THE CALCULATION OF THE FLOW BEHIND BLUFF BODIES WITH AND WITHOUT COMBUSTION

by

Stephen Bailey Pope B.Sc.(Eng), M.Sc.,
A.C.G.I., D.I.C.

Thesis submitted for the degree of

Doctor of Philosophy

in the Faculty of Engineering

University of London

Imperial College

December 1975

ABSTRACT

Measured flow properties in two-dimensional wakes are compared with the values calculated using a mean flow closure and two different Reynolds stress closure turbulence models. The comparison shows that, for wakes without recirculation, the three turbulence models predict similar values of mean velocity although the Reynolds stress models do, of course, provide a better representation of the individual stresses. For wakes with recirculation the differences between the values calculated with each turbulence model are overshadowed by large discrepancies between measurements and calculations: the length of the recirculation zone is underestimated as is the rate of spread of the downstream wake. The turbulence models are examined term by term and the dissipation equation, which is common to all three models, is identified as the source of the error. The reasons for this error and an alternative approach are suggested. A new finite-difference procedure for the solution of the equations comprising the Reynolds stress closures is described.

The transport equations for the single and joint probability distributions of scalars characterising a reacting system are derived and the unknown terms in the single probability distribution equation are modelled. Solutions of the modelled equation are presented and they demonstrate the influence of turbulent mixing and finite chemical reaction rates. These equations are employed to assess combustion models in current usage: the theoretical foundations of the models for diffusion and arbitrarily fuelled flames are consolidated while the model for premixed flames is found to be poorly based and an alternative is proposed. Calculations are made of premixed propane/air flames stabilised behind an annular V-gutter in a circular duct. The similar values of combustion efficiency and mean velocity predicted by the eddy-break-up model and the alternative proposal are in reasonable agreement with the data although the width of the flame is overestimated by approximately 30%.

ACKNOWLEDGEMENTS

This work has been carried out with the support of the Procurement Executive, Ministry of Defence and under the supervision of Professor J.H. Whitelaw.

I am grateful to members of the National Gas Turbine Establishment and to Mr. M.J. Roberts and Dr. W.P. Jones of Rolls Royce (1971) Ltd. for their continued help and interest. The various aspects of the work have benefitted from valuable comments and criticisms by Mr. P. Bradshaw, Dr. B.E. Launder and Dr. F.C. Lockwood to whom I owe my thanks. Also, extensive discussions with Mr. M.M. Ribeiro have served to broaden my view of the subject and to clarify the problems it poses. Above all, I gratefully acknowledge the encouragement, advice and guidance provided by my supervisor, Professor J.H. Whitelaw.

Finally, I should like to thank Ms. E. Barker and Ms. S.J. Chambers for performing the arduous task of typing this and other works.

CONTENTS

CHAPTER 1

INTRODUCTION

1.1 The Flows Considered

1.1.1 The Flow Behind Bluff Bodies. The investigation reported here was concerned with the turbulent flow occurring downstream of bluff bodies: both reacting and isothermal flows were considered. The flow behind a cone, which is a typical example of the isothermal case, is illustrated in figure 1.1 where three regions are distinguished.
In the first region, upstream of the trailing edge of the cone, the main feature of the flow is the divergence of the streamlines caused by the presence of the obstruction. Except in the immediate vicinity of the cone, momentum transfer by molecular and turbulent agencies is negligible.

Immediately downstream of the body a region of reversed flow occurs. While averaged streamline patterns have been measured, e.g. Chigier and Beér (1964), and are shown on the figure, a conception of the recirculation zone based on ordered flow patterns would be neglecting its essential chacteristics. A better picture, see Nicholson and Field (1949), is one of large eddies (possibly as large as the width of the body) passing to and fro across the averaged streamlines causing a great deal of mixing.

In the third region the flow is a "free boundary-layer"; that is, a region where there is a predominant flow direction along which gradients of averaged quantities are small compared with their gradients in the normal direction. The wake caused by the bluff body decays and, as the velocity returns to its free stream value, the rate at which the wake spreads across the flow decreases.

The wake described above is an idealisation of many practically occurring flows: the work performed on isothermal flows has relevance, therefore, to wakes behind aeroplanes, ships and buildings as well as to

wakes found inside engineering equipment. The flow behind inlet valves in internal combustion engines provides an example of the latter type of flow. The motivation for studying the flow behind bluff bodies was not, however, related to any of the above applications; rather, these isothermal flows were considered in order to provide an understanding of the hydrodynamics of the type of flow occurring in bluff body stabilised flames.

1.1.2 Bluff Body Stabilised Flames

In a combustion system which is homogeneous on all scales, the rate of reaction is solely a function of the thermodynamic and chemical properties. However, the gross features of reacting flows often depend only weakly on the detailed chemistry and are principally determined by the flow structure. This is because the rate of reaction is controlled not only by the chemical kinetics but also by the mixing of fuel, oxygen and thermal energy, ultimately by molecular action. Thus, for example, in high Reynolds number turbulent diffusion flames where the molecular mixing is largely independent of Reynolds number so also are the (appropriately normalised) mean velocities, temperatures and reaction rates, Spalding (1975). In the following discussion of bluff body stabilised flames, which relies on the early experimental studies reported in sub-section 1.2.2, it will be seen that mixing by the mean flow and by turbulence are of central importance.

Figure 1.2 is a sketch of a flame behind a V-gutter showing the pattern of streamlines and the location of the flame. In the region upstream of the trailing edge no reaction takes place because the flame is unable to propagate upstream faster than it is convected downstream by the flow. The flame is anchored by the recirculation zone which is a region of low flow velocity and high reaction rate; the high level of turbulence serves to supply the zone with fresh reactants and to mix them rapidly with hot

products. In exchange, the recirculation zone supplies the surrounding stream with hot products, hence initiating the flame which, as it passes downstream, spreads across the flow.

The principal use of bluff body stabilised flames is in gas turbine afterburners and it was to this application that the investigation was directed. In designing a reheat system, the engineer's principal concern is with flame stability, combustion efficiency and pollutant formulation. These aspects of reheat performance are discussed below where the predominant flow and combustion phenomena, responsible for each, are identified.

It is found that, for a given flame stabiliser and fluid composition, there is a flow velocity above which a flame cannot be stabilised. The existence of stability limits, at which the flame is said to "blow off", can be attributed to the failure of the recirculation zone to stabilise the flame as indicated above. In order to determine the mechanism responsible for this failure, consider the effect on a stabilised flame of an increase in flow velocity. The rate of supply of fuel to an elemental volume of the flow increases linearly with the velocity as does the rate of mixing. Consequently, providing that the rate at which the chemical kinetics can burn the fuel exceeds the rate of supply of energetic fuel and oxygen to the molecular scale, the reaction rate also increases linearly with the velocity. Thus, in this situation, the values of fuel concentration, temperature and density at any point in the flow are independent of the velocity. However, as the chemical kinetic rates are independent of the velocity, there is a value of flow velocity above which the molecular mixing rate exceeds the kinetic rate, resulting in lower reaction rates and, consequently, further increases in velocity result in decreased combustion and lower temperatures until the recirculation

zone is no longer able to sustain the flame. This simple model indicates that the phenomenon responsible for blow-off is an interraction between turbulence and chemical kinetics in the recirculation zone.

The combustion efficiency is determined by the rate of reaction which, in a flame well within the stability limits, is in turn determined by the mean flow and turbulence mixing. In particular, as the recirculation zone forms the base of the flame, the mixing in this region can be expected to play an important rôle in determining the combustion efficiency in all parts of the flow.

In recent years, legislation has come into force in order to limit pollution emissions from aircraft engines: consequently, although the concentrations of pollutants, principally oxides of nitrogen, are so small as not to affect the performance of combustion systems, their minimisation is an objective of the design. The formation of oxides of nitrogen depends strongly upon the temperature of the combustion gases, Newhall and Shahed (1971), and a design which produces an even temperature distribution, rather than hot and cold regions, is more likely to be successful in minimising pollutant formation.

In summary, flame stability, combustion efficiency and pollutant formation are of central interest in bluff body stabilised flames, and, to varying degrees, in most other combustion systems. The mean flow and turbulence fields have a controlling influence on the structure of the flame while the temperature field is a determining factor in pollutant formation. The recirculation zone, to which the flame owes its existence, is of particular importance and an interraction between turbulence and chemical kinetics in this region accounts for blow-off.

1.2 Description of the Research Programme

1.2.1 Preamble.

The general objective of the research was to provide a quantitative description of bluff body stabilised flames; that is, to formulate theories or models which may be used to predict the behaviour of such flows. It is useful to enumerate here the criteria by which such models are to be judged;

(i) detail - the amount of information provided

(ii) accuracy

(iii) generality

(iv) economy

Any model is unlikely to be superior to all other possibilities in all these respects and so a compromise is needed. For example, in the next sub-section where previous investigations are reported, it is seen that empirical correlations have been established between the blow-off velocity and the major flow parameters. Such correlations require a minimum of evaluation and are reasonably accurate but they only provide information about blow-off and are restricted to simple systems. On the other hand, the exact equations governing the flow provide a completely accurate and general description of every aspect of the flow but their solution is prohibitively uneconomical.

In the next sub-section, where previous related work is reported, the approach of modelling and solving transport equations for the major flow properties is seen to represent a good compromise. A chronological account of the present research programme, which represents applications and considerations of this approach, is given in sub-section 1.2.3. It will be seen that existing theories were found to be unable to describe the flows to the required accuracy and, as a consequence, the major part

of the work was involved with quantifying the errors, diagnosing their sources and devising remedies. This being the case, the work proceeded toward the overall objective in stages and the detailed objectives of each stage, stated in sub-section 1.2.4, were largely determined by the findings of the previous stages. The work comprising each stage is presented in this thesis under subject heads rather than in chronological order; the lay-out of the thesis is described in the final sub-section of this chapter.

1.2.2 State of the Art

In this sub-section, previous investigations of bluff body stabilised flames are reported in order to provide a picture of the state of knowledge at the start of the present work, 1972. The early works notably Longwell et al. (1949), Williams et al. (1949) and Longwell (1953), were concerned with measuring the stability limits under various operating condition. From these data it was possible to correlate the blow-off velocity with the dominant flow parameters and to suggest tentative models of the mechanisms involved, see, for example, Childs (1960). In order to provide a better understanding of the mechanisms, Fetting et al. (1959) and Fillippi et al. (1962) studied the effects of altering the chemical composition of the recirculation zone while Winterfeld (1965) investigated the gross hydrodynamic features of the flows. These experimental investigations provide, in part, a qualitative understanding of the flows and correlations between blow-off and the dominant flow variables. They do not, however, provide measurements of local properties such as species concentrations, temperature, velocity and turbulence properties.

The works of Howe et al. (1963), Cushing et al. (1967) and Pein et al. (1970) provide a small amount of information about the local chemical and thermodynamic properties in the flows but, due to experimental

difficulties, velocity and turbulence quantities remained unmeasured. In recognition of the important rôle played by the aerodynamics of the flow, Davies and Beér (1971), Chigier and Beér (1964), Carrody (1964), and others undertook investigations of the velocity and turbulence fields in bluff body stabilised flame type flows but in the absence of combustion. These works provide valuable information but the uncertainties in measuring in recirculation zones with hot wires or pitot probes and the absence of combustion limit their usefulness. More recently the technique of laser anemometry has been successfully applied to turbulent flames to measure both mean velocity and turbulence intensity, e.g. Durst et al. (1972a). However, while this method has great potential, results for bluff body stabilised flames obtained by 1972 were few, Durst et al. (1972b) and Durão et al. (1973).

On the theoretical front, since the late 1960's, significant advances have been made: these stem from the exploitation of digital computers to solve simultaneous partial differential equations. If the ability of computers were unbounded, the way forward would be simple; a set of equations representing the conservation of mass, momentum, energy and chemical species can be formulated which, with little uncertainty, describe the flow in every detail. The problem arises because this set of equations, applied to turbulent reacting flows, is too complicated to be solved by computers in the forseeable future. However, the engineer does not need to know every detail; the behaviour of turbulent fluctuations is not his concern. The approach appropriate to the engineer, and that adopted by many workers since the 1960's, is to solve a simpler set of equations from which ensemble averaged values of velocity, density, temperature and species concentrations can be determined.

The exact equations for the ensemble averaged velocities contain, as unknowns, the Reynolds stresses which may be estimated through turbulence

models. Prandtl's (1925) mixing length hypothesis was soon replaced by turbulence models which solved transport equations for one or more turbulence quantities. Models which solved equations for the kinetic energy and another scale of turbulence proved particularly successful: Rodi (1972) applied one such model to free shear layers while wall boundary-layers were considered by Ng (1971) and Jones (1971). Hanjalić and Launder (1972) incorporated a shear stress equation into this model in order to predict asymmetric channel flow and Launder, Morse, Rodi and Spalding (1972) concluded this phase of development by solving equations for each of the normal stresses as well. A summary of these models is provided by Launder and Spalding (1972). It should be noted that all the above works were concerned with boundary layer flows: two-equation models were used in recirculating flows, e.g. Runchal (1971), but the predictions obtained were not compared with detailed experimental data and so their accuracy for these situations could not be determined.

In addition to a turbulence model, a combustion model is required in reacting flows in order to close the set of equations. Temperature and species concentration fluctuations affect the density and reaction rates of species and, consequently, the turbulent structure; the rôle of combustion models is to account for these effects. Early investigations, e.g. Patankar and Spalding (1970) and McGuirk (1971), rather than employing a combustion model, ignored the effects of turbulence completely; this was done, not in the belief that they were negligible but, for want of a viable alternative. In order to simplify the analysis, idealised systems were considered; the two extremes of premixed and diffusion flames were considered separately with the common assumptions of a very fast single step irreversible reaction. Spalding (1971) proposed the "eddy-break-up" model for premixed flames which supposes the reaction rate to depend on the local turbulence structure. This model was used

with success by, among others, Mason and Spalding (1973) but, as will be seen later, it rests on unsure foundations. The analysis of turbulent diffusion flames stems from the work of Toor (1962): the assumption of a very fast reaction rate implies, for diffusion flames, that fuel and oxygen do not coexist. This observation allows the species concentrations, temperature and density to be evaluated from the mixture fraction, the averaged equation for which requires only a modest amount of modelling. This model is not, however, complete because the condition of non-coexistence does not mean that the averaged concentration of either fuel or oxygen is zero everywhere. In fact, due to mixture fraction fluctuations, both species can exist at the same place but at different times. Spalding (1970) suggested a transport equation for the mixture fraction fluctuations which was incorporated into the diffusion flame model by Gosman and Lockwood (1973).

This brief revue indicates the state of the art at the start of the present work: more recent advances are reported at appropriate points in the thesis. In summary, experimental investigations provided a qualitative understanding of bluff body stabilised flames although detailed measurement of local quantities were scarce. Turbulence models had been successfully used to predict boundary layer flows while work on combustion modelling, although in its infancy, suggested that reacting flows were amenable to this approach.

1.2.3 Chronicle of the Research Programme

On the basis of the past success of turbulence and combustion models, work commenced with the use of a computer program for two-dimensional recirculating flows incorporating the k- ε, two equation, turbulence model and the eddy-break-up combustion model. This computer program, a precursor of that described by Runchal (1973), formed the basis of all the calculations

performed throughout this research. A literature survey, Pope (1973), showed that experimental data for testing the procedure was in short supply. However, some initial calculations revealed that, for both isothermal and reacting flows, the calculated length of the recirculation zone was significantly less than the measured value. In light of the importance of the recirculation zone in stabilised flames, a theoretical and an experimental programme were undertaken in an attempt to overcome this defect.

At this time, the works of Launder, Morse, Rodi and Spalding (1972), Hanjalić and Launder (1972) and the results later reported by Launder, Reece and Rodi (1975) became available. They indicated that Reynolds stress closures provided a significant advantage over mean flow closures and, consequently, it was decided to incorporate a Reynolds stress model into the computer program. The modelled Reynolds stress equations had not been applied to recirculating flows before and it proved to be a difficult and time consuming task: the simplicity of the method finally adopted belies the fact that, in rejecting unviable alternatives, it represents twelve months work.

An experimental investigation was instigated with the objective of supplementing the data relating to isothermal flows behind flame stabilisers. In particular, it was intended to measure individual Reynolds stresses in order to test the new turbulence model. To this end, a rig was designed to study the flow of water around a disc baffle mounted centrally in a round tube which was to be measured by laser anemometry.

While these two tasks were in hand, partly due to the numerical difficulties being experienced with the Reynolds stress equations and partly in order to rectify an error made by Lumley (1970), the form of the effective viscosity hypothesis was considered. It was realised that the major advantage of a Reynolds stress closure could be obtained using

the two-equation model with an improved effective viscosity hypothesis. This work, Pope (1975), was successfully completed and is summarised in this thesis. The suggested effective viscosity hypothesis was not used in the calculations because, when it became available, the Reynolds stress model had been successfully incorporated into the program and results obtained.

A comparison between experimental data for isothermal wake flows and the calculations performed with the Reynolds stress model revealed that the discrepancies, although marginally less than with the k-ε model, were still prevalent. Thus, while this work on isothermal flows is useful in discovering and quantifying these errors, it did not provide a significantly better description of the flow. As more time had been spent on isothermal flows than was initially intended and as the existing data proved sufficient to test the model, the experimental programme was discontinued. The rig, which by this time had been constructed and was being commissioned, was, however, used for its initial purpose by Ms. H. Assaf, some of whose work is reported here. The author's contribution to the experimental programme is not included in this thesis.

While the work on isothermal flows was in progress, the overall objective had not been forgotten: the preliminary calculations and theoretical considerations revealed that the eddy-break-up model was not physically realistic nor could it account for the interaction between turbulence and chemical kinetics which accounts for blow-off. At the same time, the model for diffusion flames was being refined by Lockwood and Naguib (1975a) and by Elgobashi and Pun (1974) on the basis of an assumed probability distribution for the mixture fraction. In an attempt to overcome the defects of the eddy-break-up model and to unify the models for premixed and diffusion flames, the probability approach, applied to the Navier-Stokes equations by Lundgren (1967), was turned to the equations

of turbulent reacting flow. The outcome of this theoretical work was to provide a set of exact equations which clearly reflect the physical processes involved in turbulent combustion. In addition, closure approximations for these equations were suggested resulting, principally, in a model for premixed flames which accounts for the interaction between turbulence and chemical kinetics. A degenerate form of this model was obtained by assuming high reaction rates and the result can be regarded as a more soundly based form of the eddy-break-up model.

A further set of calculations were performed in order to assess the accuracy of eddy-break-up type combustion models. The calculation procedure embodied the k-ε turbulence model as well as one of the combustion models and the predictions were compared with the data of Harrison (1973 and 1974). These data include velocity and combustion efficiency measurements in a premixed propane/air flame stabilised behind an annular V-gutter.

Finally, prior to the preparation of this thesis, the implications of the theoretical and computational works performed were considered in order to assess the present status of turbulence and combustion modelling and, by highlighting the deficiencies, to suggest profitable areas for further research.

1.2.4 Objectives

The objectives of each aspect of the work described above were, in chronological order of their performance;

i to develop and test a numerical algorithm for the solution of the equations comprising Reynolds stress closures;

ii to formulate a more general effective viscosity hypothesis;

iii to calculate isothermal wakes with mean flow and Reynolds stress closures in order to assess their performance;

iv to develop a theory of turbulent combustion incorporating the effect of finite reaction rates;

v to calculate bluff body stabilised flames in order to assess the performance of combustion models;

vi to reassess the theoretical foundations of turbulence and combustion models and thereby to identify profitable areas for further research.

This research must be judged, not only by the success with which each of these objectives are achieved, but also by how far these achievements serve to fulfil the overall objective of providing a quantitative description of bluff body stabilised flames.

1.2.5 Lay-out of the Thesis

In the next four chapters the work is reported under the headings Turbulence Modelling, Combustion Modelling, Calculation Procedures and Calculations. This format, chosen to provide a coherent structure, allows each aspect of the work to be treated from beginning to end with a minimum of references to other parts of the thesis. However, the reader should bear in mind that the order of presentation does not reflect the order of performance and, consequently, several observations made in Chapters 2 and 3 represent suggestions for further work rather than ideas to be explored later in the thesis.

In Chapter 2 the turbulence models used in the calculations are introduced and the mean closure approach is discussed. These turbulence models are examined term by term and the effective viscosity hypothesis

and the dissipation equation are subjected to particularly close scrutiny. The modelling of turbulent reacting flows is discussed in Chapter 3 by reference to the probability distribution equations. A theory is developed from these equations and is used to assess the foundations of existing combustion models: in particular, in conjunction with a consideration of density fluctuations, a more soundly based form of the eddy-break-up model is proposed.

In Chapter 4 the numerical procedures for the solution of the equations comprising the various closures are outlined and the novel features used for the Reynolds stress closures are described. The results of the calculations using these procedures are presented in Chapter 5 where the performance of the models is assessed.

The main findings of the work are summarised in the final chapter; the achievements are compared with the objectives and suggestions for further work are made.

CHAPTER 2

TURBULENCE MODELLING

2.1 Introductory Remarks

In this chapter we are concerned with methods by which the average velocity, $\langle U_j \rangle$, may be determined at each point in a flow field. The exact equations for the average velocity, the Reynolds stresses and the kinetic energy of turbulence are derived and explained in this section. In section 2.2 the mean closure approach is considered and in the two subsequent sections the turbulence models used in the calculations are presented and assessed. The principal findings of this chapter are summarised in section 2.5.

For a constant density and viscosity Newtonian fluid the instantaneous velocity, U_j, is given by the Navier-Stokes equation which is an expression of the conservation of momentum in each of the three coordinate directions,

$$\rho \frac{\partial U_j}{\partial t} + \rho U_i \frac{\partial U_j}{\partial x_i} = \mu \frac{\partial^2 U_j}{\partial x_i^2} - \frac{\partial P}{\partial x_j} \qquad (2.1)$$

The continuity equation expresses the conservation of mass,

$$\frac{\partial U_i}{\partial x_i} = 0 \qquad (2.2)$$

An equation for $\langle U_j \rangle$ may be derived from equation 2.1 by decomposing the instantaneous quantities into their average and fluctuating components,

$$\begin{aligned} U_j &= \langle U_j \rangle + u_j \\ P &= \langle P \rangle + p' \end{aligned} \qquad (2.3)$$

Thus, substituting equation 2.3 into 2.1 and averaging yields,

$$\rho\frac{\partial\langle U_j\rangle}{\partial t} + \rho\langle U_i\rangle\frac{\partial\langle U_j\rangle}{\partial x_i} = \mu\frac{\partial^2\langle U_j\rangle}{\partial x_i^2} - \frac{\partial\langle P\rangle}{\partial x_j} - \rho\frac{\partial}{\partial x_i}\langle u_i u_j\rangle \qquad (2.4)$$

This equation for the averaged velocity is seen to be identical to the equation for U_j, equation 2.1, except for the inclusion of the last term which represents momentum transfer due to turbulent action. In order that equation 2.4 may be solved the Reynolds stresses, $\langle u_i u_j\rangle$, must be determined; this is the principal rôle of turbulence models.

As the Reynolds stresses form the main theme of turbulence modelling, it is appropriate at this stage to derive a transport equation for them: this is accomplished by subtracting equation 2.4 from equation 2.1, multiplying by u_k, forming a second equation by commuting the sufficies k and j, adding the two equations and averaging the result. This procedure gives the Reynolds stress equation,

$$\rho\frac{\partial}{\partial t}\langle u_j u_k\rangle + \rho\langle U_i\rangle\frac{\partial}{\partial x_i}\langle u_j u_k\rangle = -\rho\langle u_i u_k\rangle\frac{\partial\langle U_j\rangle}{\partial x_i} - \rho\langle u_i u_j\rangle\frac{\partial\langle U_k\rangle}{\partial x_i}$$

(A) (B)

$$-\frac{\partial}{\partial x_i}\left(\rho\langle u_i u_j u_k\rangle - \mu\frac{\partial}{\partial x_i}\langle u_j u_k\rangle + \langle p' u_j\rangle\delta_{ik} + \langle p' u_k\rangle\delta_{ij}\right)$$

(C)

$$+\langle p'\frac{\partial u_j}{\partial x_k}\rangle + \langle p'\frac{\partial u_k}{\partial x_j}\rangle \qquad (2.5)$$

(D)

$$-2\mu\langle\frac{\partial u_j}{\partial x_i}\frac{\partial u_k}{\partial x_i}\rangle$$

(E)

The terminology applied to the various terms is,

A - change along an averaged streamline

B - "production" due to Reynolds stress, velocity gradient interaction

C - "transport" due to turbulence and viscosity

D - "redistribution" or "pressure scrambling"

E - "dissipation" due to viscous action

The terms on the right hand side of equation 2.5 require further explanation, but first it is convenient to write the turbulent kinetic energy equation ($k \equiv \frac{1}{2} \langle u_j u_j \rangle$),

$$\rho \frac{\partial k}{\partial t} + \rho \langle U_i \rangle \frac{\partial k}{\partial x_i} = - \rho \langle u_i u_j \rangle \frac{\partial \langle U_j \rangle}{\partial x_i}$$

(A') (B')

$$- \frac{\partial}{\partial x_i} \left(\tfrac{1}{2} \rho \langle u_i u_j u_j \rangle - \mu \frac{\partial k}{\partial x_i} + \langle p' u_i \rangle \right) \qquad (2.6)$$

(C')

$$- \mu \left\langle \left(\frac{\partial u_j}{\partial x_i} \right)^2 \right\rangle$$

(E')

Production. B' in equation 2.6 is termed "the production of turbulent kinetic energy" and the name implies that it is positive. If an equation for the kinetic energy of the mean flow, $\frac{1}{2} \langle U_j \rangle^2$, were derived the same term would appear but with the opposite sign. Thus, the term represents a transfer of energy between the mean flow and the turbulence. The mean flow is ordered while the turbulence is quasi-random hence, from entropy considerations, it would be surprising if energy were extracted from the disordered turbulence and transferred to the mean flow. In fact,

measurements show that the "production" is invariably positive although there are regions in some flows where it may be negative: asymmetric channel and annulus flows provide common examples. The fact that production may at times be negative serves as a warning to theories based on a purely stochastic view of turbulence. The production of Reynolds stresses (term B in equation 2.5) generally has the same sign as the stress in question and hence tends to increase its magnitude.

Transport. The transport term in equation 2.5 is seen to be the derivative of a flux of Reynolds stress; the volume integral of the term is equal to the surface integral of the expression inside the derivative. In homogeneous turbulence the term is zero: in inhomogeneous turbulence the term serves to transfer Reynolds stresses from one part of the flow to another.

Redistribution. This term is so called because, as it does not appear in the kinetic energy equation, it only serves to transfer energy from one component of the Reynolds stress tensor to another. The redistribution term is of central interest in turbulence modelling and will be discussed at length below.

Dissipation. The dissipation of turbulent kinetic energy, ε, is identically positive: it represents the transfer of turbulence energy to thermal energy by viscous action. The partition of dissipation between the individual Reynolds stresses is a subject of controversy and will be discussed in section 2.4.

2.2 The Mean Closure Approach

2.2.1 The Problem

As a first step to determining the averaged velocity the transport equation for $\langle U_j \rangle$ has been derived, equation 2.4. However, the Reynolds stresses appear as unknowns in this equation and the Reynolds stress equations contain more unknowns. The process of deriving transport equations for each unknown could be continued ad infinitum and yet the number of unknown quantities would ever increase. This unfortunate state of affairs is an inevitable consequence of the fact that in only considering averaged quantities a full description of the flow is not possible. This is the "closure problem" which, as is all too often forgotten, is inescapable.

2.2.2 The Approach

The above considerations have shown that the direct approach of deriving a closed set of equations from which the Reynolds stresses may be deduced is not possible. However, it is possible to close the set of equations at some level by forming "constitutive relations" for the unknown quantities; that is, by supposing that the unknown quantities are related to the known quantities by a given expression. A more formal statement of this approach serves to identify its important implications: exact transport equations are derived for the set of quantities $\underline{\phi}$ and these equations contain the set of unknown quantities $\underline{\psi}$. That is,

$$\rho \frac{D\phi_\alpha}{Dt} = F_\alpha(\underline{\phi}) + G_\alpha(\underline{\psi}) \tag{2.7}$$

where ϕ_α is any one of the set $\underline{\phi}$ and F_α and G_α are known functions. In order to close the set of equations 2.7 constitutive relations are proposed,

$$\psi_\beta = H_\beta(\underline{\phi}) \tag{2.8}$$

As equations 2.7 are exact, the performance of a mean closure model depends almost entirely upon the constitutive relations which are, by nature, approximations. Let us recall the criteria, given in the Introduction, by which turbulence models are to be judged: the detail provided by the model is solely a function of the level of closure and is not influenced by the constitutive relations. However, the criteria of economy and generality require that the relations be simple and universally applicable. The success of the model depends, therefore, upon the accuracy that can be achieved with constitutive relations that are reasonably simple and universally applicable.

Before considering the accuracy that can be expected from turbulent constitutive relations, a further restriction is imposed on the form of the relation: that boundary conditions for $\underline{\phi}$ alone are sufficient to determine the solution of equations 2.7 and 2.8. This restriction, which implies that H_β makes no reference to boundary conditions except those for $\underline{\phi}$, is the essence of a constitutive relation and yet, in general, it denies the possibility of complete accuracy. A relation not in keeping with this restriction would certainly go against the criterion of economy and its generality would be doubtful. All the constitutive relations used in the models described below are subject to this restriction.

2.2.3 The Accuracy of Constitutive Relations

Consider a region of turbulent flow within which equations 2.7 and 2.8 are to be solved in a volume V. Clearly the constitutive relations, H_β, may only make reference to values of $\underline{\phi}$ within V so that if V tends to zero H_β must relate the value of ψ_β within the infinitessimal volume to the values of $\underline{\phi}$ in the same region. Thus, in the limit, ψ_β at a point must be related to $\underline{\phi}$ at the same point. As generality is required, ψ_β must be related to local values of $\underline{\phi}$ irrespective of the solution domain.

The assumptions and arguments stated above require, for complete accuracy,

(i) that the values of $\underline{\phi}$ within a flow domain are uniquely related to the values of $\underline{\phi}$ at the boundary,

(ii) that the values of $\underline{\psi}$ at any point are uniquely related to the values of $\underline{\phi}$ at that point,

and (iii) that the proposed constitutive relations between $\underline{\psi}$ and $\underline{\phi}$ are correct.

The accuracy of a turbulence model depends, therefore, upon how closely these conditions are satisfied. The closures outlined in the next section will be discussed in section 2.4 by reference to these three conditions.

2.3 Turbulence Models

Three turbulence models were employed to obtain the results presented in Chapter 5. While none of these models is new, the two Reynolds stress closures employed have not been applied to recirculating flows before. The models are quoted here together with summary justification for the modelling given by the originators. In each case, attention is restricted to the high Reynolds number form of the model: only those terms that remain finite as the Reynolds number tends to infinity are retained. A critical discussion of these models is presented in the next section.

The first model described is a mean flow closure; that is, a constitutive relation is proposed for the Reynolds stresses thus closing the mean momentum equation. It will be shown that two scaling parameters are needed to effect this closure and consequently transport equations are also solved for the kinetic energy of turbulence and its dissipation rate. These equations are also closed by modelling assumptions. The

remaining models are Reynolds stress closures: transport equations are solved for each non-zero Reynolds stress as well as for the dissipation rate of turbulent kinetic energy. The unknown terms in these equations are evaluated through relations based on known quantities.

2.3.1 The Mean Flow Closure (Model I)

Most turbulence models evolve rather than being the work of an individual. Thus, while the final form of the mean flow closure described here was proposed by Jones (1971), it stems from the works of Boussinesq (1877), Kolmogorov (1942), Prandtl (1945), Chou (1945) and Harlow and Nakayama (1967).

The Reynolds stresses are related to the mean velocity gradients by an effective viscosity hypothesis,

$$\rho \langle u_i u_j \rangle = 2/3 \ \rho k \ \delta_{ij} - \mu_{eff} \left(\frac{\partial \langle U_i \rangle}{\partial x_j} + \frac{\partial \langle U_j \rangle}{\partial x_i} \right) \qquad (2.9)$$

The velocity gradient term appearing in equation 2.9 is the only possible linear combination of velocity gradients with the same tensor properties as the Reynolds stresses: both sides of the equation are symmetric and contract to zero. It will be noted that this expression is analogous to the stress-rate of strain relation for a laminar flow; the important difference is that the effective viscosity is a function of the flow rather than of the fluid.

On dimensional grounds, at least two scaling parameters are needed to relate the Reynolds stresses to the rate of strain. These may be chosen as a velocity scale, v, and a time scale, τ. One time scale may be deduced from the velocity gradients;

$$\tau_m \equiv \left(\frac{\partial \langle U_i \rangle}{\partial x_j} \ \ \frac{\partial \langle U_i \rangle}{\partial x_j} \right)^{-\frac{1}{2}} \qquad (2.10)$$

however, as the macro time scale of turbulence, $\tau_t = k/\varepsilon$, has been

found to be independent of τ_m in simple shear flows, Lumley (1970), the two scaling parameters must be independent of the mean velocity field. Various authors' proposals for the two scaling parameters are given by Launder and Spalding (1972). A convenient choice, and the one employed here, is that of k and ε. Thus,

$$\mu_{eff} = \rho C_\mu k^2/\varepsilon \tag{2.11}$$

With a knowledge of $\langle u_i u_j \rangle$ and ε, the transport equation for k, equation 2.6, is closed except for the turbulent transport term, C'. This term is modelled, by analogy with laminar transport, as

$$\tfrac{1}{2} \rho \langle u_i u_j u_j \rangle + \langle p' u_i \rangle = - \frac{\mu_{eff}}{\sigma_k} \frac{\partial k}{\partial x_i} \tag{2.12}$$

Thus, the modelled kinetic energy equation reads,

$$\rho \frac{Dk}{Dt} = \frac{\partial}{\partial x_i} \left(\frac{\mu_{eff}}{\sigma_k} \frac{\partial k}{\partial x_i} \right) - \rho \langle u_i u_j \rangle \frac{\partial \langle U_j \rangle}{\partial x_i} - \rho \varepsilon \tag{2.13}$$

Jones' main contribution to this model was his proposed closure of the dissipation equation. However, like most previous attempts at this feat, the justification for the modelling was incorrect, the orders of magnitude of the exact and modelled terms differing in most cases, Rodi (1971). A full discussion of the modelling of the dissipation equation is given in the next section. The modelled form is,

$$\rho \frac{D\varepsilon}{Dt} = \frac{\partial}{\partial x_i} \left(\frac{\mu_{eff}}{\sigma_\varepsilon} \frac{\partial \varepsilon}{\partial x_i} \right) - \rho \frac{\varepsilon}{k} \left(C_{\varepsilon 1} \langle u_i u_j \rangle \frac{\partial \langle U_j \rangle}{\partial x_i} + C_{\varepsilon 2} \varepsilon \right) \tag{2.14}$$

The complete closure, model I, comprises the transport equations for k and ε, equations 2.13 and 2.14, together with the expressions for the Reynolds stresses and effective viscosity, equations 2.9 and 2.11.

The values of the five constants, C_μ, $C_{\varepsilon 1}$, $C_{\varepsilon 2}$, σ_k and σ_ε, used in the calculations are given in table I together with the basis for their choice.

2.3.2 The Reynolds Stress Closures (Models II and III)

Again, the models presented here represent the suggestions of several authors, the specific models being assembled first by Launder, Reece and Rodi (1975). The terms in the Reynolds stress equations representing turbulent transport, dissipation and redistribution are to be modelled; the modelling of the redistribution distinguishing the two models.

Launder et al. presented two modelled forms of the transport term. The one employed here, originally proposed by Daly and Harlow (1970), is

$$-\frac{\partial}{\partial x_i}\,\rho\langle u_i u_j u_k\rangle = \frac{\partial}{\partial x_i}\left(C_s\,\rho\,\frac{k}{\varepsilon}\langle u_i u_\ell\rangle\,\frac{\partial}{\partial x_\ell}\langle u_j u_k\rangle\right) \tag{2.15}$$

The pressure-velocity correlation contribution is ignored. The modelled term is again of the gradient diffusion type but the magnitude of the diffusive coefficient depends upon the direction. The tensor properties of each side of equation 2.15 are the same, being second order tensors symmetric in j and k. However, if the term inside the derivative is held to represent the triple correlation then the tensor properties of the exact and modelled terms differ. Noting this defect, Launder et al. proposed a more complicated model with the correct tensor properties which was not employed here because the simpler model was found to produce better agreement with experimental data.

The dissipation term was modelled on the assumption that, at high Reynolds number, the small scale turbulence is isotropic. Thus,

$$2\mu\left\langle\frac{\partial u_j}{\partial x_i}\,\frac{\partial u_k}{\partial x_i}\right\rangle = \frac{2}{3}\,\rho\,\varepsilon\,\delta_{jk} \tag{2.16}$$

As was mentioned above, this modelling is a subject of controversy and will be discussed in section 2.4. For the moment, suffice it to say that, if the dissipation is anisotropic, the neglected part has the properties of a redistribution term and hence the modelling of the pressure scrambling may be thought to include this term as well.

The redistribution term is of paramount importance for, in conjunction with the production, it governs the level of anisotropy of the Reynolds stresses. The fluctuating component of pressure appearing in the redistribution term may be eliminated by Green's theorem applied to the Poisson equation for p'. Thus, far from walls where the surface integral may be neglected,

$$\langle p' \frac{\partial u_i}{\partial x_j} \rangle = \frac{\rho}{4\pi} \int_{vol} \{ \langle (\frac{\partial^2 u_\ell u_m}{\partial x_\ell \partial x_m})^* \frac{\partial u_i}{\partial x_j} \rangle + 2 (\frac{\partial \langle U_\ell \rangle}{\partial x_m})^* \langle (\frac{\partial u_m}{\partial x_\ell})^* \frac{\partial u_i}{\partial x_j} \rangle \} \frac{d\ vol}{|\underline{x} - \underline{y}|} \qquad (2.17)$$

$$\phi_{ij,1} \qquad\qquad \phi_{ij,2}$$

where the terms with and without asterisks refer to the points $\underline{x}$ and $\underline{y}$ respectively. The first term is modelled after Rotta (1951),

$$\phi_{ij,1} + \phi_{ji,1} = -C_{\phi 1}\ \rho\varepsilon/k\ (\langle u_i u_j \rangle - 2/3\ k\ \delta_{ij}) \qquad (2.18)$$

This represents a tend towards isotropy at the rate of the turbulent time scale and has a magnitude proportional to the anisotropy. Both Reynolds stress models incorporate equation 2.18.

If the flow were homogeneous, the mean velocity gradient appearing in $\phi_{ij,2}$ can be removed from the integral which then has dimensions of Reynolds stress. The term lends itself, therefore, to be modelled as a linear combination of velocity gradients multiplied by Reynolds stresses: Launder et al. propose two such models. The first, which is embodied in model II, is

$$\phi_{ij,2} + \phi_{ji,2} = - C_{\phi 2} \left(P_{ij} - 2/3 \; P\delta_{ij}\right) \tag{2.19}$$

where P_{ij}, the production of $\langle u_i u_j \rangle$, is given by

$$P_{ij} = - \rho \langle u_i u_k \rangle \frac{\partial \langle U_j \rangle}{\partial x_k} - \rho \langle u_j u_k \rangle \frac{\partial \langle U_i \rangle}{\partial x_k} \tag{2.20}$$

and P, the production of kinetic energy, is equal to $\frac{1}{2} P_{ii}$. The term tends to counteract anisotropy by diminishing the effects of anisotropic production. Equation 2.19 does not, however, satisfy one of the requirements of the exact expression. Launder et al. proposed a second closure which is in accord with this restraint;

$$\begin{aligned} \phi_{ij,2} + \phi_{ji,2} = & - (C_{\phi 2} + 8)/11 \quad (P_{ij} - 2/3 \; P \; \delta_{ij}) \\ & - (30C_{\phi 2} - 2)/55 \quad \rho k \left(\frac{\partial \langle U_i \rangle}{\partial x_j} + \frac{\partial \langle U_j \rangle}{\partial x_i}\right) \\ & - (8C_{\phi 2} - 2)/11 \; (D_{ij} - 2/3 \; P \; \delta_{ij}) \end{aligned} \tag{2.21}$$

$$\text{where } D_{ij} = - \rho \langle u_i u_k \rangle \frac{\partial \langle U_k \rangle}{\partial x_j} - \rho \langle u_j u_k \rangle \frac{\partial \langle U_k \rangle}{\partial x_i} \tag{2.22}$$

Equation 2.21 is the closure employed by model III.

Each unknown term in the Reynolds stress equation has now been modelled and the result reads

$$\begin{aligned} \rho \frac{D}{Dt} \langle u_i u_j \rangle = & \frac{\partial}{\partial x_\ell} \left(C_s \rho \frac{k}{\varepsilon} \langle u_\ell u_k \rangle \frac{\partial \langle u_i u_j \rangle}{\partial x_k}\right) + P_{ij} - 2/3 \; \rho\varepsilon \; \delta_{ij} \\ & - C_{\phi 1} \rho \; \varepsilon/k \; (\langle u_i u_j \rangle - 2/3 \; k\delta_{ij}) + (\phi_{ij,2} + \phi_{ji,2}) \end{aligned} \tag{2.23}$$

the second part of the redistribution term being given by equation 2.19 and 2.21 for models II and III respectively.

The dissipation equation used with the two Reynolds stress models is the same as for model I, equation 2.14, except that the transport is modelled in a similar way to that of the Reynolds stresses. Thus

$$\rho \frac{D\varepsilon}{Dt} = \frac{\partial}{\partial x_i} \left(C_\varepsilon \rho \frac{k}{\varepsilon} \langle u_i u_j \rangle \frac{\partial \varepsilon}{\partial x_j} \right) + \frac{\varepsilon}{k} \left(C_{\varepsilon 1} P - \rho C_{\varepsilon 2} \varepsilon \right) \qquad (2.24)$$

Six constants appear in each model, $C_{\phi 1}$, $C_{\phi 2}$, $C_{\varepsilon 1}$, $C_{\varepsilon 2}$, C_s and C_ε: the values used in the calculations are given in table I.

2.3.3 Wall Functions

As the models described above are intended for flow regions with high Reynolds numbers, a special treatment is needed close to a wall. Rather than introducing low Reynolds number terms into the models and solving the equations up to the wall (a region of high variation of turbulent quantities), instead, the near wall region is approximated by Couette flow solutions based on the logarithmic law of the wall.

Let the subscripts w and p refer to points on and near the wall respectively and y be the normal distance from the wall. The following normalised distance and velocity are defined:

$$y_p^+ \equiv \rho \left(k_p C_\mu^{\frac{1}{2}}\right)^{\frac{1}{2}} y_p / \mu \qquad (2.25)$$

$$u_p^+ \equiv \frac{1}{\kappa} \ell n \, E y_p^+ \qquad (2.26)$$

The wall shear stress is then given by,

$$\tau_w = \mu \left(\frac{\partial \langle U \rangle}{\partial y}\right)_w = \frac{\langle U_p \rangle}{y_p} \frac{y_p^+}{u_p^+} \qquad (2.27)$$

The value of ε near the wall is prescribed by,

$$\varepsilon_p = (C_\mu^{\frac{1}{2}} k_p)^{3/2}/\kappa y_p \tag{2.28}$$

and the integral of ε from the wall to y_p, which is required for the kinetic energy and Reynolds stress equations, is given by

$$\int_o^{y_p} \varepsilon \, dy = (C_\mu^{\frac{1}{2}} k_p)^{3/2} u^+_p \tag{2.29}$$

The flux of Reynolds stresses to the wall is zero. The wall law constants κ and E take the values 0.4 and 8.8 respectively.

2.4 Assessment of the Closures

In this section we consider the success that may be expected of the closures described in the previous section. The detail provided by these models is satisfactory and they are quite general; also, it will be seen in Chapter 4 that they are adequately economical. The question that remains is: For a given situation, what accuracy may be expected? The answer lies in the closeness to which each model satisfies the three requirements enumerated in section 2.2.3.

2.4.1 The Effective Viscosity Hypothesis

The second condition applied to an effective viscosity hypothesis requires that the value of $\langle u_i u_j \rangle$ at any point be uniquely related to the values of k, ε and $\frac{\partial \langle U_i \rangle}{\partial x_j}$ at the same point. However, as can be seen from equation 2.5, the Reynolds stresses may be transported both by the mean and fluctuating velocities and so, for the condition to be satisfied, the flow must be such that the transport terms are negligible.

This implies that the velocity gradients and Reynolds stresses must be nearly homogeneous. Further, for a high Reynolds number nearly homogeneous flow, it is reasonable to assume that all macro-scales of turbulence are proportional and so the two scaling parameters, k and ε , together with the velocity gradients are sufficient to determine the Reynolds stresses. As the restriction to near homogeneity ensures that the first condition is satisfied, it only remains to be considered whether the effective viscosity hypothesis, equations 2.9 and 2.11, is the correct relation between stress and rate of strain.

In a nearly homogeneous shear flow, with $\partial \langle U_1 \rangle / \partial x_2$ as the only non-zero velocity gradient, Champagne et al. (1970) measured

$$a_{11} = .3$$
$$a_{22} = -.18$$
$$a_{33} = -.12$$
$$a_{12} = .33$$

where $a_{ij} = \langle u_i u_j \rangle / k - {}^2/_3 \delta_{ij}$

whereas, at best, equation 2.9 predicts

$$a_{11} = a_{22} = a_{33} = 0 \quad , \quad a_{12} = .33$$

Thus, as the mechanism that causes the inequality of the normal stresses cannot be accounted for with the isotropic viscosity hypothesis, it must be concluded that the form of the relation is incorrect. Pope (1975) considered the possibility of a more general effective visocity hypothesis both for three dimensional flows and for flows expressible in two dimensional Cartesian coordinates. The main findings of this work are summarised here.

By defining the following non-dimensional quantities,

$$a_{ij} = \langle u_i u_j \rangle / k - {}^2/3\, \delta_{ij} \quad , \tag{2.30}$$

$$s_{ij} = \tfrac{1}{2}\, k/\varepsilon \left(\frac{\partial \langle U_i \rangle}{\partial x_j} + \frac{\partial \langle U_j \rangle}{\partial x_i} \right) \quad , \tag{2.31}$$

$$\omega_{ij} = \tfrac{1}{2}\, k/\varepsilon \left(\frac{\partial \langle U_i \rangle}{\partial x_j} - \frac{\partial \langle U_j \rangle}{\partial x_i} \right) \quad , \tag{2.32}$$

the problem may be reformulated as that of determining the tensor H_{ij} such that

$$a_{ij} = H_{ij}\,(s, \omega). \tag{2.33}$$

A consideration of the properties of the tensors, a, s and ω, reveals that the most general expression for H_{ij} is a finite tensor polynomial in terms of all the linearly independent second order tensors, T_{ij}, with zero trace that may be formed from s and ω with coefficients, G, depending upon the invariants of s and ω. Thus,

$$H_{ij} = \sum_{\lambda} G^{\lambda}\, T^{\lambda}_{ij} \tag{2.34}$$

For simplicity the following abbreviated notation will be introduced:

$$s\omega = s_{ik}\, \omega_{kj}, \quad s\omega s\omega = s_{ik}\, \omega_{kl}\, s_{lm}\, \omega_{mj}, \quad \text{etc.}$$

$$s^2 = s_{ik} s_{kj}\,, \quad \{s^2\} = s_{ik}\, s_{ki}, \text{ etc.}$$

$$I = \delta_{ij}\,, \quad I_2 = \delta^2{}_{ij} = \begin{cases} 1, & i = j \neq \alpha \\ 0, & i \neq j \text{ and } i = j = \alpha \end{cases}$$

where, for two dimensional flows, α is the direction of invariance. (This is equivalent to considering the matrices associated with the tensors).

In this notation, for the general three dimensional case there are ten tensors, T, and five variants,

$$T^1 = s \qquad T^2 = s\omega - \omega s$$

$$T^3 = s^2 - I\{s^2\}/3 \qquad T^4 = \omega^2 - I\{\omega^2\}/3$$

$$T^5 = \omega s^2 - s^2\omega \qquad T^6 = \omega^2 s + s\omega^2 - 2I\{s\omega^2\}/3$$

$$T^7 = \omega s\omega^2 - \omega^2 s\omega \qquad T^8 = s\omega s^2 - s^2\omega s$$

$$T^9 = \omega^2 s^2 + s^2\omega^2 - 2I\{s^2\omega^2\}/3$$

$$T^{10} = \omega s^2\omega^2 - \omega^2 s^2\omega$$

and $\{s^2\}$, $\{\omega^2\}$, $\{s^3\}$, $\{\omega^2 s\}$, $\{\omega^2 s^2\}$.

For the two dimensional case there are three tensors and two invariants,

$$T^0 = {}^1/_3 I - \tfrac{1}{2} I_2$$

$$T^1 = s$$

$$T^2 = s\omega - \omega s$$

and $\{s^2\}$ and $\{\omega^2\}$.

The significance of equation 2.34 is now seen to be that the Reynolds stresses are a known function of a finite number of known tensors and the same number of unknown scalars. The unknown scalars are in turn a function of a finite number of known invariants. For example, the task of formulating an effective viscosity hypothesis for two dimensional flows has been reduced to that of determining three scalars which may be functions of only two invariants. The influence of the functions may be demonstrated by writing in full the values of $\underline{a}$ given by equations 2.33 and 2.34 for the two dimensional flow measured by Champagne et al. (1970).

$$a_{11} = -1/6\, G^0 \quad . \quad . \quad . \quad -\tfrac{1}{2} G^2 \left(k/\varepsilon \frac{\partial \langle U_1 \rangle}{\partial x_2}\right)^2$$

$$a_{22} = -1/6\, G^0 \quad . \quad . \quad . \quad +\tfrac{1}{2} G^2 \left(k/\varepsilon \frac{\partial \langle U_1 \rangle}{\partial x_2}\right)^2$$

$$a_{33} = 1/3\, G^0$$

$$a_{12} = \tfrac{1}{2} G^1 k/\varepsilon \frac{\partial \langle U_1 \rangle}{\partial x_2}$$

$$a_{13} = a_{23} = 0$$

It is seen that G^1 does not influence the normal stresses and that G^0 and G^2 do not influence the shear stress. A finite value of G^2 causes a_{11} and a_{22} to differ and G^0 enables a_{33} to depart from zero. Clearly if G^0 and G^2 are set to zero, as is the case in an isotropic viscosity hypothesis, then the observed differences between the normal stresses cannot be predicted. This inherent deficiency in isotropic viscosity hypotheses suggests that they will provide an inadequate closure for more complex flows, where more than one component of Reynolds stress is required to close the mean momentum equations.

It has been shown that the general form of an effective viscosity hypothesis is equation 2.34 and that the values of G implied by the isotropic viscosity hypothesis are incorrect. As it has also been shown that in a homogeneous flow the Reynolds stresses are uniquely related to k, ε and $\frac{\partial \langle U_i \rangle}{\partial x_j}$, it is not surprising to find that for this situation the modelled Reynolds stress equations reduce to a relation, albeit implicit, between these quantities. Thus, the unknown functions, G, may be deduced from the modelled Reynolds stress equation: this was done for the case of two dimensional flows. As we wish to apply the model to flows that are only nearly homogeneous, it is desirable

to approximate the transport terms in the modelled Reynolds stress equations. Rodi (1972) suggested the following approximation.

$$(\text{transport of } \langle u_i u_j \rangle) \simeq \frac{\langle u_i u_j \rangle}{k} \text{ (transport of k)} = \frac{\langle u_i u_j \rangle}{k} (P - \rho\varepsilon) \qquad (2.35)$$

Substituting equation 2.35 into the Reynolds stress equation of model III, equations 2.21 and 2.23, yields,

$$a = -g [b_1 s + b_2 (as + sa - 2I \{as\}/3) - b_3 (a\omega - \omega a)] \qquad (2.36)$$

where $b_1 = 8/15$

$b_2 = (5-9C_{\phi 2})/11$

$b_3 = (7C_{\phi 2} + 1)/11$

$g = (C_{\phi 1} + P/\rho\varepsilon - 1)^{-1}$

By exploiting the tensor properties of T, the values of G appropriate to equation 2.36 may be deduced and lead to the proposed effective viscosity hypothesis,

$$H = -2C_\mu [s + gb_3 (s\omega - \omega s) + gb_2 \{s^2\} (2I/3 - I_2)] \qquad (2.37)$$

where

$$C_\mu = \tfrac{1}{2} b_1 g (1 - 2\{\omega^2\} b_3^2 g^2 - 2/3\, b_2^2 g^2 \{s^2\})^{-1} \qquad (2.38)$$

The choice of G^1, and consequently C_μ, is of paramount importance as it dictates the predicted shear stress level. Figure 2.1 shows the variation of C_μ, given by equation 2.38, as a function of σ and Ω, where

$$\sigma \equiv (\tfrac{1}{2}\{s^2\})^{\frac{1}{2}}$$

and $$\Omega \equiv (-\tfrac{1}{2}\{\omega^2\})^{\frac{1}{2}}$$

This variation of C_μ may be compared with previous suggestions indicated below.

Model I	C_μ = constant
Rodi (1972)	$C_\mu = C_\mu\ (P/\varepsilon)$
Bradshaw et al. (1967)	$C_\mu \alpha\ \sigma^{-1}$

(a $\alpha\ s/\sigma$ may be considered as a tensor invariant expression of Bradshaw et al.'s hypothesis, a_{12} = constant).

While the two latter expressions are in accord with the present proposal in that they predict a diminution of C_μ with increasing σ, none of the above expressions allows for any dependence of C_μ upon the rotation invariant, Ω. This omission is tantamount to assuming that the Reynolds stresses are materially indifferent; that is, to assuming that the Reynolds stresses are unaffected by solid body rotations. The use of this unfounded assumption is most likely responsible for the short-comings of these isotropic viscosity hypotheses in predicting flows with streamline curvature, see for example Bradshaw (1973).

On the basis of the above considerations, the effective viscosity hypothesis of model I may be assessed as follows:

(i) for nearly homogeneous flows the Reynolds stresses may be uniquely related to k, ε and velocity gradients: that is, a constitutive relation for $\langle u_i u_j \rangle$ is possible.

(ii) the form of the relation is incorrect; the assumption that the principal axes of stress and rate of strain are coincident is not borne out by experiments.

(iii) the lack of dependence of the dominant parameter, C_μ, upon the rate of strain and rotation invariants suggests that

the model will become more inaccurate as the flow departs from homogeneity and plane shear respectively.

2.4.2 The Dissipation Equation

The dissipation equations of all three models, equations 2.14 and 2.24, differ only in the turbulent transport term. Attention will be focussed here on the source term, S_ε , which is common to all models. This term is possibly the most important part of the turbulence models: assuming that the viscosity hypothesis or the modelled redistribution term provide an adequate description of the Reynolds stresses, then the predominant unknown in the kinetic energy equation is the dissipation. Thus, the source term not only affects the dissipation but it has an important, though indirect, effect upon the kinetic energy. As these two quantities, k and ε, serve to set the turbulent scales, an error in S_ε may be expected to produce considerable errors not only in k and ε but also in the predicted velocity field. Rodi (1972), who solved equations for k and for the quantity $k^{5/2}/\varepsilon$, examined the influence of changing the constants in the model on the spreading rate of four free shear flows: while a 5% increase in C_μ resulted in a 2.5% increase in the spreading rate, the same increase in the constants analogous with $C_{\varepsilon 1}$ and $C_{\varepsilon 2}$ resulted in 14% and -8% increases respectively. This observed sensitivity of the spreading rate to changes in S_ε confirms the important rôle played by the source term in governing the rate of change of the turbulent scales.

Before assessing the modelling of the source term, the mechanism of the dissipative process will be considered. Dissipation is defined as the negative source term in the kinetic energy equation associated with viscous processes, i.e.

$$\varepsilon \equiv \frac{\mu}{\rho} \left\langle \left(\frac{\partial u_i}{\partial x_i}\right)^2 \right\rangle \qquad (2.39)$$

If the Reynolds number of a flow were increased by decreasing μ , it would be found that, below some value of μ, ε remained constant. Thus, while equation 2.39 defines ε , it is not very useful conceptually. In order to obtain a more meaningful definition of ε the spectral energy equation is considered,

$$\frac{DE(\kappa)}{Dt} = P(\kappa) - \frac{\partial}{\partial x_i} F_{x_i}(\kappa) - \frac{\partial F_\kappa(\kappa)}{\partial \kappa} - \frac{\mu \kappa^2}{\rho} E(\kappa) \qquad (2.40)$$

where $E(\kappa)$ is the energy per unit wave number, κ, and $P(\kappa)$ is the production spectrum. The next two terms represent the gain of energy due to transport in position and wave number spaces respectively; the final term is the dissipation spectrum. Integration of equation 2.40 with respect to κ from zero to infinity gives the kinetic energy equation; from the definition of $E(\kappa)$,

$$k = \int_0^\infty E(\kappa)\, d\kappa \qquad (2.41)$$

$$\varepsilon = \int_0^\infty \frac{\mu \kappa^2}{\rho} E(\kappa)\, d\kappa \qquad (2.42)$$

The nature of the spectral energy equation is such that, at high Reynolds numbers, the dissipation term is only significant at high wave numbers whereas the other terms (except the transport in wave number space) are only significant at low wave numbers, see for example Tennekes and Lumley (1972). Consequently, wave numbers κ_1 and κ_2 $(\kappa_1 < \kappa_2)$ may be chosen such that

$$\int_{\kappa_1}^\infty E(\kappa)\, d\kappa < \gamma \qquad (2.43)$$

$$\int_{\kappa_1}^{\infty} P(\kappa) - \frac{\partial}{\partial x_i} F_{x_i}(\kappa) \, d\kappa < \gamma \tag{2.44}$$

and

$$\int_{o}^{\kappa_2} \frac{\mu}{\rho} \kappa^2 E(\kappa) \, d\kappa < \gamma \tag{2.45}$$

where γ is an arbitrarily small number. Thus, integrating the spectral energy equation between κ_1 and infinity yields

$$F_\kappa(\kappa_1) = \int_{\kappa_1}^{\infty} \kappa^2 \frac{\mu}{\rho} E(\kappa) \, d\kappa = \varepsilon \tag{2.46}$$

Hence, dissipation may be regarded as the flux of energy through wave number space in the region $\kappa_1 < \kappa < \kappa_2$.

The advantage of the conception of dissipation given by equation 2.46 over its definition, equation 2.39, is twofold: first, the objective of finding an expression for ε which is independent of μ is achieved and, secondly, $F_\kappa(\kappa_1)$ pertains to lower wave numbers than does ε. The significance of the second point is that changes in $F_\kappa(\kappa_1)$ may be attributed to changes in $E(\kappa)$ in the range $0<\kappa<\kappa_1$, the same range that is influenced by known quantities such as $<u_i u_j>$ and $\frac{\partial <U_j>}{\partial x_i}$. The physical implications of formulating a constitutive relation for the source of dissipation now become apparent: at a given point in space, changes in $F_\kappa(\kappa_1)$ must be assumed to be uniquely related to changes in $E(\kappa)$ which in turn must be uniquely related to known quantities.

It was stated above that changes in $F_\kappa(\kappa_1)$ could be attributed to changes in $E(\kappa)$ and so the first assumption appears reasonable. However, as the flux of energy in wave number space is not instantaneous, a change in $E(\kappa)$ will not have an immediate effect upon $F_\kappa(\kappa_1)$. The characteristic

time scale of the energy transfer is τ_t and consequently, as τ_t is not small compared with the time scale of the mean flow, changes in $F_\kappa(\kappa_1)$ at a point are due to changes in $E(\kappa)$ within a significant volume around the point. Thus, in order to satisfy the first assumption, the flow should be such that the behaviour of $E(\kappa)$ within a volume may be determined from its behaviour at a point: this implies either homogeneity or some form of similarity, that is

$$E(\kappa) = E^*(\kappa^*)\ k^{3/2}\ \tau_t \qquad (2.47)$$

where $\kappa^* \equiv \kappa(k^{\frac{1}{2}}\tau_t)$ is the normalised wave number and E^*, the normalised energy spectrum, is not a function of $\underline{x}$. The full transport equation for $E(\kappa)$ may not be written in self similar form because μ, appearing in the last term, is independent of the turbulent scales. However, as the low wave number part of the spectrum is independent of this term, the rest of the equation may take similar form providing that all the quantities are homogeneous when normalised by the scaling parameters which in turn must change at a constant rate. Thus, in these circumstances, the source term can be related to local quantities and indeed it follows directly that the dissipation equation must have the following form:

$$\rho \frac{D\varepsilon}{Dt} = \rho \frac{\varepsilon^2}{k} \times \text{const.} \qquad (2.48)$$

The condition of similarity is seen to be sufficient for a constitutive relation for S_ε to be possible; it only remains to determine the constant in equation 2.48. As the normalised Reynolds stresses and rates of strain are also constant their invariants may be used to complete the constitutive relation; further, as the conditions of similarity imply that the rates of strain determine the Reynolds stresses, only the rate of strain invariants need be considered. The dissipation equation

incorporated in the models presented in section 2.3 was developed and tested in two-dimensional, near-equilibrium boundary-layer and free shear flows where only one velocity gradient was significant. Thus, it is not surprising that the source term was modelled as a linear function of the only non-zero independent invariant of the rate of strain tensor. Since, in general, there are five independent invariants there is clearly scope for extending the modelling to more general situations. Bradshaw (1973) and Priddin (1975) have criticised the form of the dissipation equation in particular relation to flows with streamline curvature and such flows will be poorly represented by the present source term. In this context, the rotation invariant, $-\{\omega^2\}$, is of particular interest: in a two-dimensional shear flow without streamline curvature it is equal to the rate of strain invariant, $\{s^2\}$. Thus, the dimensionless parameter $(\{\omega^2\} + \{s^2\}) / (\{\omega^2\} - \{s^2\})$, which is unity for solid body rotation, zero for parallel shear flow and -1 for plane strain, may be introduced into the dissipation equation to account for streamline curvature without altering its performance in parallel shear flows.

Equation 2.48 is a direct consequence of the conditions for similarity: the significance of the preceding discussion is that similarity is not only a sufficient condition for a constitutive relation for S_ε to be possible but it is also a necessary condition. It must be conceded, therefore, that any modelled dissipation equation, closed by quantities pertaining to low wave numbers, has no foundation in non-similar flows. Few flows, and none of practical importance, are exactly similar; it is important, therefore, to assess the degree of non-similarity in various types of flow and to estimate the possible error in their calculation due to the inappropriate dissipation equation.

In shear flows, such as boundary layers, jets and wakes, the Reynolds stresses and velocity gradients normalised by the scaling

parameters are approximately homogeneous; the values of $\langle u_i u_j \rangle / k$ and $P/\rho\varepsilon$ vary slowly across the flow. In addition, for boundary layers and for free shear flows that exhibit profile similarity, the rate of change of the scaling parameters is constant. Thus, these flows display approximate similarity and can be expected to be fairly well represented by a turbulence model incorporating the dissipation equation.

For more complex flows, such as the flow behind a bluff body, neither of these properties may be assumed. In order to estimate the magnitude of the changes in the scaling parameters, consider the turbulent time scale, $\tau_t = k/\varepsilon$, in a plain jet with centre-line velocity U_o and half width $y_{\frac{1}{2}}$. Applying the effective viscosity hypothesis of model I to this situation τ_t may be deduced.

$$1 \simeq P/\rho\varepsilon = C_\mu \left(\frac{k}{\varepsilon} \frac{\partial \langle U_i \rangle}{\partial x_j}\right)^2 \simeq C_\mu \tau_t^2 \left(\tfrac{1}{2} U_o / y_{\frac{1}{2}}\right)^2 \qquad (2.49)$$

$$\text{thus;} \qquad \tau_t \simeq C_\mu^{-\frac{1}{2}} \left(2 \frac{y_{\frac{1}{2}}}{U_o}\right) \simeq 7 \; y_{\frac{1}{2}}/U_o \qquad (2.50)$$

A physical interpretation of equation 2.50 is that the time taken for energy to pass from the lowest to the highest wave numbers of the energy spectrum is equal to the time taken for a particle on the centre-line to pass seven half-widths downstream. This observation highlights the difficulty of relating the source of dissipation to local quantities.

The rate of change of τ_t may be estimated by taking the Lagrangian derivative of equation 2.50;

$$\frac{D\tau_t}{Dt} = \tfrac{1}{2} U_o \frac{d}{dx} \left(C_\mu^{-\frac{1}{2}} \; 2 \frac{y_{\frac{1}{2}}}{U_o}\right) = \left(C_\mu^{-\frac{1}{2}} + 1\right) \frac{dy_{\frac{1}{2}}}{dx} \simeq .42 \qquad (2.51)$$

(The value of $\frac{dy_{\frac{1}{2}}}{dx}$ is taken as .103, a value obtained by several workers, see Rodi (1972): the multiplier, $\frac{1}{2}$, indicates that the derivative is taken at the half width.) It is interesting to note that, assuming diffusion to be negligible and that production is equal to dissipation, the modelled dissipation equation gives,

$$\frac{D\tau_t}{Dt} = C_{\varepsilon 2} - C_{\varepsilon 1} = .45 \qquad (2.52)$$

As in general τ_t is large compared with the mean flow time scale and $D\tau_t/Dt$ is not small compared with unity, τ_t will not change at an approximately constant rate in rapidly changing flows such as those behind bluff bodies. Consequently it must be concluded that calculations of such flows will probably be subject to an error due to the inapplicability of the dissipation equation: the magnitude of the error is difficult to estimate but calculations, presented in Chapter 5, suggest that it is large.

The expected failure of the dissipation equation in rapidly changing flows is attributable to the impossibility of relating the source of dissipation to local quantities: neither $<u_i u_j>$ nor $\partial <U_i>/\partial x_j$ provide sufficient information about changes in the energy spectrum. An alternative approach is to solve a modelled equation for $E(\kappa)$ and to determine k and ε from equations 2.41 and 2.46. This approach is attractive because it introduces additional information and obviates the need for a dissipation equation: the unknown terms, $P(\kappa)$, $F_x(\kappa)$ and $F_\kappa(\kappa)$, may be expected to be well approximated by functions of the known quantities even in rapidly changing flows. The disadvantage is one of economy: the additional independent variable, κ, increases the dimensionality of the solution space by one and consequently the computational effort needed to solve the equations, although not prohibitive, is increased considerably.

2.4.3 The Redistribution Term

Equation 2.17 provides an exact expression for the pressure-velocity gradient correlation in terms of velocity alone. The appearance of a volume integral in this expression immediately calls in question the validity of modelling the term by local quantities. In order to assess the possible error in the modelling for inhomogeneous flows, the behaviour of $\phi_{ij,2}$ is considered as the flow departs from homogeneity. The two point correlation may be expressed as the sum of a symmetric and an anti-symmetric part,

$$< u_i(\underline{x}) \; u_m \; (\underline{x} + \underline{r}) > = R_{im} \; (\underline{x}, \underline{r}) + R'_{im} \; (\underline{x}, \underline{r}) \tag{2.53}$$

where $R_{im} \; (\underline{x}, \underline{r}) = R_{im} \; (\underline{x}, -\underline{r})$ (2.54)

and $R'_{im} \; (\underline{x}, \underline{r}) = -R'_{im} \; (\underline{x}, -\underline{r})$ (2.55)

Thus, expressing the averaged velocity gradient as a Taylor's series and neglecting third order terms, the second part of equation 2.17 may be written as,

$$\frac{2\pi}{\rho} \; \phi_{ij,2} = - \frac{\partial <U_1>}{\partial x_m} \int_{vol} \frac{\partial^2 R_{im}}{\partial r_j \partial r_\ell} \frac{d\underline{r}}{|r|}$$

$$+ \frac{\partial <U_1>}{\partial x_m} \frac{\partial}{\partial x_j} \int_{vol} \frac{\partial R'_{im}}{\partial r_1} \frac{d\underline{r}}{|r|} +$$

$$+ \frac{\partial}{\partial x_n} \left(\frac{\partial <U_1>}{\partial x_m}\right) \frac{\partial}{\partial x_j} \int_{vol} r_n \frac{\partial R_{im}}{\partial r_1} \frac{d\underline{r}}{|r|}$$

$$- \frac{\partial}{\partial x_n} \left(\frac{\partial <U_1>}{\partial x_m}\right) \int_{vol} r_n \frac{\partial^2 R'_{im}}{\partial r_j \partial r_1} \frac{d\underline{r}}{|r|} \tag{2.56}$$

For homogeneous flows, the derivatives of velocity gradients and of the volume integrals are zero as is the anti-symmetric part of the correlation, R'. Thus, while the first term is non-zero even in homogeneous turbulence, the remaining terms are each products of two quantities, both of which are zero for homogeneous flows: that is, all the second order terms are identically zero. (Rotta (1951) came to the same conclusion but assumed R' to be zero). The significance of this finding is that the first term, which is essentially a local quantity, may be expected to represent $\phi_{ij,2}$ even as the flow departs from homogeneity: however, near walls, where the surface integral cannot be neglected and where high derivatives of the mean velocity are significant, this may not be the case. Thus, in spite of the volume integral, it is reasonable to assume that $\phi_{ij,2}$ can be related to local quantities. The nature of $\phi_{ij,1}$ is less well understood but, as it pertains to smaller length scales than does $\phi_{ij,2}$, it can also be expected to be locally determined.

The specific form of $\phi_{ij,2}$ employed in model III, equation 2.21, is a direct result of assuming the first volume integral in equation 2.56 to be linearly proportional to Reynolds stresses. The same result was obtained by Naot et al. (1973) who assumed a function for the two point correlation. As the modelling of this term appears to be soundly based both mathematically and physically there is little point in considering more complex forms until the present model is found to be deficient. The expression for $\phi_{ij,2}$ used by model II, equation 2.19, which may be regarded as a truncated form of equation 2.21, has the advantage of simplicity and consequently economy. The resulting loss of accuracy may be estimated from the calculations presented in Chapter 5.

The first part of the redistribution term is considered in conjunction with the anisotropic part of dissipation. Both terms, if finite, have the effect of redistributing Reynolds stresses even in the absence of mean

rates of strain. Launder et al. followed Rotta (1951) in suggesting a modelled form of $\phi_{ij,1}$ and assumed the dissipation to be isotropic. The latter contention is supported by Lumley (1970) who argued that the anisotropic part of the dissipation tensor decreases as the square root of Reynolds number. Ribeiro (1975), on the other hand, by a multi-linear modelling of the two point joint probability distribution concluded that $\phi_{ij,1}$ is zero and that the dissipation is significantly anisotropic. Measurements of dissipation by Townsend (1954) and Uberoi (1957), though difficult to perform, support Ribeiro's thesis.

As far as forming a closure is concerned, the source of the redistributive effect is immaterial. Measurements of the decay of anisotropic grid turbulence could serve to quantify this effect but the data of Uberoi (1957), Uberoi (1963) and Tucker and Reynolds (1968) present a confused picture, there being little agreement between the three similar investigations. This being the case, the physical basis of the modelled term must remain unsatisfactory until the experimental and theoretical tools that are applied to small length scales become more convincing.

2.4.4 The Turbulent Transport Terms

The remaining terms represent turbulent transport and are all modelled as simple gradient diffusion. As turbulent transport is zero in homogeneous flows, its modelling may be expected to have a minor influence on the prediction of the gross features of an inhomogeneous flow. This contention is supported by Rodi (1972) who found that a 5% decrease in the diffusive constants resulted in only a 0.4% increase in the spreading rates of free shear flows. There are, however, flows in which the diffusion of Reynolds stresses is important: Launder et al. (1975) predicted the asymmetric channel flow of Hanjalic and Launder (1972) using models II and III. The prediction of model III are very close to the data while those of model II, although reasonable, are less accurate. Thus, simple gradient

diffusion provides an adequate representation of the turbulent transport which is the predominant feature of this flow. It is to be expected, therefore, that the models will not be found lacking due to the closure of the turbulent transport terms.

2.5 Summary

This chapter has been concerned with presenting and assessing methods of determining the Reynolds stresses in order to close the mean momentum equations. The three turbulence models used in the calculations were a mean flow closure, model I (equations 2.9, 2.11, 2.13 and 2.14) and two Reynolds stress closures, models II and III (equations 2.19, 2.21, 2.23 and 2.24). The wall functions presented in sub-section 2.3.3 and the values of the constants given in table I complete these closures.

A consideration of the mean closure approach revealed that the accuracy of the models depends upon the satisfaction of the three conditions enumerated in sub-section 2.2.3. The three models were examined in light of these considerations and the isotropic viscosity hypothesis and the dissipation equations were found to be particularly suspect. While an effective viscosity approach is valid in nearly homogeneous flows, the isotropic viscosity hypothesis fails to reflect experimental observations. An improved effective viscosity hypothesis was proposed (equations 2.37 and 2.38) which has the advantages of providing a realistic model of the whole of the Reynolds stress tensor and accounting for the effects of streamline curvature. The form of the dissipation equation was found to be appropriate to similar flows only. The lack of dependence of the source of dissipation on the rotation invariant may also account for the poor behaviour of the models in similar flows with significant streamline curvature. For non-similar flows it was concluded that the dissipation is without physical foundation and that considerable inaccuracies may be

incurred. A model based on the spectral energy equation was suggested as a possible means of overcoming this defect.

CHAPTER 3

COMBUSTION MODELLING

3.1 Introductory Remarks

The previous chapter was concerned with devising methods for describing an inert isothermal flow field: the principal aim was to determine the average velocity, $< U_i >$. We are concerned here with determining not only $<U_i>$ but also the averaged values of chemical and thermodynamic quantities which characterise a turbulent reacting flow: the determination of the temperature, $<T>$, the density, $<\rho>$, and the mass fraction of chemical species, $<m_\alpha>$, forms the principal objective of combustion modelling.

A practical combustion system may contain many complexities: the fuel may take the form of liquid droplets or solid particles and the reaction may proceed through literally hundreds of radicals; soot formation and significant heat transfer by radiation are common. Even if the flow were laminar it would be difficult, therefore, to formulate a closed set of equations to describe the flow; the reaction rates in particular are subject to large uncertainties. As a first step to understanding such complex systems, the restricted case of single phase, gaseous,adiabatic flows in which the Reynolds number is high and the Mach number is low is considered here. Bluff body stabilised flames, furnace flames and the flow in gas turbine combustion chambers are, to varying degrees of approximation, encompassed by these restrictions. In some circumstances the gross features of such turbulent flames are found to be independent of the detailed chemistry involved, see for example Spalding (1975). There is reason to believe, therefore, that a theory of turbulent combustion, based upon instantaneous equations which contain some uncertainties, may nevertheless be successful.

The difference between a turbulent reacting flow and an inert isothermal flow may be attributed to two agencies; the effect of the reaction on the turbulence and the effect of the turbulence on the reaction. The former is due to changes in the viscosity and more especially in the density due to the reaction: this aspect of the problem has been considered by Favre (1969), Bilger (1975) and Bray (1973 and 1974). In section 3.4 the influence of density variations is considered, employing the approach advocated by Favre and Bilger. The second effect, that of the turbulence on the reaction, is of prime concern here and presents the most serious obstacle to formulating a closed set of averaged equations which describe the flow. In the next section, the probability approach, which has been applied to the Navier-Stokes equations by Lundgren (1967) and others, is applied to the equations of turbulent reacting flows. The resultant theory provides a useful mathematical and conceptual framework on which an understanding of the mechanisms involved in turbulent combustion can be built. Further insight is gained by applying the theory to idealised situations, for which solutions of the equations are presented. It is appropriate to mention that since Lundgren's (1967) work, several other authors, notably Dopazo and O'Brien (1973), have exploited the potential advantages of this and allied approaches to turbulent reacting flows: a recent review of such works is provided by Murthy (1974). Consequently, the theory developed in section 3.2, although independent of these works, is not entirely novel: however, the level of closure chosen in sub-section 3.2.2 distinguishes the present work. In section 3.3, where the present theory is compared with combustion models currently in use, the physical foundations of these models are examined.

In the context of the prediction of bluff body stabilised flames, the theory of section 3.2 offers the potential advantage over existing models of obviating the need to assume very rapid reactions. However, as the

application of the theory to idealised situations showed that its quantitative performance is suspect and as the incorporation of the proposed theory in a solution procedure for practical flow situations is beyond the scope of the present work, the assumption of rapid reactions was retained. Thus, the calculations of bluff body stabilised flames, reported in Chapter 5, were performed with a degenerate form of the theory incorporating the assumption of rapid reactions. Calculations were also made with the eddy-break-up model for comparison purposes and the details of the two models are given in section 3.5.

The principal findings of this chapter are summarised in section 3.6.

3.2 A Theory of Turbulent Combustion

In this section a theory of turbulent combustion is presented in which assumptions are made in order to produce the simplest set of equations that retain the essence of the problem. As some of these assumptions are unrealistic, they are best regarded as axioms: the contention that the resultant axiomatic theory reflects the physical situation is supported by the observation that the gross features of turbulent flames are often independent of their detail structure, Spalding, (1975). That is, a simple set of equations is considered and is expected to display the same gross behaviour as do the complex set of equations which represent the system in every detail.

A reacting system can be characterised by the mass fraction of each chemical species, the temperature and the pressure: an equation of state relates these quantities to the density. Both the mass fractions and the temperature are assumed to obey the transport equation

$$\frac{\partial \rho \phi_\alpha}{\partial t} + \frac{\partial}{\partial x_i} (\rho U_i \phi_\alpha) = \frac{\partial}{\partial x_i} (\Gamma \frac{\partial \phi_\alpha}{\partial x_i}) + S_\alpha(\underline{\phi}, P) \qquad (3.1)$$

The last term in equation 3.1 implies that the source of the scalar is not a function of the velocity field. This is always true when ϕ_α represents a mass fraction but, when ϕ_α represents temperature, kinetic heating must be negligible. The molecular transport of the scalars is assumed to be of the simple gradient diffusion type with equal coefficients. While such an assumption would undoubtedly lead to errors if a laminar flow were predicted with equation 3.1, the discussion of section 2.4.2 indicates that the details of molecular transport are irrelevant to the behaviour of a high Reynolds number flow.

The further assumption of low Mach number is made to remove the dependence of S_α and ρ upon fluctuations of pressure. Thus,

$$S_\alpha(\underline{\phi},P) = S_\alpha(\underline{\phi},\langle P\rangle) = S_\alpha(\underline{\phi}) \tag{3.2}$$

and $$\rho(\underline{\phi},P) = \rho(\underline{\phi},\langle P\rangle) = \rho(\underline{\phi}) \tag{3.3}$$

Providing the source terms and the equation of state are known, equations 2.1, 2.2, 3.1 and 3.3 form a closed set. An equation for $\langle\phi_\alpha\rangle$ may be derived from equation 3.1 by decomposing ϕ_α into its average and fluctuating values,

$$\phi_\alpha = \langle\phi_\alpha\rangle + \phi'_\alpha \tag{3.4}$$

There results,

$$\frac{\partial}{\partial t}\langle\rho\rangle\langle\phi_\alpha\rangle + \frac{\partial}{\partial x_i}\langle\rho U_i\rangle\langle\phi_\alpha\rangle = \frac{\partial}{\partial x_i}\left(\Gamma\frac{\partial\langle\phi_\alpha\rangle}{\partial x_i}\right) - \frac{\partial}{\partial x_i}\langle[\rho U_i]\,\phi'_\alpha\rangle$$

$$- \frac{\partial}{\partial t}\langle\rho'\phi'_\alpha\rangle + \langle S_\alpha(\underline{\phi})\rangle \tag{3.5}$$

(where $[\rho U_i] \equiv \rho U_i - \langle\rho U_i\rangle$)

The principal unknown term in equation 3.5 is the average reaction rate, $<S_\alpha(\phi)>$; the average density, $<\rho(\underline{\phi})>$, is also unknown. As these averaged quantities may be highly non-linear it is incorrect to assume that

$$<S_\alpha(\underline{\phi})> = S_\alpha(<\underline{\phi}>) \tag{3.6}$$

Indeed, it will be shown below that in some circumstances $<S_\alpha(\underline{\phi})>$ is independent of S_α. The main objective of the theory is to overcome the difficulty of modelling such non-linear terms and to this end the probability distribution of $\underline{\phi}$ is considered.

3.2.1 The Joint Probability Distribution Equation

First, probability is mathematically defined and some useful consequences of the definition are shown. The instantaneous probability of ϕ_α, $p(\phi_\alpha)$, is defined such that the probability of ϕ_α being in the range

$$\tilde{\phi}_\alpha < \phi_\alpha < \tilde{\phi}_\alpha + d\tilde{\phi}_\alpha \text{ is } p(\tilde{\phi}_\alpha)\ d\tilde{\phi}_\alpha.$$

Clearly, the instantaneous value of $p(\tilde{\phi}_\alpha)d\tilde{\phi}_\alpha$ is either zero or unity and so $p(\tilde{\phi}_\alpha)$ may be identified as the Dirac delta function:

$$p(\tilde{\phi}_\alpha) \equiv \delta(\tilde{\phi}_\alpha - \phi_\alpha) \tag{3.7}$$

where $\tilde{\phi}_\alpha$ is the new independent variable representing probability space. From this definition it follows that for any good function, h,

$$\int_{-\infty}^{\infty} h(\tilde{\phi}_\alpha)\ p(\tilde{\phi}_\alpha)\ d\tilde{\phi}_\alpha = h(\phi_\alpha) \tag{3.8}$$

and consequently,

$$<h(\phi_\alpha)> = \int_{-\infty}^{\infty} h(\tilde{\phi}_\alpha) < p(\tilde{\phi}_\alpha)> d\tilde{\phi} \tag{3.9}$$

The joint probability of a set of n scalars, $\underline{\phi} \equiv (\phi_1, \phi_2 \ldots \phi_n)$, is defined as the product of the individual proabilities of each scalar.

$$p(\tilde{\underline{\phi}}) = \prod_{\alpha=1}^{n} p(\tilde{\phi}_\alpha) = \prod_{\alpha=1}^{n} \delta \quad (\tilde{\phi}_\alpha - \phi_\alpha) \tag{3.10}$$

Again, from the definition of $p(\tilde{\underline{\phi}})$ it follows that

$$\int_{-\infty}^{\infty} h(\tilde{\underline{\phi}}) \; p(\tilde{\underline{\phi}}) \; d\underline{\phi} = h(\underline{\phi}) \tag{3.11}$$

and consequently

$$\langle h \; (\underline{\phi}) \rangle = \int_{-\infty}^{\infty} h(\tilde{\underline{\phi}}) < p(\tilde{\underline{\phi}}) > \; d\tilde{\underline{\phi}} \tag{3.12}$$

Thus, it is seen that with a knowledge of $<p(\tilde{\underline{\phi}})>$ the average reaction rate, $<S_\alpha(\underline{\phi})>$, can be determined from equation 3.12.

Two further results which will be used extensively below are

$$\int_{-\infty}^{\infty} \tilde{\phi}_\alpha^m \; \frac{\partial^n}{\partial \tilde{\phi}_\alpha^n} [p(\tilde{\phi}_\alpha) \; h(\tilde{\phi}_\alpha)] \; d\tilde{\phi}_\alpha = 0, \quad m < n$$

$$= (-1)^n \; m!/(m-n)! \int_{-\infty}^{\infty} \tilde{\phi}_\alpha^{(m-n)} \; p(\tilde{\phi}_\alpha) h(\tilde{\phi}_\alpha) \; d\tilde{\phi}_\alpha, \; n \leq m \tag{3.13}$$

and

$$\frac{\partial p}{\partial t} (\tilde{\phi}_\alpha) = \frac{\partial}{\partial t} \delta(\tilde{\phi}_\alpha - \phi_\alpha) = \frac{\partial \phi_\alpha}{\partial t} \frac{\partial \quad (\tilde{\phi} \; - \phi_\alpha)}{\partial \phi_\alpha} = - \frac{\partial \phi_\alpha}{\partial t} \frac{\partial \delta(\tilde{\phi}_\alpha - \phi_\alpha)}{\partial \tilde{\phi}_\alpha} = - \frac{\partial \phi_\alpha}{\partial t} \frac{\partial p(\tilde{\phi}_\alpha)}{\partial \tilde{\phi}_\alpha} \tag{3.14}$$

From equation 3.14 it is evident that a transport equation for $p(\tilde{\phi}_\alpha)$ may be deduced by multiplying equation 3.1 by $- \frac{\partial p(\tilde{\phi}_\alpha)}{\partial \tilde{\phi}_\alpha}$. Further, by multiplying the resulting equation by $\prod_{\substack{\gamma=1 \\ \gamma \neq \alpha}}^{n} p(\tilde{\phi}_\gamma)$ and summing for all α, a

transport equation for $p(\tilde{\underline{\phi}})$ is obtained, namely

$$\frac{\partial}{\partial t}[\rho p(\tilde{\underline{\phi}})] + \frac{\partial}{\partial x_i}\rho U_i p(\tilde{\underline{\phi}}) = -\sum_{\alpha=1}^{n} \frac{\partial p}{\partial \tilde{\phi}_\alpha}(\tilde{\underline{\phi}})\left[\frac{\partial}{\partial x_i}\Gamma\frac{\partial \phi_\alpha}{\partial x_i} + S_\alpha(\underline{\phi})\right] \qquad (3.15)$$

After manipulation, equation 3.15 may be averaged to give the joint probability distribution equation

$$\rho(\tilde{\underline{\phi}})\frac{\partial}{\partial t}<p(\tilde{\underline{\phi}})> + \rho(\tilde{\underline{\phi}})\frac{\partial}{\partial x_i}<U_i>\ p(\tilde{\underline{\phi}})> \quad =$$

$$\frac{\partial}{\partial x_i}\{\Gamma\frac{\partial}{\partial x_i}<p(\tilde{\underline{\phi}})> - \rho(\tilde{\underline{\phi}})<p(\tilde{\underline{\phi}})\ u_i>\}$$

(A) (B)

$$-\sum_{\alpha=1}^{n}\frac{\partial}{\partial \tilde{\phi}_\alpha}\{<p(\tilde{\underline{\phi}})>\ S_\alpha(\tilde{\underline{\phi}}) + \sum_{\beta=1}^{n}\frac{\partial}{\partial \tilde{\phi}_\beta}<p(\tilde{\underline{\phi}})\Gamma\frac{\partial \phi_\alpha}{\partial x_i}\ \frac{\partial \phi_\beta}{\partial x_i}>\} \qquad (3.16)$$

(C) (D)

The terminology applied to the various terms is as follows,

A - transport in $\underline{x}$-space by laminar diffusion

B - transport in $\underline{x}$-space by turbulent convection

C - transport in $\tilde{\underline{\phi}}$-space due to the source terms

D - transport in $\tilde{\underline{\phi}}$-space by molecular action

The laminar diffusion term, which is negligible at high Reynolds number, contains no unknown correlations. The turbulent convection term contains the unknown correlation $<p(\tilde{\underline{\phi}})\ u_i>$ which represents a flux of $<p(\tilde{\underline{\phi}})>$ in $\underline{x}$-space. While this correlation is unfamiliar, it is directly analogous to more common terms like $<\phi'\ u_i>$ and its behaviour is expected to be similar. The most notable feature of equation 3.16 is that the term in

S_α contains no unknowns, and so there are no problems of modelling as was the case with $<S_\alpha(\underline{\tilde{\phi}})>$. The term $<p(\underline{\tilde{\phi}})> S_\alpha(\underline{\tilde{\phi}})$ represents a flux of $<p(\underline{\tilde{\phi}})>$ in probability space due to the source.

The final term in equation 3.16 poses the greatest problem to understanding as it pertains to the microscale. However, its rôle may be demonstrated by integrating its moments to form a source term in equations for $<\phi_\gamma>$ and $<\phi'^2_\gamma>$,

$$\frac{\partial<\phi_\gamma>}{\partial t} = \ldots\ldots 0 \qquad (3.17)$$

$$\frac{\partial<\phi'^2_\gamma>}{\partial t} = \ldots\ldots - 2\int_{\infty}^{\infty} < p(\underline{\tilde{\phi}})\ \Gamma(\frac{\partial \phi_\gamma}{\partial x_i})^2 > d\underline{\tilde{\phi}}$$

$$= \ldots\ldots - 2\Gamma< (\frac{\partial \phi_\gamma}{\partial x_i})^2 > \qquad (3.18)$$

Equation 3.17 indicates that the term does not influence the value of $<\phi_\gamma>$: the same conclusion may be reached without reference to a particular diffusion hypothesis. As the source term in equation 3.18 is identically non-positive, the effect of molecular action is to reduce the value of $<\phi'^2_\gamma>$. While this result does depend upon the specific form of molecular diffusion, the irreversibility of dissipative processes guarantees that the source is non-positive. Unfortunately, a satisfactory closure approximation has not been found for this term. However, the probability distribution of a single scalar is more amenable to analysis and is examined further.

3.2.2 The Single Probability Distribution Equation

Clearly, the transport equation for the probability distribution of a single scalar is given by equation 3.16 with n=1. As the potentially

non-linear density is seen to produce no problems and the treatment given below is essentially demonstrative, for simplicity, the density will be assumed constant and equal to unity: the laminar diffusion term, which makes no contribution at high Reynolds number, is also omitted. Thus, the transport equation for $< p(\tilde{\phi})>$ reads,

$$\frac{D}{Dt}<p(\tilde{\phi})> = - \frac{\partial}{\partial x_i} <p(\tilde{\phi})\ u_i> - \frac{\partial}{\partial \tilde{\phi}} \{<p(\tilde{\phi})> S(\tilde{\phi}) + \frac{\partial}{\partial \tilde{\phi}} <p(\phi)\ \Gamma(\frac{\partial \phi}{\partial x_i})^2 >\} \quad (3.19)$$

As was mentioned above, the probability velocity correlation is similar to terms such as $<\phi' u_i>$. Consequently, it can be modelled in an analogous manner as

$$<p(\tilde{\phi})\ u_i> = - C_1\ k^2/\varepsilon\ \frac{\partial}{\partial x_i} < p(\tilde{\phi})> \quad (3.20)$$

The molecular action term contains the expression

$$G(\tilde{\phi}) \equiv <p(\tilde{\phi})\Gamma\ (\frac{\partial \phi}{\partial x_i})^2 >$$

which is the correlation of two quantities: $\Gamma\ (\frac{\partial \phi}{\partial x_i})^2$ pertains to small fluctuations on the microscale while $p(\tilde{\phi})$ is dominated by large fluctuations associated with the macroscale. It appears, therefore, that the two quantities are uncorrelated. Thus,

$$G(\tilde{\phi}) = < p(\tilde{\phi}) > <\Gamma(\frac{\partial \phi}{\partial x_i})^2 > \quad (3.21)$$

And, following the conventional modelling of $<\Gamma(\frac{\partial \phi}{\partial x_i})^2 >$,

$$G(\tilde{\phi}) = C_2 <p(\tilde{\phi})> \frac{\varepsilon}{k} < \phi'^2 > \quad (3.22)$$

The modelled form of equation 3.19 then becomes

$$\frac{D}{Dt}\langle p(\tilde{\phi})\rangle = \frac{\partial}{\partial x_i} C_1 k^2/\varepsilon \frac{\partial}{\partial x_i}\langle p(\tilde{\phi})\rangle$$

$$- \frac{\partial}{\partial \tilde{\phi}} \{\langle p(\tilde{\phi})\rangle S(\tilde{\phi}) + C_2 \frac{\varepsilon}{k} \langle \phi'^2 \rangle \frac{\partial}{\partial \tilde{\phi}} \langle p(\tilde{\phi})\rangle\} \qquad (3.23)$$

This equation will be examined for inert flows ($S(\tilde{\phi}) = 0$). Integrating the equation to form equations for $\langle \phi \rangle$ and $\langle \phi'^2 \rangle$ produces

$$\frac{D}{Dt}\langle \phi \rangle = \frac{\partial}{\partial x_i} C_1 k^2/\varepsilon \frac{\partial \langle \phi \rangle}{\partial x_i} \qquad (3.24)$$

$$\frac{D}{Dt}\langle \phi'^2 \rangle = \frac{\partial}{\partial x_i} C_1 k^2/\varepsilon \frac{\partial}{\partial x_i}\langle \phi'^2 \rangle + 2C_1 \frac{k^2}{\varepsilon} \left(\frac{\partial}{\partial x_i}\langle \phi \rangle\right)^2 - 2C_2 \frac{\varepsilon}{k}\langle \phi'^2 \rangle \qquad (3.25)$$

These equations are seen to be identical to those used by, for example, Lockwood and Naguib (1975a) and, for consistency with these authors, the constants C_1 and C_2 take values of 0.127 and 0.925 respectively. While the consistency of equation 3.23 with previous models is encouraging, it provides no check on the behaviour of the equation in probability space and hence the modelling of G in particular is not validated. To this end, the decay of the probability distribution in a stagnant, homogeneous flow is considered. Equation 3.23 reduces to

$$\frac{\partial}{\partial t}\langle p(\tilde{\phi})\rangle = - C_2 \frac{\varepsilon}{k} \langle \phi'^2 \rangle \frac{\partial^2}{\partial \tilde{\phi}^2}\langle p(\tilde{\phi})\rangle \qquad (3.26)$$

which has a solution

$$\langle p(\tilde{\phi}, t)\rangle = (\hat{\phi}\sqrt{2\pi})^{-1} \exp\left\{-\tfrac{1}{2}\left(\frac{\tilde{\phi} - \langle \phi \rangle}{\hat{\phi}}\right)^2\right\} \qquad (3.27)$$

where $\hat{\phi}(t) \equiv \langle \phi'^2 \rangle^{\frac{1}{2}} = \hat{\phi}_o \exp\{- C_2 \frac{\varepsilon}{k} (t - t_o)\}$ (3.28)

That is, for this situation, an initially Gaussian probability distribution remains Gaussian while its standard deviation decreases exponentially at a rate proportional to the turbulent time scale. Similarly, a steady, stagnant flow in which $<\phi>$ varies linearly with $\underline{x}$ yields the following solution of equation 3.23:

$$<p(\tilde{\phi},\underline{x})> = (\hat{\phi}\sqrt{2\pi})^{-1} \exp\{-\tfrac{1}{2}(\frac{\tilde{\phi}-<\phi>}{\hat{\phi}})^2\} \qquad (3.29)$$

where $$\hat{\phi} = (\frac{C_2}{C_1}\frac{\partial<\phi>}{\partial x_i}\frac{\partial<\phi>}{\partial x_i})^{\frac{1}{2}} k^{3/2}/\varepsilon \qquad (3.30)$$

Again, the probability distribution is Gaussian with a standard deviation proportional to the gradient of $<\phi>$ multiplied by the turbulent length scale. These solutions of the modelled probability distribution equation are in accord with intuition and thus support the modelling assumptions. However, in spite of the good performance of the model for the situations considered above, it will be shown that modelling G by equation 3.22 is not appropriate to more general situations.

Consider the probability distribution shown on figure 3.1. The main features of this distribution may be realised in turbulent reacting flows; the distribution is bounded at $\tilde{\phi}_1$ and $\tilde{\phi}_4$ where there is a delta function. In the region $\tilde{\phi}_1 < \tilde{\phi} < \tilde{\phi}_4$, $<p(\tilde{\phi})>$ may not be zero because this would imply infinite gradients of ϕ; however, a region $\tilde{\phi}_2 < \tilde{\phi} < \tilde{\phi}_3$ may occur in which $<p(\tilde{\phi})>$ is arbitrarily small. From consideration of the definition of G, for the general probability distribution outlined above, the following properties of G may be deduced.

(i) $G \geqslant 0$

(ii) $G = 0$ for $\tilde{\phi} \leqslant \tilde{\phi}_1$ and $\tilde{\phi} \geqslant \tilde{\phi}_4$

(iii) $\frac{\partial^2 G}{\partial \tilde{\phi}^2} \leqslant 0$ for $\tilde{\phi}_2 < \tilde{\phi} < \tilde{\phi}_3$

The third condition is required because, if $\frac{\partial^2 G}{\partial \tilde{\phi}^2}$ were positive, negative values of $\langle p(\tilde{\phi}) \rangle$ would occur. Further, by integrating equation 3.19 twice with respect to $\tilde{\phi}$ it is seen, from the other terms, that

(iv) G is finite and continuous.

It is apparent that, for the probability distribution of figure 3.1, the model for G given by equation 3.22 violates all the conditions except for the first. These four conditions are sufficient to suggest a modelled form of G: condition (iv) requires that G be an integral function of the potentially discontinuous and infinite $\langle p(\tilde{\phi}) \rangle$ while condition (ii) suggests the form

$$G(\tilde{\phi}) = C_2 \frac{\varepsilon}{k} \hat{\phi} H(\tilde{\phi}) \tag{3.31}$$

where $\hat{\phi} = \langle \phi'^2 \rangle^{\frac{1}{2}}$,

$$H(\tilde{\phi}) = \int_{-\infty}^{\tilde{\phi}} g\left(\frac{\tilde{\phi}-\phi^*}{\hat{\phi}}\right) \langle p(\phi^*) \rangle \, d\phi^* \int_{\tilde{\phi}}^{\infty} g\left(\frac{\phi^*-\tilde{\phi}}{\hat{\phi}}\right) \langle p(\phi^*) \rangle \, d\phi^* \tag{3.32}$$

and g is any continuous function with $g(0) = 0$.
Conditions (i) and (iii) require that g be non-negative and that its second derivative be non-positive. Thus, equations 3.31 and 3.32 form a model for G which is consistent with the four conditions imposed by the exact expression. However, a function g cannot be chosen that results in the desired Gaussian behaviour for the idealised flows considered above. It must be concluded, therefore, that the modelling of G is not completely satisfactory although predictions based on it can be expected to be qualitatively correct. In the absence of experimental data, the choice of

$$g(y) = \ln (1+y) \tag{3.33}$$

used in subsequent calculations was based on an intuitive appraisal of the shape of $<p(\tilde{\phi})>$ for various functions for g. The more obvious choice of $g(y) = y$ results in unrealistic multi-model distributions. With the revised closure approximation for G the modelled equation becomes

$$\frac{D}{Dt}<p(\tilde{\phi})> = \frac{\partial}{\partial x_i} C_1 k^2/\varepsilon \frac{\partial}{\partial x_i}<p(\tilde{\phi})>$$

$$- \frac{\partial}{\partial \tilde{\phi}} \{S(\tilde{\phi})<p(\tilde{\phi})> + C_2 \frac{\varepsilon}{k} \hat{\phi} \frac{\partial H}{\partial \tilde{\phi}}(\tilde{\phi})\} \qquad (3.34)$$

The equation for $<\phi'^2>$ which results from integrating this equation is no longer consistent with that employed by Lockwood and Naguib and so C_2 may not be evaluated directly. The value 4.5 used in subsequent calculations does, however, predict approximately the same values of $<\phi'^2>$.

3.2.3 Applications of the Theory

In order to study the probability distributions predicted by the modelled equation, a steady, homogeneous, isotropic flow was considered in which equal quantities of fluid with values of $\tilde{\phi}_1$ and $\tilde{\phi}_2$ were homogeneously introduced and an equal amount of the resulting mixture was withdrawn, the residence time being τ_R. The form of equation 3.34 appropriate to the situation is

$$\tfrac{1}{2}[\delta(\tilde{\phi}-\tilde{\phi}_1) + \delta(\tilde{\phi}-\tilde{\phi}_2)] - <p(\tilde{\phi})> = \frac{\tau_R}{\tau_t} \hat{\phi} C_2 \frac{\partial^2 H(\tilde{\phi})}{\partial \tilde{\phi}^2} \qquad (3.35)$$

The time scale ratio, τ_R/τ_t, ($\tau_t \equiv k/\varepsilon$) is of great physical significance for it determines the degree of mixing. Equation 3.35 was solved numerically for various values of the time scale ratio and the resulting distributions of $<p(\tilde{\phi})>$ are shown on Figure 3.2. It is seen that two

limiting cases exist.

$$\text{as} \quad \tau_R/\tau_t \to 0, \quad \langle p(\tilde{\phi})\rangle \to \tfrac{1}{2}\,[\delta(\tilde{\phi}-\tilde{\phi}_1) + \delta(\tilde{\phi}-\tilde{\phi}_2)] \tag{3.36}$$

$$\text{as} \quad \tau_R/\tau_t \to \infty\ , \quad \langle p(\tilde{\phi})\rangle \to \delta(\tilde{\phi}-\langle\phi\rangle) \tag{3.37}$$

These two results are an inevitable consequence of the restrictions imposed on the modelling of G. The real test of the modelling is the predicted values of $\langle p(\tilde{\phi})\rangle$ for intermediate values of the time scale ratio. In the absence of experimental data the predictions can only be appraised intuitively: there is no feature of the predictions that is contrary to expectations.

The behaviour of the modelled equation with a finite source term is studied by considering a similar situation to that described above. In this case, a one step reaction takes place between homogeneously premixed fuel and oxidant to form a single product. ϕ represents the mass fraction of product which lies in the range $\tilde{\phi}_1 \leq \phi \leq \tilde{\phi}_2$. The reactants are added to the system at $\tilde{\phi}=\tilde{\phi}_1$ and the resultant mixture is withdrawn. For this situation equation 3.34 becomes

$$\frac{1}{\tau_R}\,[\delta(\tilde{\phi}-\tilde{\phi}_1) - \langle p(\tilde{\phi})\rangle] = \frac{\partial}{\partial\tilde{\phi}}\,[\langle p(\tilde{\phi})\rangle\, S(\tilde{\phi}) + \frac{C_2\hat{\phi}}{\tau_t}\,\frac{\partial H}{\partial\tilde{\phi}}\,(\tilde{\phi})] \tag{3.38}$$

The specific form of the reaction rate will not be defined at this point except to set it to zero at $\tilde{\phi}=\tilde{\phi}_1$ and $\tilde{\phi}=\tilde{\phi}_2$ and positive for $\tilde{\phi}_1 < \tilde{\phi} < \tilde{\phi}_2$. $\tilde{\phi}=\tilde{\phi}_2$ corresponds to a situation where all the reactants have reacted, hence $S(\tilde{\phi}_2) = 0$: at $\tilde{\phi}=\tilde{\phi}_1$ where there are pure reactants, in a typical premixed flame, the temperature is too low for reaction to take place, thus $S(\tilde{\phi}_1)=0$. The time scale of the reaction, τ_k, is taken as the inverse of the maximum value of $S(\tilde{\phi})$, and the normalised reaction rate,

$S^*(\tilde{\phi})$, is given by

$$S^*(\tilde{\phi}) = \tau_k S(\tilde{\phi}) \tag{3.39}$$

Equation 41 may now be written in the form

$$\delta(\tilde{\phi}-\tilde{\phi}_1) - \langle p(\tilde{\phi})\rangle = \frac{\partial}{\partial\tilde{\phi}}\left[\frac{\tau_R}{\tau_K}\langle p(\tilde{\phi})\rangle S^*(\tilde{\phi}) + C_2\hat{\phi}\ \frac{\tau_R}{\tau_t}\ \frac{\partial H(\tilde{\phi})}{\partial\tilde{\phi}}\right] \tag{3.40}$$

The averaged reaction rate may be obtained from equation 3.40 by multiplying by $\tilde{\phi}$ and integrating

$$\langle S(\phi)\rangle = (\langle\phi\rangle - \tilde{\phi}_1)/\tau_R \tag{3.41}$$

The form of the sdution of equation 3.40 will be demonstrated for the nine situations characterised by each of the time scale rations being either zero, finite or infinite. These solutions are more clearly demonstrated by taking the definite integral of equation 3.40:

$$\int_{\infty}^{\tilde{\phi}} \delta(\tilde{\phi}-\tilde{\phi}_1) - \langle p(\tilde{\phi})\rangle\, d\tilde{\phi} = \frac{\tau_R}{\tau_K}\langle p(\tilde{\phi})\rangle S^*(\tilde{\phi}) + \frac{\tau_R}{\tau_t}\ C_2\hat{\phi}\ \frac{\partial H(\tilde{\phi})}{\partial\tilde{\phi}} \tag{3.42}$$

Inspection of equation 3.42 reveals two important conclusions. First, a trivial solution, given by

$$\langle p(\tilde{\phi})\rangle = \delta(\tilde{\phi}-\tilde{\phi}_1)\ ;\ \langle\phi\rangle = \tilde{\phi}_1;\ \langle S(\phi)\rangle = 0\ , \tag{3.43}$$

exists regardless of the values of the time scale ratios. (For this solution, each term in equation 3.42 is zero). Secondly, a necessary condition for another solution to exist is that both time scale ratios be non-zero. If τ_R/τ_K is zero, $\langle S(\phi)\rangle$ is zero and hence equation 3.41 becomes the trivial solution. Physically, fluid at $\phi=\phi_1$ is introduced tending to decrease $\langle\phi\rangle$ as the mixing term cannot alter the value of $\langle\phi\rangle$ the result is a tendency toward the trivial solution. If τ_R/τ_t is

zero, the fluid introduced at $\tilde{\phi}=\tilde{\phi}_1$ has no way to pass to higher mass fractions since $<p(\tilde{\phi})>S^*(\tilde{\phi})$ at $\tilde{\phi}=\tilde{\phi}_1$ is zero. This observation highlights the importance of the process referred to as back-mixing whereby, hot combustion products mix with cold reactants, raising their temperature until reaction is possible. Thus, the five situations characterised by combinations of time scale ratios in which one or both is zero result in the trivial solution only.

The first situation of practical interest is that in which $\tau_R/\tau_t \rightarrow \infty$ which τ_R/τ_K remains finite. In order that the mixing term in equation 3.42 remains finite $\hat{\phi}$ must tend to zero. Thus, the probability distribution will tend to a single delta function which, clearly, is centred on $<\phi>$ i.e.

$$< p(\tilde{\phi})> \;=\; \delta(\tilde{\phi} - <\phi>) \tag{3.44}$$

The averaged reaction rate is given by

$$<S(\phi)> \;=\; \int_{\infty}^{\infty} S(\tilde{\phi}) \;\; <p(\tilde{\phi})> \, d\tilde{\phi} \;\; = \;\; S(<\phi>) \tag{3.45}$$

and hence, from equation 3.41

$$<\phi> \;=\; \tilde{\phi}_1 + S^* \, (<\phi>) \; \tau_R/\tau_K \tag{3.46}$$

It is seen that in this situation, which corresponds to a perfectly stirred reactor, equation 3.6 is valid, i.e.

$$<S(\phi)> \;=\; S(<\phi>)$$

It should also be noted that equation 3.46 may have one or more than one solution; one being the trivial solution. As an extension of this situation it is seen that as τ_R/τ_K tends to infinity also, in order to satisfy equation 3.46, $<\phi>$ must take a value such that $S^*(<\phi>)$ is close to zero. Thus, in the case where both time scale ratios are infinite

a solution is given by

$$<p(\tilde{\phi})> = \delta(\tilde{\phi}_2-\tilde{\phi}) \tag{3.47}$$

that is, all the reactants are converted into products.

The final case for which an analytic solution is presented is that in which τ_R/τ_K tends to infinity while τ_R/τ_t remains finite. It is for this situation that the eddy-break-up model of Mason and Spalding (1973) is intended. The form of the solution is again found by examining 3.42 and noting that the reaction rate term can remain finite only by $<p(\tilde{\phi})>$ being comprised of delta functions at $\tilde{\phi}_1$ and $\tilde{\phi}_2$:

$$<p(\tilde{\phi})> = a\,\delta(\tilde{\phi}-\tilde{\phi}_1) + (1-a)\,\delta(\tilde{\phi}-\tilde{\phi}_2) \tag{3.48}$$

Substituting $<\phi>$ given by equation 3.48 into equation 3.41 gives

$$<S(\phi)> = (1-a)\,(\tilde{\phi}_2-\tilde{\phi}_1)\,/\,\tau_R \tag{3.49}$$

Now, if equation 3.42, with $<p(\tilde{\phi})>$ given by equation 3.48, is evaluated at the limit as $\tilde{\phi}$ tends to $\tilde{\phi}_{1+}$ there results

$$(1-a) = \frac{\tau_R}{\tau_K} \lim_{\tilde{\phi}\to\tilde{\phi}_{1+}} <p(\tilde{\phi})>\, S^*(\tilde{\phi}) + C_2\,\frac{\tau_R}{\tau_t}\,\hat{\phi} \lim_{\tilde{\phi}\to\tilde{\phi}_{1+}} \frac{\partial H(\tilde{\phi})}{\partial\tilde{\phi}} \tag{3.50}$$

As the limit of the first term is zero, equations 3.49 and 3.50 may be combined to give

$$<S(\phi)> = 2\,C_2/\tau_t\;\hat{\phi}\,\hat{\phi}_{max} \lim_{\tilde{\phi}\to\tilde{\phi}_{1+}} \frac{\partial H(\tilde{\phi})}{\partial\tilde{\phi}} \tag{3.51}$$

where

$$\hat{\phi}_{max} = \tfrac{1}{2}\,(\tilde{\phi}_2-\tilde{\phi}_1) \tag{3.52}$$

is the maximum value that $\hat{\phi}$ may obtain. The notable result is that, as τ_R/τ_K tends to infinite, the averaged reaction rate remains finite and

is independent of both τ_R/τ_K and $S^*(\tilde{\phi})$. As is implied by the name of the eddy-break-up model, the reaction rate is directly proportional to the rate of back-mixing. Evaluating the limit of the differential, the averaged reaction rate is given by

$$< S(\phi) > = \tfrac{1}{2} C_2/\tau_t \quad \frac{\hat{\phi}^2}{\phi_{max}} \quad \ln(1 + \frac{2\,\hat{\phi}_{max}}{\hat{\phi}}) \tag{3.53}$$

Comparing this result with the eddy-break-up model

$$<S(\phi)> = C_{EBU}\ \hat{\phi}/\tau_t \tag{3.54}$$

a relation for the eddy-break-up "constant" is obtained;

$$C_{EBU} = \tfrac{1}{2} C_2 \quad \frac{\hat{\phi}}{\hat{\phi}_{max}} \quad \ln(1 + \frac{2\hat{\phi}_{max}}{\hat{\phi}}) \tag{3.55}$$

The variation of C_{EBU} with $\hat{\phi}/\hat{\phi}_{max}$ is shown on figure 3.3 and should be compared with the values of .53 and 1.0 used by Mason and Spalding (1973) and Khalil et al. (1975) respectively. It appears that C_{EBU} given by equation 3.55 is too large, however, the assumption of very fast chemistry in the flow situations of the above authors may not be completely valid. It may certainly be expected that near complete combustion the reaction rate will be very rapid but, at the cold end of the probability distribution the reaction rate will still be small. Thus, in this situation a delta function may be expected at $\phi=\phi_2$ but not at $\phi=\phi_1$. The effect of finite rate chemistry over a region of probability space is to decrease the averaged reaction rate and hence to make the effective eddy-break-up constant smaller than that predicted by equation 3.55. While this is a possible explanation of the discrepancy between the constants and while the influence of finite but large reaction rates should be borne in mind, the calculations presented in Chapter 5 reveal the same discrepancy; consequently, it must be conceded that this result of the

theory is quantitatively incorrect.

It is worth noting that had the function, g, been chosen as $g(y) = y$ then the theory would predict the eddy-break-up model with $C_{EBU} = C_2$; the value of C_2 appropriate to the new function, g, would, of course, be different from that quoted above.

In each of the above cases, where one or both of the time scale ratios tend either to zero or infinity, it has been shown that the probability distribution is known a priori. The solution of the probability distribution equation is, therefore, unnecessary. However, these situations are idealised and in practice both time scales are finite; it is for situations of this type that the probability approach is intended. Equation 3.40 was solved numerically for various values of one time scale ratio while the other was held at unity. Figure 3.4 shows the predicted reaction rate against τ_R/τ_K for $\tau_R/\tau_t = 1$ and figure 3.5 shows the reaction rate against τ_R/τ_t for $\tau_R/\tau_K = 1$. The normalised reaction rate was given by

$$S^*(\tilde{\phi}) = 4(\tilde{\phi}_2-\tilde{\phi}_1)\,(\tilde{\phi}-\tilde{\phi}_1)\,(\tilde{\phi}_2-\tilde{\phi}_1)^{-2} \qquad (3.56)$$

In both cases the predictions follow the expected trends but there is no basis for a quantitative assessment of the model's performance.

3.2.4 Conclusion on the Theory

The starting point of the theory was the transport equations for the scalars characterising the chemical and thermodynamic aspects of the flow, equation 3.1. From these equations, without any physical input (save the exclusion of pressure fluctuation influence), the joint probability distribution equation was deduced, equation 3.16. This equation overcomes the problems associated with the non-linearities in the density and the

source terms. The joint probability is seen to be transported in position space by laminar diffusion and by turbulent and mean flow convection and in probability space by the source term and by turbulent mixing on the microscale. It is the interrelation of the two latter agencies that accounts for the influence of turbulent mixing on the average reaction rate: if the reaction rate is very high in some region of probability space then the averaged reaction rate depends upon the rate at which the averaged probability is transported to that region.

The simplified case of the single probability equation was considered further: a model for the term representing turbulent mixing on the microscale was suggested and was used to predict an idealised combustion system. While the modelling is not completely satisfactory, the predictions can be expected to be qualitatively correct. These predictions demonstrate the interrelation of the reaction rate and the micromixing for different time scale ratios of the system.

The achievements of the theory are threefold;

(i) the joint probability distribution equations provide a useful mathematical and conceptual picture of the behaviour of turbulent reacting flows,

(ii) the modelled single probability distribution equation can be solved to predict any combustion system characterised by a single scalar, and (iii) the assumptions and inaccuracies in existing models may be judged by reference to the results of the theory.

The third point forms the subject of the next section.

3.3 A Criticism of Existing Models

In recent years combustion models have been developed for incorporation into flow solution algorithms. We are concerned, in this section, with comparing the present theory with such models that are in current use. These models may be divided into three classes depending upon the

nature of the flame being considered. Mason and Spalding (1973) developed the "eddy-break-up" model for use in premixed flames. Khalil, Spalding and Whitelaw (1975) also used this model for some of their calculations. Diffusion flames have been studied with a model based on probability distributions by Elgobashi and Pun (1974) and Lockwood and Naguib (1975a). The third class of flame, that which is neither premixed nor diffusion, has been studied by Khalil, Spalding and Whitelaw (1975) and by Lockwood and Naguib (1975b).

Many of the assumptions and equations are common to all the models: the combustion is supposed to proceed by a single step irreversible reaction,

$$1 \text{ kg. fuel} + s \text{ kg. oxidant} \rightarrow (1+s) \text{ kg. products} \qquad (3.57)$$

The transport equation for the mass fraction of each species is given by equation 3.1: the averaged form of this equation, equation 3.5, is modelled as, for example,

$$\langle \rho \rangle \frac{D}{Dt} \langle m_{fu} \rangle = \frac{\partial}{\partial x_i} \frac{\mu_{eff}}{\sigma_{fu}} \frac{\partial}{\partial x_i} \langle m_{fu} \rangle + \langle S_{fu} \rangle \qquad (3.58)$$

where m_{fu}, m_{ox} and m_{pr} are the mass fractions of fuel oxidant and products respectively. An equation for the average mixture fraction, $\langle f \rangle$,

$$f = m_{fu} - m_{ox}/s \quad , \qquad (3.59)$$

may be deduced from equation 3.58,

$$\langle \rho \rangle \frac{D}{Dt} \langle f \rangle = \frac{\partial}{\partial x_i} \frac{\mu_{eff}}{\sigma_f} \frac{\partial \langle f \rangle}{\partial x_i} \qquad (3.60)$$

It may be noticed that in formulating these transport equations, the influence of density fluctuations has been ignored; consequently, attention is focussed here on the other aspects of the models. The influence of density fluctuations is discussed in the next section.

In order to determine the temperature an equation for the enthalpy, $<h>$, is solved.

$$h \equiv m_{fu} H_{fu} + T \sum_{\alpha} C_{p\alpha}(T)\, m_{\alpha} \tag{3.61}$$

where H_{fu} is the heat of reaction, C_p the specific heat and the summation is for all species. The form of the enthalpy equation is the same as that for $<f>$ there is no source term. Equation 3.61 may be rearranged to give,

$$T(h, m_{\alpha}) = (h - m_{fu} H_{fu}) \left(\sum_{\alpha} C_{P_{\alpha}}(T)\, m_{\alpha} \right)^{-1} \tag{3.62}$$

With a knowledge of the temperature, the density may be obtained from the gas law

$$\rho\,(T, m_{\alpha}) = P\{R\, T \sum_{\alpha} m_{\alpha}/W_{\alpha}\}^{-1} \tag{3.63}$$

where R is the universal gas constant and W the molecular weight. A further equation that is used by each model is that for the fluctuations of the scalars;

$$g_{\phi} \equiv <\phi'^2> \tag{3.64}$$

$$<\rho> \frac{Dg_{\phi}}{Dt} = \frac{\partial}{\partial x_i} \frac{\mu_{eff}}{\sigma_g} \frac{\partial g_{\phi}}{\partial x_i} + C_{g1}\, \mu_{eff} \left(\frac{\partial <\phi>}{\partial x_i}\right)^2 - C_{g2} <\rho> \frac{\varepsilon}{k}\, g_{\phi} \tag{3.65}$$

For an arbitrarily fuelled system the equations for $<m_{fu}>$, $<f>$ and $<h>$ could be solved if $<S_{fu}>$, $<T(h,m_{\alpha})>$ and $<\rho(h,m_{\alpha})>$ were known. The models for premixed and diffusion flames exploit the restrictions of their respective systems to facilitate or avoid the determination of these unknown quantities and to reduce the number of transport equations that need be solved.

3.3.1 Premixed Flames

Mathematically, a homogeneously premixed flame is characterised by the boundary and initial conditions of $<f>$ being constant (and equal to $<f_o>$). The solution of equation 3.60 then becomes trivial,

$$<f> = <f_o> \tag{3.66}$$

and consequently, from equation 3.59, all the mass fractions may be related to $<m_{fu}>$ by,

$$<m_{ox}> = s(<m_{fu}> - <f_o>) \tag{3.67}$$

$$<m_{pr}> = 1 - <m_{fu}> - <m_{ox}> \tag{3.68}$$

Thus, the transport equation for $<f>$ need not be solved. The closure is completed by modelling the unknown terms as,

$$<S_{fu}> = -<\rho>\frac{\varepsilon}{k} C_{EBU} g_{fu}^{\frac{1}{2}} \tag{3.69}$$

$$<T(h, m_{fu})> = T(<h>, <m_{fu}>) \tag{3.70}$$

and $$<\rho(T, m_{fu})> = \rho(<T>, <m_{fu}>) \tag{3.71}$$

The eddy-break-up model, equation 3.69, was discussed in section 3.2.3 where the theory gave a similar result. There are two points, however, that require further comment. First, the assumption of a very high reaction rate may not be valid in practical situations; Runchal (1973), Khalil et al. (1975) and others have taken the reaction rate as the minimum of that given by the eddy-break-up model and that given by

$$<S_{fu}> = S_{fu}(<m_{fu}>, <T>) \tag{3.72}$$

The fact that the eddy-break-up model predicts a higher value than does equation 3.72 (which represents an upper bound) confirms that, in parts of the flow, the assumption of very fast reaction breaks down.

The second point relates to the value ascribed to g_{fu}. If the assumption of very fast reaction is consistently applied, g_{fu} must take its highest possible value: however, in this model, a transport equation for g_{fu} is solved, equation 3.65. Further, equation 3.65 is appropriate to fluctuations of scalars without sources and so, when it is applied to g_{fu}, a term, of order of magnitude $\langle\rho\rangle\, g_{fu}^{\frac{1}{2}} \langle S_{fu}\rangle$, is neglected. These two points indicate that the eddy-break-up model as a whole is far removed from the physical situation it is supposed to represent. Nevertheless, it has been used by its originators and others to produce some useful results and it contains the valuable assertion that the averaged reaction rate scales with the turbulent time scale.

The error in approximating the temperature and density by equations 3.70 and 3.71 depends upon the situation. If the mean specific heat is constant then the temperature, given by equation 3.62, is a linear function of h and m_{fu} and hence equation 3.70 is valid. The density, on the other hand, varies approximately as the inverse of temperature. Thus, if the temperature is bounded by $T_1 < T < T_2$, the error in equation 3.71 is given by,

$$0 \geq \frac{\rho\langle T\rangle - \langle\rho(T)\rangle}{\langle\rho(T)\rangle} \geq \frac{T_1 - T_2}{T_2 + T_1} \qquad (3.73)$$

Taking T_1 and T_2 to be 700°K and 2000°K, values typical of the flows reported in Chapter 5, it is seen that the density may be underestimated by as much as 50%. Bearing in mind that changes in density have a major effect upon the hydrodynamics, this possible error is a serious one. Equation 3.71 represents the lower bound of density and implies that the probability distribution of m_{fu} is a delta function centred on $\langle m_{fu}\rangle$:

the probability distribution consistent with the assumption of a very high reaction rate is

$$\langle\rho(m_{fu})\rangle = (m_2-m_1)^{-1}\{(m_2-\langle m_{fu}\rangle)\,\delta(m_1-m_{fu}) + (\langle m_{fu}\rangle - m_1)\,\delta(m_2-\langle m_{fu}\rangle)\} \quad (3.74)$$

where m_1 and m_2 are the minimum and maximum values that m_{fu} may take. The corresponding expression for density is

$$\langle\rho(m_{fu})\rangle = \frac{m_2 - \langle m_{fu}\rangle}{m_2 - m_1}\,\rho(m_1) + \frac{\langle m_{fu}\rangle - m_1}{m_2 - m_1}\,\rho(m_2) \quad (3.75)$$

which represents the upper bound. Thus, the average density lies between the values given by equation 3.71 and equation 3.75 and, for consistency, the latter expression is preferable.

A major criticism of this model is that it is restricted to situations where the assumption of very high reaction rates is valid: if the assumption were valid then the form of the eddy-break-up model would be appropriate and the temperature and density could be evaluated, without error, by way of the probability distribution, equation 3.74. What is needed, then, is a model that predicts the average reaction rate and probability distribution when the reaction rate is not high. The theory propounded in the last section lends itself to this end.

Applying the assumptions and restrictions made for premixed flames to the theory leads to the conclusion that all quantities can be expressed as functions of m_{fu}, h and $\langle P\rangle$ only. Further, as h is nearly homogeneous in premixed flames, only a small error is incurred by assuming that, for any quantity, ϕ,

$$\phi(m_{fu}, h, \langle P\rangle) = \phi(m_{fu}, \langle h\rangle, \langle P\rangle) \quad (3.76)$$

(Equation 3.76 is exact if the incoming fuel/air stream has a uniform temperature and if all confining surfaces are adiabatic). Thus, the

system may be characterised by the single scalar, m_{fu}, and so the solution of the single probability distribution equation for $<p(\tilde{m}_{fu})>$ provides the required closure. That is, the modelled transport equation for $<p(\tilde{m}_{fu})>$, which takes account of finite reaction rates, can be solved and the values of the average mass fractions, density and temperature can be obtained from

$$<\phi(m_{fu}, h, <P>)> = \int_{-\infty}^{\infty} <p(m_{fu})> \phi(\tilde{m}_{fu}, <h>, <P>)\, d\tilde{m}_{fu} \qquad (3.77)$$

In considering this approach to model premixed flames the objection can be raised that the inclusion of the additional independent variable, $\tilde{m}_{fu}$, increases the dimensionality of the solution space by one and, consequently, reduces the economy of the solution procedure a great deal. It would be glib to retort that simple answers to complicated problems should not be expected. Rather, it is to be hoped that the solution of the probability equations, as a research exercise, will indicate which of the many possible simplifications to the equation are appropriate and, hence, lead to a more economical procedure. In this context, the work of Bray and Moss (1974) is worthy of comment. These authors proposed a closure based on an assumed probability distribution expressed in parametric form: these parameters are functions of $<m_{fu}>$ and g_{fu} for which modelled transport equations were suggested. While this model was not deduced from the probability equations, such a route could be chosen and the number of parameters could be increased to provide more accuracy and generality.

3.3.2 Diffusion Flames

The model for diffusion flames is based upon the assumption that fuel and oxygen are not co-present. For most situations this assumption is justified; the fuel and oxygen streams are separated by a hot flame front and so, at any interface between fuel and oxygen, the temperature

is sufficiently high for the reaction to be very rapid. With this assumption, from the definition of the mixture fraction the following relations are obtained,

$$\begin{aligned} m_{fu} &= 0 \text{ for } f<0 \quad ; \quad m_{fu} = f \text{ for } f \geq 0 \\ m_{ox} &= -fs \text{ for } f<0 \quad ; \quad m_{ox} = 0 \text{ for } f \geq 0 \end{aligned} \tag{3.78}$$

Also, if the inlet temperatures of the two streams are uniform then h is given by

$$h = h_{ox} + (h_{fu} - h_{ox}) \ (f - f_{ox}) \ / \ (f_{fu} - f_{ox}) \tag{3.79}$$

where the subscripts 'ox' and 'fu' indicate the inlet values of the quantities in the oxygen and fuel streams respectively. Clearly, as the mass fractions and enthalpy are known functions of f so also are the temperature and density. Thus, the values of m_{fu}, m_{ox}, ρ and T are all known functions of f: however, as these functions are non-linear, the values of $\langle m_{fu} \rangle$, $\langle m_{ox} \rangle$, $\langle \rho \rangle$ and $\langle T \rangle$ are not directly related to $\langle f \rangle$.

Elgobashi and Pun (1974) and Lockwood and Naguib (1975a) overcame this problem by assuming a probability distribution for f. Thus, for example,

$$\langle T(f) \rangle = \int_{-\infty}^{\infty} \langle p(\tilde{f}) \rangle \ T(\tilde{f}) \ d\tilde{f} \tag{3.80}$$

The probability distribution was assumed to be a 'clipped-Gaussian', that is

$$\begin{aligned} &\tilde{f} > f_{fu} \text{ and } \tilde{f} < f_{ox} \ , \langle p(\tilde{f}) \rangle = 0 \\ &f_{ox} < \tilde{f} < f_{fu} \quad , \langle p(\tilde{f}) \rangle = N(\tilde{f}) = (\sigma\sqrt{2\pi})^{-1} \exp\left(-\tfrac{1}{2} \left(\frac{\tilde{f}-\mu}{\sigma}\right)^2\right) \end{aligned} \tag{3.81}$$

$$\langle p(f_{ox}) \rangle = \delta(\tilde{f}-f_{ox}) \int_{-\infty}^{f_{ox}} N(\tilde{f}) \ d\tilde{f}$$

and $$\langle p(f_{fu}) \rangle = \delta(\tilde{f}-f_{fu}) \int_{f_{fu}}^{\infty} N(\tilde{f}) \ d\tilde{f}$$

The two parameters in this distribution, σ and μ, can be determined from $<f>$ and g_f for which transport equations are solved. The clipped-Gaussian is probably the most physically realistic distribution that can be expressed in terms of two parameters: the limiting cases of $<f> \to f_{fu}$ and $g_f^{\frac{1}{2}}/(f_{fu}-f_{ox}) \to 0$ are accounted for correctly. However, the determination of σ and μ and the subsequent evaluation of the integrals, such as equation 3.80, entails a considerable amount of computational effort. Khalil et al. (1975) and Gosman and Lockwood (1973) used a simpler form of $<p(\tilde{f})>$ which, though physically less plausible, requires a minimum of computational effort,

$$<p(\tilde{f})> = \tfrac{1}{2}\,\delta\,(\tilde{f} - f_+) + \tfrac{1}{2}\,\delta\,(\tilde{f} - f_-) \qquad (3.82)$$

where $$f_{\pm} = <f> \pm g_f^{\frac{1}{2}} \qquad (3.83)$$

In situations where the assumption of rapid reaction is valid, the only uncertainty in the model is the determination of $<p(\tilde{f})>$. If the theory of the previous section were applied to these situations, rather than assuming a probability distribution, a transport equation for $<p(\tilde{f})>$ would be solved. However, as the equation for $<p(\tilde{f})>$ is computationally expensive to solve and the uncertainty in its modelling is no less than that in the assumption of a clipped-Gaussian distribution, this approach is not advocated. The comparison of measurements with the predictions of Elgobashi and Pun (1974) and Lockwood and Naguib (1975a) is favourable and suggests that their model provides a good description of diffusion flames.

3.3.3 Arbitrarily Fuelled Flames

The assumptions made at the beginning of this section lead to the conclusion that an arbitrarily fuelled flame can be characterised by m_{fu},

f and h. In the case of premixed and diffusion flames it was shown that either m_{fu} or f is redundant: further, for both situations, it was argued that the influence of enthalpy is adequately accounted for by its average value, that is,

$$< \phi(m_{fu}, f, h) > = < \phi(m_{fu}, f, < h>) > \qquad (3.84)$$

Thus, the single probability distributions $<p(\tilde{m}_{fu})>$ and $<p(\tilde{f})>$ provides a complete description of premixed and diffusion flames respectively. For arbitrarily fuelled flames, while equation 3.84 can again be employed to remove the dependence on h, both m_{fu} and f must be retained. Consequently, a knowledge of the joint probability $< p(\tilde{m}_{fu},\tilde{f})>$ is required to provide a complete description of this situation. (In fact, the joint probability $<p(\tilde{m}_{pr},\tilde{f}) >$, which contains the same information, will be considered).

Before considering the model of Lockwood and Naguib (1975b) the theory of the previous section is applied to this problem. This is done for two reasons; first, the theory makes the physical assumptions more precise and comprehensible and secondly, a model, similar to that of Lockwood and Naguib, was independently derived from the theory. The assumption of a very high reaction rate is again made: this denied the co-presence of the fuel/air mixture and products for premixed flames and of fuel and air in diffusion flames. For arbitrarily fuelled flames the consequence is that fuel, air and products may not co-exist. Thus, the joint probability $<p(\tilde{m}_{pr},\tilde{f})>$ may be expressed as the sum of three single probabilities,

$$\begin{aligned} < p(\tilde{m}_{pr},\tilde{f}) > = & < p_1(\tilde{f})> \ \delta(\tilde{m}_{pr}) \ + \\ & \text{(no products)} \\ & < p_2(\tilde{f}) > \delta(1 + s\tilde{f} - \tilde{m}_{pr}) + \\ & \text{(no fuel)} \\ & < p_3(\tilde{f})> \delta\ (1 - \tilde{f} - \tilde{m}_{pr}) \qquad (3.85) \\ & \text{(no oxygen)} \end{aligned}$$

A sketch of such a distribution is shown of figure 3.6. It is seen that $\langle p_2(\tilde{f})\rangle$ is zero for positive $\tilde{f}$ and $\langle p_3(\tilde{f})\rangle$ is zero for negative $\tilde{f}$. Thus, the two distributions may be summed to form one distribution without loss of information,

$$\langle p_A(\tilde{f})\rangle \equiv \langle p_2(\tilde{f})\rangle + \langle p_3(\tilde{f})\rangle \tag{3.86}$$

The subscript 'A' stands for 'activated species', a term introduced by Lockwood and Naguib to indicate that, in this region, the energy is sufficient for reactions to be rapid.

The problem of determining the joint probability has now been reduced to that of determining two single probabilities: averaged quantities may be evaluated through,

$$\begin{aligned}\langle \phi(f,m_{pr})\rangle &= \int_{-\infty}^{\infty}\int_{-\infty}^{\infty} \phi(\tilde{f},\tilde{m}_{pr}) \langle p(\tilde{f},\tilde{m}_{pr})\rangle \, d\tilde{f}\, d\tilde{m}_{pr} \\ &= \int_{-\infty}^{\infty} \phi(\tilde{f},0)\langle p_1(\tilde{f})\rangle + \phi(\tilde{f}, 1+s\tilde{f})\langle p_2(\tilde{f})\rangle + \phi(\tilde{f}, 1-\tilde{f})\langle p_3(\tilde{f})\rangle \, d\tilde{f} \\ &= \int_{-\infty}^{\infty} \phi_1(\tilde{f}) \langle p_1(\tilde{f})\rangle + \phi_A(\tilde{f}) \langle p_A(\tilde{f})\rangle \, d\tilde{f}\end{aligned} \tag{3.87}$$

The last equality serves to define ϕ_1 and ϕ_A. The behaviour of $\langle p_1(\tilde{f})\rangle$ and $\langle p_A(f)\rangle$ is unknown and so, for want of a better assumption, their shapes are presumed to be the same, that is,

$$(1-A)^{-1}\langle p_1(\tilde{f})\rangle = A^{-1}\langle p_A(\tilde{f})\rangle = \langle p(\tilde{f})\rangle \tag{3.88}$$

where A, the mass fraction of activated species, is given by

$$A \equiv \int_{-\infty}^{\infty} \langle p_A(\tilde{f})\rangle \, d\tilde{f} \tag{3.89}$$

There is no direct evidence either to support or to refute the assumption of equation 3.88 but at least it satisfies the required mathematical restrains: the integrals of each term are identically unity and for the limiting cases of A = 0 or 1 the equation is correct. It is seen, from equation 3.88, that only $< p(\tilde{f})>$ and A need be determined. As there is no difference between the quantity f in this situation and in diffusion flames, the same modelling of $< p(\tilde{f})>$ may be used; that is $< p(\tilde{f})>$ is assumed to be a clipped-Gaussian given by equation 3.81, based on the values of $<f>$ and g_f.

The theory of the last section lends itself well to the task of formulating a transport equation for the novel quantity A. From the definition of the various single probabilities, an alternative definition of A is,

$$A \equiv \int_{-\infty}^{\infty} \int_{o+}^{\infty} <p(\tilde{m}_{pr},\tilde{f})> \, d\tilde{m}_{pr} \, d\tilde{f} \qquad (3.90)$$

Thus, writing the joint probability equation, equation 3.16, for $< p(\tilde{m}_{pr},\tilde{f})>$ and integrating between the limits indicated by equation 3.90 leads to an exact transport equation for A,

$$\frac{\partial}{\partial t} <\rho_A> A + \frac{\partial}{\partial x_i} <\rho_A><U_i> A = - \frac{\partial}{\partial x_i} <\rho \, u_i A> + \lim_{\tilde{m}_{pr} \to o+} \frac{\partial}{\partial \tilde{m}_{pr}} <p(\tilde{m}_{pr}) \; \Gamma (\frac{\partial m_{pr}}{\partial x_i})^2> \qquad (3.91)$$

where $< \rho_A > \equiv \int_{-\infty}^{\infty} <p_A(\tilde{f})> \rho_A (\tilde{f}) \, d\tilde{f}$ (3.92)

The final term in equation 3.91, which will be denoted by S_A, is familiar; it is the expression from which the reaction rate in premixed flames was deduced in sub-section 3.2.3. The same modelling applied to the present term gives,

$$S_A = C_2 \langle \rho_A \rangle \varepsilon/k \, (1-A) \int_0^\infty \langle p(\tilde{m}_{pr}) \rangle \, g(\tilde{m}_{pr}/\hat{m}_{pr}) \, d\tilde{m}_{pr} \qquad (3.93)$$

The form of this expression is more comprehensible if the function $g(y)$ is chosen as $g(y) = y$: it was noted above that this choice leads to the eddy-break-up model in premixed flames. Hence,

$$S_A = C_2 \langle \rho_A \rangle \varepsilon/k \, (1-A) \langle m_{pr} \rangle / \hat{m}_{pr} \qquad (3.94)$$

Modelling the turbulent transport term in the normal way, the modelled equation for A is,

$$\frac{\partial}{\partial t} \langle \rho_A \rangle A + \frac{\partial}{\partial x_i} \langle U_i \rangle \langle \rho_A \rangle A = \frac{\partial}{\partial x_i} C_1 \langle \rho_A \rangle \frac{k^2}{\varepsilon} \frac{\partial A}{\partial x_i} + C_2 \langle \rho_A \rangle \varepsilon/k \, \frac{(1-A)}{\hat{m}_{pr}} \langle m_{pr} \rangle \qquad (3.95)$$

The proposed closure for arbitrarily fuelled flames is now complete. To summarise, transport equations may be solved for $\langle f \rangle$, g_f and A and the values of $\langle f \rangle$ and g_f used to determine the clipped-Gaussian probability distribution, $\langle p(\tilde{f}) \rangle$. Averaged quantities may then be determined through equations 3.87 and 3.88 by

$$\langle \phi(f, m_{pr}) \rangle = \int_{-\infty}^{\infty} \langle p(\tilde{f}) \rangle \, [(1-A) \, \phi_1 (\tilde{f}) + A \phi_A (\tilde{f})] \, d\tilde{f} \qquad (3.96)$$

This closure may be compared with that of Lockwood and Naguib (1975b): while these authors suggested determining averaged quantities through equation 3.96 they did not explicitly assume the equality of the activated and unactivated probability distributions, equation 3.88. The principal difference between the two closures is Lockwood and Naguib's alternative proposal,

$$S_A = C_A \langle \rho \rangle \varepsilon/k \, [A(1-A)]^{\frac{1}{2}} \qquad (3.97)$$

However, although this modelled source term has a different form from equation 3.94, it is, in fact, almost identical. Thus, the two closures are, to all intents and purposes, the same and the subsequent discussion applies equally to them both.

The first point to note is that the closure is compatible with the models for diffusion and premixed flames; if A is everywhere unity, characterising a diffusion flame, then the closure is identical to that described in sub-section 3.3.2. If, on the other hand, $\langle f \rangle$ is uniform then the closure reduces to that of sub-section 3.3.1 with the assumption of a very high reaction rate; equation 3.94 becomes equation 3.74 and the transport equation for A becomes an equation for $\langle m_{pr} \rangle$ with the source term given by the eddy-break-up model. To a large extent, therefore, the closure for arbitrarily fuelled flames may be assessed by reference to the criticism of the models for premixed and diffusion flames. In particular, it must again be conceded that in some situations the assumption of very high reaction rates is inapplicable. For example, the closure will provide a poor representation of a diffusion flame which has lifted off the burner, where the reaction rate is a controlling factor. On the other hand, as demonstrated by Lockwood and Naguib, a premixed jet burning in air is predicted accurately by the closure.

3.4 The Effect of Density Variations

The last two sections were concerned with the effect of turbulence on the reaction rate: here, the influence of the reaction on the mean flow and the turbulence is considered. The chemical and thermodynamic properties of the fluid affect the velocity field through the density and viscosity which appear in the continuity and momentum equations. The discussion of sub-section 2.4.2 indicates that, at high Reynolds number, the flow field is independent of the magnitude of the viscosity and, consequently, attention

is focussed on the influence of density variations. Density variations may be caused by temperature gradients, species concentration gradients or by the compressibility of the fluid: in combustion systems all the three agencies may act together, causing the density to vary by as much as an order of magnitude.

The principal difficulty in formulating a closed set of averaged equations for variable density flows is caused by the appearance of density in the term representing convection,

$$\frac{D\rho\phi}{Dt} = \frac{\partial\rho}{\partial t}\phi + \frac{\partial}{\partial x_i}\rho U_i\phi \qquad (3.98)$$

Bray (1973) derived the exact transport equations for mean velocity, species concentration and turbulent kinetic energy by decomposing the instantaneous quantities in the normal way, i.e.

$$\begin{aligned} U_i &= \langle U_i \rangle + u_i \\ \rho &= \langle \rho \rangle + \rho' \\ \phi &= \langle \phi \rangle + \phi' \end{aligned} \qquad (3.99)$$

In addition to the terms arising in constant density flows, five density fluctuation correlations result from the decomposition of the convective term; namely, $\langle \rho' u_i \rangle$, $\langle \rho' u_i u_j \rangle$, $\langle \rho' u_i u_j u_k \rangle$, $\langle \rho' \phi' \rangle$ and $\langle \rho' u_i \phi \rangle$. Bearing in mind that the density may vary by an order of magnitude, none of these correlations may be neglected; indeed, it is shown in the next section that, in one of the flows calculated in Chapter 5, $\langle \rho \rangle \langle \phi \rangle$ may be six times greater than $\langle \rho\phi \rangle$; that is, $\langle \rho' \phi' \rangle$ is approximately 80% of $\langle \rho \rangle \langle \phi \rangle$ but of opposite sign. Further, the modelling of these correlations is hindered by the paucity of turbulence measurements in reacting flows which are also insufficient to provide a direct test of any proposed model.

An alternative approach, which overcomes some of these problems and results in a simpler set of equations, is to decompose the instantaneous quantities in terms of their mass averages. This approach, which was proposed by Favre (1969), is best demonstrated by means of the Favre joint probability distribution, introduced by Bilger (1975):

$$\overline{p}\,(\tilde{\underline{U}},\tilde{\underline{\phi}}) \equiv \frac{1}{\langle\rho\rangle}\int_0^\infty \langle \delta(\underline{U}-\tilde{\underline{U}})\;\delta(\underline{\phi}-\tilde{\underline{\phi}})\;\;\delta(\rho-\tilde{\rho})\rangle\;\tilde{\rho}\;\;d\tilde{\rho} \qquad . \tag{3.100}$$

$\overline{p}$ is seen to be the joint probability of the velocity, $\underline{U}$, and the set of scalars, $\underline{\phi}$, weighted with the density. The mass averaged mean quantities and correlations (indicated by overbars) are given by the moments of the joint probability distribution;

$$\begin{aligned}
\overline{U}_j &\equiv \iint \overline{p}\,(\tilde{\underline{U}},\tilde{\underline{\phi}})\;\;\tilde{U}_j\;d\tilde{\underline{U}}\;d\tilde{\underline{\phi}} \\
\phi_\alpha &\equiv \iint \overline{p}\,(\tilde{\underline{U}},\tilde{\underline{\phi}})\;\;\tilde{\phi}_\alpha\;d\tilde{\underline{U}}\;d\tilde{\underline{\phi}} \\
\overline{u_i''\phi''} &\equiv \iint \overline{p}\,(\tilde{\underline{U}},\tilde{\underline{\phi}})\;(\tilde{U}_i-\overline{U}_i)(\tilde{\phi}_\alpha-\overline{\phi}_\alpha)\;d\tilde{\underline{U}}\;d\tilde{\underline{\phi}}\;,\ \text{etc.}
\end{aligned} \tag{3.101}$$

It should be noted that, with mass averages thus defined, terms like $\overline{u_i''}$ and $\overline{\phi_\alpha''}$ are identically zero: an alternative definition of mass averages, see for example Libby (1972), does not lead to this property.

It is readily shown that transport equations for the moments of $\overline{p}$ are virtually identical to those for constant density flows, Bilger (1975). The only difference is that correlations containing the divergence of $\underline{u}''$ do not vanish and that terms involving molecular transport adopt a slightly different form. Unlike the averaged equations based on the normal decomposition of $\underline{U}$, ρ and $\underline{\phi}$, no correlations with ρ' occur. Thus, for example, the continuity relation and the equations for $\overline{U}_j$ and $\overline{u_i''u_j''}$ (excepting viscous terms) are given by their constant density equivalents

with u_i'' replacing u_i and overbars replacing averaging brackets, $\langle\ \rangle$. The fact that the exact expressions pertaining to molecular action adopt a slightly different form is of no consequence since it was argued in sub-section 2.4.2 that, at high Reynolds number, the microscale is determined by the macroscale which does retain the same form. The fact that the divergence of the velocity vector, $\underline{u}''$, is not zero is more serious for it indicates that u_i'' behaves differently from u_i. However, the only manifestation of this different behaviour in the Reynolds stress equations is that the pressure-rate-of-strain term does not contact to zero; that is, the kinetic energy equation has the additional source term, $\overline{p'\partial u_i''/\partial x_i}$.

It appears, then, that the practice of mass averaging not only produces a simpler set of equations but also, as the transport equations for all the moments of are essentially the same as their constant density counterparts, the same modelling assumptions may be made. This contention is supported by the calculations of Libby (1972) and by Bilger (1975). Thus, the terms $\overline{u_i''\phi''}$, $\overline{u_i''\varepsilon''}$ and $\frac{1}{2}\overline{u_i''u_j''u_j''}$ may be modelled by the simple gradient diffusion hypothesis,

$$\overline{u_i''\phi''} = -\frac{C_u}{\sigma_\phi}\frac{\bar{k}^2}{\bar{\varepsilon}}\frac{\partial\tilde{\phi}}{\partial x_i} \qquad \text{etc.,} \tag{3.102}$$

while the isotropic viscosity hypothesis must be slightly modified to take account of the divergence of $\underline{\tilde{U}}$;

$$\overline{u_i''u_j''} = 2/3\,\bar{k}\,\delta_{ij} - C_\mu\frac{\bar{k}^2}{\bar{\varepsilon}}\left(\frac{\partial\tilde{U}_i}{\partial x_j} + \frac{\partial\tilde{U}_j}{\partial x_i} - 2/3\,\frac{\partial\tilde{U}_\ell}{\partial x_\ell}\,\delta_{ij}\right) \tag{3.103}$$

The modelling of the additional term $\overline{p'\partial u_i''/\partial x_i}$ is more difficult; Libby (1972) suggested a modelled form for inert flows with significant Mach numbers while Bray (1974) suggested that, in low Mach number reacting

flows, the analagous term, $\langle p' \partial u_i/\partial x_i \rangle$, is negligible. In view of the lack of experimental data, the existing deficiencies of the turbulence model and of Bray's suggestion, the term will be neglected here.

With these modelling assumptions, equations for $\overline{U}$, $\overline{k}$ and $\overline{\varepsilon}$ and any one of the combustion models described in the previous section form a closure, save for the determination of $\langle \rho \rangle$ and $\langle S_\alpha \rangle$. As $\langle \rho \rangle$ and $\langle S_\alpha \rangle$ are related to $\langle \underline{\phi} \rangle$, rather than to $\overline{\underline{\phi}}$, a relation for $\langle \underline{\phi} \rangle$ must be obtained. Since all the combustion models assume a probability distribution for $\underline{\phi}$, $\langle \underline{\phi} \rangle$ may be determined without further modelling assumptions. For example, for premixed flames, it follows from the definition of $\overline{\phi}$ that

$$\langle m_{fu} \rangle = \overline{m}_{fu} + \int \langle p(\tilde{m}_{fu}) \rangle (1 - \rho(\tilde{m}_{fu})/\langle \rho \rangle) \tilde{m}_{fu} \, d\tilde{m}_{fu} \qquad (3.104)$$

The advantage of mass averaging is seen to be that a closed set of equations, from which $\langle \underline{\phi} \rangle$ may be determined, is obtained without modelling velocity-density correlations. While these correlations must be modelled in order to extract information about the unweighted velocity field, any inaccuracy in such modelling does not propagate through the system of equations.

The mean velocity was the only measured function of the velocity field in the reacting flows calculated in Chapter 5. It should be noted that the technique of laser anemometry, which is well suited to combustion situations, measures the unweighted velocity: the precise quantities measured by hot wires or Pitot probes, which were used to perform these measurements, are less certain. Assuming that the unweighted velocity was measured, in order to compare the measured and calculated velocities $\langle U_i \rangle$ must be determined. Bray (1974) suggested the following form of modelling,

$$\langle U_i \rangle = \overline{U}_i - \langle \rho' u_i \rangle / \langle \rho \rangle$$

$$\simeq \overline{U}_i + \frac{C_\mu}{\sigma_\rho} \frac{\overline{k}^2}{\overline{\varepsilon}} \frac{1}{\langle \rho \rangle} \frac{\partial \langle \rho \rangle}{\partial x_i} \qquad (3.105)$$

where σ_ρ is of order unity. This modelling, which may be expected to be of the right order of magnitude, predicts $\langle \rho' u_i \rangle$ to be negligibly small compared with $\langle \rho \rangle \langle U_i \rangle$ in the flows calculated in Chapter 5. Consequently, the term will not be discussed further save to emphasise that the modelling of $\langle \rho' u_i \rangle$ and other velocity-density correlations has no influence on the calculated values of $\overline{U}_i$, $\overline{k}$ and $\langle \underline{\varphi} \rangle$.

In conclusion, the close similarity between the transport equations for mass averaged quantities in reacting flows and the equations for constant density flows suggests that the same modelling may be applied to each. Consequently, a closed set of equations is obtained without modelling velocity-density correlations. The only additional modelling required is in relating unweighted quantities to their mass averaged values. Any inaccuracy in this modelling for one quantity does not affect the other quantities.

3.5 The Combustion Models Employed

In Chapter 5 calculations of bluff-body stabilised flames are presented: the details of the two combustion models used are described in this section. The calculations pertain to the combustion of a premixed, uniform temperature, propane/air mixture downstream of an annular V-gutter in a circular duct.

The first model, Model A, comprises the closure outlined in sub-section 3.3.1 together with the k-ε turbulence model: the influence of density fluctuations is ignored. This represents the standard form of the eddy-break-up model used by Mason and Spalding (1973), Khalil et al. (1975) and others in which the probability distribution of $\tilde{m}_{fu}$ is assumed to be a single delta function centred on $\langle m_{fu} \rangle$. Model B may be regarded

as an extension of model A in the light of the considerations of this chapter; the reaction rate and probability distribution are determined from the theory of section 3.2 with the assumption of rapid reaction. The effects of density fluctuations are accounted for in the manner described in the previous section, that is, transport equations are solved for the mass averaged quantities. Before the two combustion models are described in more detail, the determination of the distributions $\rho(\tilde{m}_{fu} < P >)$ and $T(\tilde{m}_{fu})$, which are common to both, is described below.

In section 3.3, only three "species", fuel, oxygen and products, were considered: here, the nitrogen in the air is accounted for and the products are assumed to comprise of carbon dioxide and water. In spite of this, because the incoming stream is homogeneously premixed and the reactants are assumed to combine in fixed proportions by,

$$C_3H_8 + 5O_2 \rightarrow 3\,CO_2 + 4\,H_2O\,,$$

the mass fractions of each species can again be related to m_{fu};

$$\begin{aligned} m_{N_2} &= (m_{N_2})_o \\ m_{O_2} &= (m_{O_2})_o - 5((m_{fu})_o - m_{fu})\, W_{O_2}/W_{fu} \\ m_{CO_2} &= 3((m_{fu})_o - m_{fu})\, W_{CO_2}/W_{fu} \\ m_{H_2O} &= 4((m_{fu})_o - m_{fu})\, W_{H_2O}/W_{fu} \end{aligned} \qquad (3.106)$$

where W_α and $(m_\alpha)_o$ are the molecular weight and inlet mass fraction of species α. Further, due to the known composition of the inlet stream, the values of $(m_{fu})_o$ and (M_{N_2}) are related,

$$(M_{N_2})_o = 3.31 \ (M_{O_2})_o \tag{3.107}$$

and $$(M_{N_2})_o + (M_{O_2})_o + (m_{fu})_o = 1 \tag{3.108}$$

Consequently, the mass fraction of each species can be expressed as a linear algebraic function of m_{fu} and $(m_{fu})_o$.

In the flows calculated in Chapter 5, the temperature of the inlet stream is uniform and the heat transfer to the walls is small compared with the heat release due to combustion. Consequently, the enthalpy is uniform and equal to its inlet value, h_o. Thus, the temperature and density distributions are related to m_{fu} through equations 3.62 and 3.63 by;

$$T(\tilde{m}_{fu}) = (h_o - \tilde{m}_{fu} H_{fu}) \left(\sum_\alpha C_{P\alpha}(T) m_\alpha(\tilde{m}_{fu})\right)^{-1} \tag{3.109}$$

$$\rho(\tilde{m}_{fu}) = <p>\{R T(\tilde{m}_{fu}) \sum_\alpha m_\alpha(\tilde{m}_{fu})/W_\alpha\}^{-1} \tag{3.110}$$

The values of R and H_{fu} are taken as 8.3143 kJ/kg mole ^oK and 4.63747×10^4 kJ/kg respectively (Gordon and McBride (1971)). For each of the five species, the specific heats are determined from a fourth order polynomial in temperature; the coefficients are taken from the data assembled by Gordon and McBride (1971).

Model A. Transport equations are solved for $<U_i>$, k, ε, $< m_{fu} >$ and g_{fu}. The reaction rate is modelled by the eddy-break-up model as,

$$<S_{fu}> = -<\rho>\varepsilon/k \ C_{EBU} \ g_{fu}^{\frac{1}{2}} \tag{3.111}$$

and the closure is completed by determining $< \rho>$ and $< T >$ by,

$$< \rho > = \rho(< m_{fu} >) \tag{3.112}$$

$$< T > = T(< m_{fu} >) \tag{3.113}$$

Model B. Transport equations are solved for $\overline{U}_i$, $\overline{k}$, $\overline{\varepsilon}$ and $\overline{m}_{fu}$ and the form of these equations is identical to those for the unweighted quantities. In contrast to model A, the probability distribution is taken as a double delta function, equation 3.74. The values of $< m_{fu} >$, $<\rho >$ and $<T >$, which are determined from this probability distribution, are most easily expressed in terms of the mass averaged combustion efficiency;

$$\eta \equiv (m_2 - \overline{m}_{fu})/(m_2 - m_1) \tag{3.114}$$

$$<m_{fu} > = m_2 - (m_2 - \overline{m}_{fu})\, \overline{\eta}\, \{ 1 - (1 - \overline{\eta})(1 - \rho_2/\rho_1)\}^{-1} \tag{3.115}$$

$$<\rho > = \rho_1 \{1 - (1 - \overline{\eta})\, (1 - \rho_2/\rho_1)\}^{-1} \tag{3.116}$$

$$T = T_2 + (T_1 - T_2)\, \overline{\eta}\, \{1 - (1 - \overline{\eta})(1 - \rho_2/\rho_1)\}^{-1} \tag{3.117}$$

where m_1 and m_2 are the minimum and maximum fuel mass fractions and ρ_1, ρ_2, T_1 and T_2 are the corresponding densities and temperatures. It should be noted that, for small η , these relations give,

$$<\rho > <\eta> \simeq \rho_1/\rho_2 \; <\rho\, \eta >$$

As ρ_1/ρ_2 is approximately equal to six in one of the flows calculated in Chapter 5, it is seen that the neglect of density-mass-fraction correlations is totally inconsistent with the assumption of rapid reaction.

The reaction rate given by the theory of section 3.2, equation 3.53, does not take density variations into account: in the absence of any

evidence to the contrary, it is assumed that, the expression for $G(\tilde{\phi})$, from which the reaction rate is deduced, may be modified to incorporate density variations as

$$G(\tilde{\phi}) = C_2 \frac{\overline{\varepsilon}}{\overline{k}} \hat{\phi} \int_{-\infty}^{\tilde{\phi}} \rho^{\frac{1}{2}} (\phi^*) \overline{P}(\phi^*) g(\frac{\tilde{\phi} - \phi^*}{\hat{\phi}}) \, d\phi^* \int_{\tilde{\phi}}^{\infty} \rho^{\frac{1}{2}}(\phi^*) \overline{P}(\phi^*) g(\frac{\phi^* - \tilde{\phi}}{\hat{\phi}}) \, d\phi^* \tag{3.118}$$

where $\hat{\phi}$ is equal to $(\overline{\phi''^2})^{\frac{1}{2}}$. This leads to the reaction rate of fuel used by model B;

$$\langle S_{fu} \rangle = - C_2 \langle \rho \rangle \frac{\overline{\varepsilon}}{\overline{k}} (m_2 - m_1) \overline{\eta} (1-\overline{\eta}) \ln (1+1/[\overline{\eta}(1-\overline{\eta})]^{\frac{1}{2}} (\rho_2/\rho_1)^{\frac{1}{2}}/ (1 - (1-\overline{\eta}) \rho_2/\rho_1) \tag{3.119}$$

The constants C_{EBU} and C_2 were evaluated so as to maximise the agreement between the calculated and measured combustion efficiencies. Their values, 1.1 and 1.0 respectively, differ significantly from the value of $C_{EBU} = .53$ suggested by Mason and Spalding (1973) and $C_2 = 4.5$ used in section 3.2. These differences will be discussed in Chapter 5.

3.6 Summary

This chapter has been concerned with modelling the averaged equations of turbulent reacting flow. The joint probability distribution equations have been derived and have been shown to provide a useful mathematical and conceptual picture of the behaviour of reacting systems. For premixed flames, the modelled single probability distribution equation offers the potential advantage over existing models of obviating the need to assume rapid reactions: however, the quantitative performance of the particular model proposed is suspect. The application of the theory of section 3.2 to arbitrarily fuelled flames produced a model similar to that of Lockwood

and Naguib (1975b) and clarified its physical foundation.

A discussion of the influence of density variations indicated that a closed set of equations for mass averaged quantities can be obtained without modelling velocity-density correlations. While these correlations must be modelled in order to determine unweighted quantities, any inaccuracy in the modelling for one quantity does not affect other quantities.

The two combustion models employed to perform the calculations reported in Chapter 5 are described in section 3.5. The first, model A, represents the standard form of the eddy-break-up model in which fluctuations are ignored: the probability distribution of the fuel mass fraction is assumed to be a single delta function. Model B incorporates the effects of fluctuations by solving for mass averaged quantities and assumes a double delta function probability distribution. The reaction rate employed, equation 3.119, is based on the theory presented in section 3.2.

CHAPTER 4

CALCULATION PROCEDURES

4.1 Introductory Remarks

In the last two chapters, a variety of turbulence and combustion models were introduced which, together with the momentum and continuity equations, form a closed set of equations. These equations were solved numerically to produce the results reported in Chapter 5; the numerical procedures used are described and discussed in this chapter.

It could be said that numerical procedures are of secondary importance in the study of turbulent flows; providing they give a true solution of the equations, their constitution is of no great importance. If present computational powers were limitless and inexpensive this would be the case but, as things stand, an improved numerical procedure results in a saving in computer expense and allows calculations to be made of more complex flows or with more complex models. Thus, to a large extent, the ability to test models is limited by the capabilities of existing computers and computational techniques. As the testing of hypotheses is an integral part of the scientific method, the development of turbulence and combustion models depends upon relating theories to experimental observations through a solution procedure. Consequently, the three components, modelling, computational procedures and experimental results, are of equal importance and a limitation on any one of them handicaps the advance of knowledge. Indeed, it is not unreasonable to speculate that, had Chou, Kolmogorov and their contemporaries had today's computational tools, the present state of knowledge would have been attained fifteen years ago.

All the flows considered are two-dimensional and steady: that is, all averaged quantities can be expressed as functions of only two spatial coordinates and their values do not vary in time. This being the case,

the principal rôle of the calculation procedure is to solve the transport equations constituting the closure in only two independent variables. These equations, which are elliptic, can be written in the common form,

$$\frac{\partial}{\partial x_i} \rho U_i \phi = \frac{\partial}{\partial x_i} \Gamma_{ij} \frac{\partial \phi}{\partial x_j} + S_\phi \qquad (4.1)$$

where ϕ represents any one of the quantities $\langle U_i \rangle$, k, ε, $\langle u_i u_j \rangle$, $\langle m_{fu} \rangle$, g_{fu} or their mass average equivalents and the source, S_ϕ, and the diffusivity, Γ_{ij}, depend upon the quantity in question. Henceforth, for brevity and in order to retain the common form, the averaging symbols are omitted. Thus, U_i appearing in equation 4.1 represents $\overline{U}_i$ if ϕ is a mass averaged quantity and $\langle U_i \rangle$ if ϕ is unweighted.

The direct solution of the set of simultaneous equations 4.1 is hindered by the facts that no equation exists for the pressure and that the continuity relation is not included. Thus, as well as solving equations 4.1 explicitly for ϕ, the calculation procedure must also determine the pressure and ensure that mass is conserved.

The results reported in Chapter 5 were obtained using two different calculation procedures: the procedure for the reacting flows, for which model I was used, is outlined in the next section. The principles on which this scheme is based have been reported in the open literature by Patankar and Spalding (1973) and the specific details are given by Runchal (1973). It was found that significant changes to this procedure were necessary in order to solve the equations comprising the Reynolds stress closures. The principles of the new procedure for these equations, described in section 4.3, are applicable not only to flows characterised by two-dimensional elliptic equations but also to three-dimensional flows. As a result, a means is provided for testing and using Reynolds stress closures in more complex flows than the two-dimensional boundary-layer type flows previously

considered. The performance of the procedures is discussed in section 4.4.

4.2 The Basic Procedure

As mentioned above, the details of this numerical scheme are given by Runchal (1973). The purpose of this section is to present an outline of the principal features of the procedure used for reacting flows and to introduce the nomenclature that will be used in the next section.

Most of the flows calculated, when considered in polar-cylindrical coordinates, have no variation in the circumferential direction while the others may be expressed in two-dimensional Cartesian coordinates. In order that the equations have the same form in the two different coordinate systems, the coordinates are defined as follows: in polar-cylindrical coordinates, x is the axial direction and r=y is the radial direction. In Cartesian coordinates, x and y are the mutually orthogonal directions and r is equal to unity. Thus, for example, in both systems,

$$\nabla^2 \phi = \frac{\partial^2 \phi}{\partial x^2} + \frac{1}{r} \frac{\partial}{\partial y} \left(r \frac{\partial \phi}{\partial y} \right) \tag{4.2}$$

In this coordinate system, with U and V denoting the velocities in the x and y directions, the general transport equation, equation 4.1 becomes,

$$\frac{\partial}{\partial x} (\rho U \phi) + \frac{1}{r} \frac{\partial}{\partial y} (r \rho V \phi) - \frac{\partial}{\partial x} \left(\Gamma_x \frac{\partial \phi}{\partial x} \right) - \frac{1}{r} \frac{\partial}{\partial y} \left(r \Gamma_y \frac{\partial \phi}{\partial y} \right) = S_\phi \tag{4.3}$$

In the Appendix, this equation is written in full for each of the variables.

A finite-difference method is used to solve equation 4.3. Figure 4.1 shows part of a finite-difference grid where the values of ϕ are assumed known at the nodes P, N, S, E and W. Equation 4.3 is integrated over the indicated control volume to give,

$$\left[\int_{y_-}^{y_+} r(\rho U\phi - \Gamma_x \frac{\partial\phi}{\partial x})\,dy\right]_{x_-}^{x_+} + \left[r\int_{x_-}^{x_+} (\rho V\phi - \Gamma_y \frac{\partial\phi}{\partial y})\,dx\right]_{y_-}^{y_+} = \int_{y_-}^{y_+}\int_{x_-}^{x_+} r\,S_\phi\,dx\,dy \tag{4.4}$$

and the following finite-difference approximations are then made:

$$\int_{y_-}^{y_+} r\rho U\phi\,dy\,\Big|_{x_+} \simeq \tfrac{1}{2}(\phi_P + \phi_E)\,(\rho U)_{x_+}\int_{y_-}^{y_+} r\,dy = C_{x_+}(\phi_P + \phi_E) \tag{4.5}$$

$$\int_{y_-}^{y_+} r\Gamma_x \frac{\partial\phi}{\partial x}\,dy\,\Big|_{x_+} \simeq \frac{\phi_E - \phi_P}{x_E - x_P}(\Gamma_x)_{x_+}\int_{y_-}^{y_+} r\,dy = D_{x_+}(\phi_E - \phi_P) \tag{4.6}$$

$$\int_{y_-}^{y_+}\int_{x_-}^{x_+} r\,S_\phi\,dx\,dy \simeq (S_\phi)_{x_P}\int_{y_-}^{y_+}\int_{x_-}^{x_+} r\,dy\,dx = (S_\phi)_{x_P}\,\mathrm{Vol} \tag{4.7}$$

and similarly for the integrals with respect to x and for the lower limits of the integrals. The values of $(\rho U)_{x_+}$, $(\Gamma_x)_{x_+}$ etc., if not known at the required locations, are determined by linear interpolation. Thus, with

$$A_E \equiv D_{x_+} - C_{x_+} \tag{4.8}$$

$$A_W \equiv D_{x_-} + C_{x_-} \quad \text{etc.,} \tag{4.9}$$

substituting equations 4.5 to 4.9 into equation 4.4 gives

$$\phi_p\,\Sigma A = \Sigma\,(\phi A) + (S_\phi)_{x_p}\,\mathrm{Vol} \tag{4.10}$$

where the summation is over N, S, E and W. This equation provides a

relationship between the value of ϕ_p and its neighbours but, in some circumstances, its physical implications are unacceptable. If, for example, C_{x_-} is positive and greater than D_{x_-} then A_w will be negative and so equation 4.10 implies that an increase of ϕ_W causes a decrease in ϕ_p. Gosman et al. (1969) suggest a modification to equations 4.8 and 4.9 in order to overcome this implausibility, i.e.

$$\text{if } |C_{x_+}| > D_{x_+} \quad , \quad A_E = |C_{x_+}| - C_{x_+} \tag{4.11}$$

$$\text{if } |C_{x_-}| > D_{x_-} \quad , \quad A_W = |C_{x_-}| + C_{x_-} \quad \text{etc.} \tag{4.12}$$

The physical interpretation and justification of these modifications which are used in both procedures, are given by Gosman et al. (1969).

If the pressure is known, then equation 4.10, written for each variable at each grid node, forms a closed set of algebraic equations. However, there is no guarantee that the resultant velocity field would satisfy the continuity equation. The two problems of determining the pressure and conserving mass are overcome by adjusting the pressure field so as to satisfy continuity. The procedure for adjusting the pressure requires a specific justaposition of the velocity and pressure nodes, see figure 4.2. The mass flow, G, through each face of the cell centred on P_p, is approximated by,

$$G_{x_+} \simeq \tfrac{1}{2}(\rho_p + \rho_E)\, U_E \int_{y_-}^{y_+} r\, dy = B_{x_+}\, (\rho)_{x_+}\, U_E \tag{4.13}$$

$$G_{y_+} \simeq \tfrac{1}{2}(\rho_p + \rho_N)\, V_N \int_{x_-}^{x_+} r\, dx = B_{y_+}\, (\rho)_{y_+}\, V_N \tag{4.14}$$

and similarly,

$$G_{x_-} = - B_{x_-} (\rho)_{x_-} U_p \tag{4.15}$$

$$G_{y_-} = - B_{y_-} (\rho)_{y_-} V_p \tag{4.16}$$

Now, the continuity relation requires that $\Sigma G = 0$ and the pressure field is changed by an amount P^* so that the corresponding changes in (ρ) and U, (ρ^*) and U^*, result in changes in G, G^*, such that

$$\Sigma G + \Sigma G^* = 0 \tag{4.17}$$

The change in density is given, through the equation of state by,

$$(\rho^*)_{x_-} = \tfrac{1}{2}(P_P^* + P_W^*) \left(\frac{\partial \rho}{\partial P}\right)_{x_-} \tag{4.18}$$

and the change in velocity is approximated by linearising the finite difference equation for U, equation 4.10,

$$U_p^* \simeq (P_W^* - P_P^*) \frac{Vol}{(x_P - x_W) \Sigma A}$$

$$= (P_W^* - P_P^*) DU_p \tag{4.19}$$

Consequently, neglecting second order terms,

$$G_{x_-}^* \simeq B_{x_-} [(\rho^*)_{x_-} U_p + (\rho)_{x_-} U_p^*]$$

$$= - \tfrac{1}{2} B_{x_-} U_p \left(\frac{\partial \rho}{\partial P}\right)_{x_-} (P_P^* + P_W^*) - B_{x_-} (\rho)_{x_-} DU_p (P_W^* - P_P^*)$$

$$= - C_{x_-} (P_P^* + P_W^*) - D_{x_-} (P_W^* - P_P^*) \tag{4.20}$$

Thus, defining finite-difference coefficients, A, as before (equations 4.8 and 4.9) an equation for P* is obtained:

$$P_p^* \Sigma A = \Sigma (P^*A) - \Sigma G \qquad (4.21)$$

The non-linearity of the finite difference equations requires that they be solved iteratively: equation 4.10 is solved for U and V and then equation 4.21 is solved for P*. The pressure, density and velocities are then incremented by P*, ρ^*, U* and V*. Equation 4.10 is then solved for all the other quantities. This procedure is repeated until all the equations are satisfied simultaneously and the mass sources, ΣG, are zero.

The above description of the procedure is not comprehensive: details of other features, such as under-relaxation, the treatment of boundaries and the solution of the finite-difference equations, can be found in the original source, Runchal (1973). However, the information given about the coordinate system, the disposition of the grid nodes and the finite-difference approximations is sufficient for the reader to appreciate the remainder of this chapter.

4.3 The Reynolds Stress Closure Procedure

The necessity of modifying the basic procedure for the Reynolds stress closures is caused, not by the form of the Reynolds stress equations, but by the different form taken by the momentum equations. In the case of the mean flow closure, where the isotropic viscosity hypothesis is employed, the gradient of the Reynolds stresses appearing in the momentum equation may be written as

$$-\frac{\partial}{\partial x_i}\rho\langle u_i u_j\rangle = \frac{\partial}{\partial x_i}\left(\mu_{eff}\frac{\partial U_j}{\partial x_i}\right) + \left\{\frac{\partial}{\partial x_i}\left(\mu_{eff}\frac{\partial U_i}{\partial x_j}\right) - \tfrac{2}{3}\rho\frac{\partial k}{\partial x_j}\right\} \qquad (4.22)$$

The first term on the right hand side, which is predominant, is incorporated into the basic procedure by setting $\Gamma_x = \Gamma_y = \mu_{eff}$ in equation 4.3 and the final term forms part of the source. The same treatment cannot be applied to the Reynolds stress closures because they do not provide an explicit relationship between stress and rate of strain. Consequently, the whole of the Reynolds stress gradient term is included in the source and the diffusivities are set to zero.

If the basic procedure were applied to the Reynolds stress closure, the set of finite-difference equations would differ from those appropriate to model I in two important aspects: the interlinkage between stress and rate of strain would be removed from the velocity equations and the shear stress $<uv>$ would be determined at different locations. Consider first the way in which the term $-\frac{\partial}{\partial x}\rho<uv>$, appearing in the V-velocity equation, is treated by the basic procedure incorporating the isotropic viscosity hypothesis;

$$\int_{x_-}^{x_+} -\frac{\partial}{\partial x}\rho<uv>\,dx = [\rho<uv>]_{x_-} - [\rho<uv>]_{x_+}$$

$$\simeq (\Gamma_x)_{x_-}\frac{(V_p-V_W)}{(x_p-x_W)} + (\Gamma_x)_{x_+}\frac{(V_E-V_p)}{(x_E-x_p)} + S' \qquad (4.23)$$

where S' represents the contribution of velocity gradients other than $\frac{\partial V}{\partial x}$. The last equality in this equation is used in the implicit part of the finite-difference equations and provides the interlinkage between stress and rate of strain: an increase in V_p causes $[\rho<uv>]_{x_-}$ to decrease and $[\rho<uv>]_{x_+}$ to increase and, consequently, the whole expression decreases causing V_p to tend to its original value. Also, the appearance of V_E and V_W in equation 4.23 provide a linkage between V_p and its neighbouring values.

By way of contrast, consider the form taken by equation 4.23 when the values of $\langle uv \rangle$ are determined explicitly from the isotropic viscosity hypothesis at the pressure nodes. This is analogous to applying the basic procedure to the Reynolds stress closures since, assuming the transport of $\langle uv \rangle$ to be small, the value of $\langle uv \rangle$, which would be calculated at the pressure nodes, is largely determined by the local velocity gradients. In this case, assuming for simplicity a grid with equal spacing, δx, and homogeneous diffusivities, Γ,

$$[\rho\langle uv \rangle]_{x_-} - [\rho\langle uv \rangle]_{x_+} \simeq \frac{\Gamma}{4\delta x} \{ (2 V_{WW} + V_{WWN} + V_{WWS}) - 2 (2V_p + V_N + V_S) - (2 V_{EE} + V_{EEN} + V_{EES}) \} + S' \qquad (4.24)$$

This expression does not compare favourably with equation 4.23 because it is a less accurate approximation of the exact term and, in addition, it provides no linkage between V_p and its neighbours, V_E and V_W. The latter defect, that only alternate grid lines are linked, explains why the author's attempts to solve the Reynolds stress closures by the basic procedure failed; the values of the velocities and Reynolds stresses, rather than converging to their correct values, diverged with successive iterations.

In order to overcome these difficulties, a new procedure was developed which calculates the equation for $\langle uv \rangle$ on a different grid, see figure 4.3. With this juxtaposition of grid nodes, the terms $\frac{\partial}{\partial x} \rho\langle uv \rangle$ in the V-equation and $\frac{1}{r} \frac{\partial}{\partial y} r\rho\langle uv \rangle$ in the U-equation can be evaluated without interpolation and the velocity gradients $\frac{\partial U}{\partial y}$ and $\frac{\partial V}{\partial x}$, which have a predominant effect on the shear stress, can be determined directly at the $\langle uv \rangle$ nodes. Consequently, the new procedure obviates the need for interpolation and, although the interlinkage of stress and rate of strain cannot be retained within the velocity equations, it will be shown that

the $\langle uv \rangle$ and velocity equations are coupled in a stable manner. A small increase in $\langle uv \rangle_p$ from its correct value results in increases in U_p and V_p and decreases in U_s and V_w, causing $\partial U/\partial y$ and $\partial V/\partial x$ to increase at the $\langle uv \rangle_p$ node. The effect of these increased velocity gradients is to decrease, through the source term in the $\langle uv \rangle$ equation, the value of $\langle uv \rangle_p$ towards its correct value.

For an inert, isothermal flow, the new procedure entails the solution of the equations for U, V and $\langle uv \rangle$ on their respective grids and of the equations for $\langle u^2 \rangle$, $\langle v^2 \rangle$, $\langle w^2 \rangle$, ε and P^* at the pressure nodes. The formulation of the finite-difference equations is straightforward and the details are not reported here. The approximations made are generally the same as in the basic procedure but, for axisymmetric flows, they are modified near the axis to take account of the information that,

$$\text{as } r \to 0, \quad \langle uv \rangle \quad \alpha \; r \tag{4.25}$$

$$\text{and as } r \to 0, \quad \langle v^2 \rangle - \langle w^2 \rangle \quad \alpha \; r^2 \tag{4.26}$$

For example, equation 4.5, written for $\langle uv \rangle$, is altered to give,

$$\int_o^{y+} r \rho U \langle uv \rangle dy \Big|_{x_+} = \int_o^{y_+} r^2 \rho U \left(\frac{\langle uv \rangle}{r}\right)_p \; dy \Big|_{x_+}$$

$$\simeq \tfrac{1}{2} \frac{(\langle uv \rangle_p + \langle uv \rangle_E)}{r_p} \; (\rho U)_{x_+} \int_o^{y_+} r^2 \, dy \tag{4.27}$$

With these modifications consistently applied, no problems were encountered near the axis of symmetry in spite of the fact that, as r tends to zero, two of the terms in the $\langle uv \rangle$ equation become infinite.

A quantitative assessment of the new procedure is given in the next section.

4.4 Discussion of the Procedures

The basic procedure described in Section 4.2 is well established; it has been tested and used by several authors, e.g. Runchal (1973) and Khalil, Spalding and Whitelaw (1975). The procedure is coded as a Fortran program which, on a CDC 6600 digital computer, has storage and time requirements of 17,000 + 32/ (grid node) words and .0006 sec/ (iteration x grid node x equation) respectively. The combustion calculations reported in Chapter 5 were obtained by this procedure, solving eight equations on a 24 x 25 grid. It was found that 450 iterations were required to achieve a converged solution and hence the time taken was 21 minutes. These statistics are discussed below where they are compared with those of the new procedure.

Since the new procedure described in Section 4.3 differs significantly from the basic procedure, tests were carried out to ensure that, for any grid size below some limit, the solutions were the same. Figure 4.4 shows calculated values of mean axial velocity and the corresponding normal stress along the centre-line of a wake behind a disc in a uniform free stream. The results show that the numerical accuracy is reasonable even with a 14 x 14 grid. The calculated values of velocity and Reynolds stresses at other locations in the field showed similar accuracy. The size of the grids used with this procedure to perform the calculations reported in Chapter 5 varied, depending upon the complexity of the flow in question; the flows with recirculation, Carmody (1964) and Durão and Whitelaw (1974), were calculated on a 30 x 30 grid to ensure that no significant error could be attributed to numerical inaccuracy. 25 x 16 and 30 x 30 grids was used for the essentially boundary-layer type flows of Chevray and Kovasznay (1969) and Chevray (1968) respectively. The large grid, used for the latter case, was necessary because the solution domain was extended a considerable distance into the free stream.

The Fortran program for this procedure, which included the facility of solving the same scalar equations for reacting flows as the basic procedure, had storage and time requirements of 16,000 + 20/(grid node) words and .0003 sec/(iteration x grid node x equation). The number of iterations required to obtain a converged solution was found to depend on the complexity of the flow; for the flow of Carmody (1964) 600 iterations were needed while for the simpler flow of Chevray (1968) only 200 iterations were required. The resultant time requirements for these two calculations were 27 and 9 minutes respectively.

A comparison of the storage and time requirements of the two procedures shows that the new procedure is more economical in both respects. This fact is solely attributable to programming efficiency because the additional grid and the complicated source terms in the Reynolds stress equations inevitably leads to an increase in computational effort. For a 20 x 20 grid, the new procedure requires 24,000 words and 1 sec/iteration to calculate an isothermal flow with one of the Reynolds stress closures. This performance may be regarded as satisfactory but the number of iterations required, which is approximately the same for both procedures, causes the total time requirement to be, at least, twenty times that of analogous parabolic procedures. In spite of this shortcoming, which urgently requires investigation, the new procedure is no more expensive of computer time than the basic procedure and, as will be seen in the next Chapter, has been successfully employed to calculate recirculating flows with Reynolds stress closures.

CHAPTER 5

CALCULATIONS

In this chapter, the results of calculations of isothermal and reacting flows are reported. The next section is concerned with isothermal wake flows calculated with each of the three turbulence models described in section 2.3. These calculations, which were performed with the procedure of section 4.3, are compared with experimental data in order to assess the accuracy of each model. These results have been reported elesewhere, Pope and Whitelaw (1976) but, as they are central to the present work, they are presented and discussed here. Section 5.2 is concerned with reacting flows: the two combustion models described in section 3.5 are used in conjunction with the procedure of section 4.2 to calculate premixed propane/air flames stabilised behind an annular V-gutter. A comparison with experimental data allows an assessment of the combustion models and of the assumptions on which they are based.

5.1 Isothermal Flows

In this section the calculations of isothermal wake flows are reported. Each of the four flows considered (described below) was calculated with all three turbulence models described in section 2.3: this allows a comparison of the three models as well as an assessment of their performance by reference to the experimental data. The flows considered and the available experimental data are described in the next sub-section. As the same sets of equations are solved to calculate each of these flows, the calculations are distinguished solely through the applied boundary conditions which are also described in the next sub-section. In sub-section 5.1.2, where the results of the calculations are presented, it is seen that the boundary

conditions for some of the flows are not known with certainty. Consequently, test calculations are also reported by which the error in the predictions due to uncertainties in the boundary conditions may be assessed. In the final sub-section the results are discussed and conclusions are made about the performance of the turbulence models.

5.1.1 Description of Flows Considered

A literature survey, Pope (1973), of experimental information relating to near-wake flows, with and without recirculation , showed that available data was in short supply. The papers by Chevray (1968) and Chevray and Kovasznay (1969) pertain to the wake downstream of an ellipsoid and of a long, thin, flat plate respectively: in both cases, the region of recirculation immediately downstream of the body was negligibly small but, as the axial velocity gradients were of the same order of magnitudes as the radial gradients, the solution of the equations in elliptic form is appropriate. Carmody (1964) reported similar measurements downstream of a disc and, in this case, the region of recirculating flow was extensive and encompassed by the measurements. The recent measurements of Durão and Whitelaw (1974) and Durão (1975) are also helpful in this connection since they relate to the wake downstream of an annular jet: they were obtained using a laser-Doppler anemometer, rather than the hot wires of previous authors and this helps to remove any bias which might result from the consideration of hot-wire data alone.

The measurements of Chevray included values of mean axial and radial velocities and all the non-zero Reynolds stresses at various locations downstream of his ellipsoid. The values of each dependent variable except dissipation were available at the trailing edge of the ellipsoid which was chosen as the inlet plane of the solution domain. The dissipation at inlet was assumed to be equal to the production of turbulent kinetic energy.

Chevray and Kovasznay measured the mean axial velocity and the Reynolds stresses, $\langle u^2 \rangle$, $\langle v^2 \rangle$ and $\langle uv \rangle$, downstream of a thin, plane plate. The measurements at the trailing edge, which was again chosen as the inlet plane of the solution domain, show fully developed turbulent boundary-layer profiles. Consequently, the inlet value of the normal velocity was assumed to be zero while values of $\langle w^2 \rangle$ were taken from the boundary-layer data of Klebanoff (1954): again, the dissipation was equated to the production of turbulent kinetic energy.

The measurements of Carmody are also extensive and are particularly relevant to blunt body stabilised flames in that they were performed downstream of a disc (or radius R) in a free stream (with velocity U_E). The separated nature of this flow provides a greater test of the present turbulence models than the flows of Chevray and Chevray and Kovasznay but it should be remembered that it also presents a more formidable measurement problem. The measurements of axial velocity were obtained with a Pitot tube and, as a result, static pressure was also measured: the reported values of $\langle u^2 \rangle$ and $\langle uv \rangle$ were obtained using hot wires. In the recirculation zone, the high turbulence intensity and the steep velocity gradients undoubtedly cause significant errors in the measurements: also, the disturbance of this reversed flow region due to the presence of the measuring probes introduces uncertainties. For these reasons, the measurements downstream of the recirculation zone can be expected to be more accurate.

The inlet plane of the solution domain was taken coincident with the disc where the values of axial velocity were taken from the data. The radial velocity quoted by the author was evaluated from the continuity equation and consequently is subject to a large error. The values used were obtained by solving for the flow upstream of the disc, assuming it to be inviscid, using the measured axial velocity as a boundary condition. The validity of this approach was confirmed by the observation that, at

the inlet plane, the dynamic head, calculated from the measured axial velocity and pressure and the predicted radial velocity, was nearly constant. The inlet values of the normal stresses were set at .002 U_E^2 while the dissipation was set through the length scale with $l/R = .03$. These nominal free-stream values may be expected not to influence the calculations very much as in the region immediately downstream of the disc, a great deal of turbulence is produced.

The measurements of Durão and Whitelaw (1974) pertain to an annular jet; the inner radius of the jet being 0.72 times the outer radius, R. Close to the outlet of the jet a region of reversed flow occurred in the vicinity of the centre-line thus initiating a wake which decayed further downstream. The outer region of the flow resembled a decaying jet and, for $x/R > 100$ where the wake has vanished, the measurements show self-preserving jet profiles. Upstream of the nozzle there was a contraction thus ensuring that the turbulence intensity at exit was small. The value of the mean velocity components at the jet outlet are not reported but further measurement, Durão (1975), indicated that the axial velocity is uniform and that the radial component is negligible. These measurements served as boundary conditions for velocity while the turbulence quantities were prescribed with the same nominal values as those for the flow of Carmody.

The wall functions, described in sub-section 2.3.3, are used adjacent to the discs of Carmody and Durão and Whitelaw thus completing the specification of boundary conditions at the inlet plane. The boundary conditions for the other three sides of the rectangular solution domain are common to all the flows. A plane or axis of symmetry is located at y=0 where the symmetric quantities, U, k, ε, $\langle u^2 \rangle$, $\langle v^2 \rangle$ and $\langle w^2 \rangle$, have zero normal gradients; V and $\langle uv \rangle$, being anti-symmetric, are zero. The "free-stream" boundary was located sufficiently far into the free-stream to make the resulting calculations independent of its location.

Turbulence quantities were ascribed nominal values while the axial velocity took its known free-stream value, U_E; the radial velocity boundary condition is specified, therefore, through the continuity relation. For all the flows considered, far downstream of the inlet plane, the flow becomes boundary-layer like in nature; that is, $U >> |V|$ and normal gradients are far larger than those in the axial direction. In these circumstances the equations become parabolic and, hence, the out-flow boundary condition, $\frac{\partial \phi}{\partial x} = 0$ (for all quantities), which is only approximately correct, results in a negligible error upstream. The outflow boundary was located sufficiently far downstream of the last axial position of interest to ensure that no error was incurred due to these boundary conditions.

5.1.2 Presentation of Results

The closed sets of equations provided by each of the three turbulence models and the above boundary conditions were solved by the numerical scheme described in section 4.3: the results of these calculations are presented here.

The flow of Chevray (1968). The calculated profiles of U/U_E are shown on figures 5.1 and of $\langle uv \rangle / U^2_E$ on figure 5.2. The figures show the results of calculations obtained with each of the three turbulence models and demonstrate the effect of a 20% decrease in the initial values of ε and a doubling of the initial values of V. The experimental data are indicated on the figures for comparison purposes.

It can be seen from figure 5.1 that each of the three models results in values of mean velocity which are virtually the same except in the vicinity of the symmetry axis where small differences occur. In general, the non-dimensional calculated velocity values are lower than the measurements: the comparison suggests that the mixing is too low in the vicinity of the symmetry axis and that this suppresses the development of

the wake. However, the calculated shear stress is greater than the measured values thus refuting this supposition and suggesting instead that the measurements do not satisfy the axial momentum equation. The discrepancy could stem from the measured values of V used as inlet conditions in the calculations: these values are undoubtedly subject to a possible error which could be as large as a factor of two. For this reason, the calculations were repeated with initial V-values which were twice the measured values. As can be seen, the U-profiles at downstream locations became larger than the measured values.

The comparison between measured and calculated values of non-dimensional shear stress, shown on figure 5.2, again shows that all models result in similar trends to the measurements. In the upstream region the shear stress predicted by model I is far less than that predicted by the Reynolds stress models. This reflects the fact that model I takes no account of the convection of the individual stresses. Once again, the influence of the initial V-profile is large and does not allow any quantitative assessment of the ability of the three models to predict shear stress.

The Flow of Chevray and Kovasznay (1969). For this flow, the uncertainty in the V-velocity at the trailing edge (assumed zero) and hence its influence can be expected to be significantly less than in the data of Chevray (1968). Consequently, this flow can be expected to provide a more reliable test of the turbulence models. Figure 5.3 allows a comparison between measured and calculated values of the mean axial velocity: shear stress values are shown on figure 5.4; and normal stresses on figure 5.5.

As was the case with the flow configurations of Chevray, the three models result in calculated values of mean velocity which are virtually identical. On this occasion, however, the agreement between measurements

and calculations is excellent. The predictions of shear stress are adequate and, once again, they do not allow any model to be identified as a clear improvement over any other: this is made particularly clear by the differences which result from a 20% increase in the assumed initial values of ε. The agreement between the measurements and calculations of figures 5.3 and 5.4 is certainly sufficiently good to provide confidence in the initial values used for the calculations. The differences between the measured values of $< u^2 >$ and $< v^2 >$ and those calculated with each of the models is, therefore, particularly significant. It can readily be seen that model III provides calculated values which are in good agreement with experiment; model II is slightly less satisfactory and model I, which predicts $< u^2 > = < v^2 >$, is inadequate. The influence of the assumed initial ε profile does not alter this conclusion.

The flow of Carmody (1964). Unlike the two flows considered above, the flow of Carmody contains a significant region of reversed flow: the results presented here represent the first calculations of such flows with Reynolds stress closures. Figures 5.6 and 5.7 present comparisons between measured and calculated mean values: figure 5.6 is concerned with growth rate and centre-line velocity and figure 5.7 with normalised velocity profiles at downstream locations. Figure 5.8 is concerned with shear-stress profiles and figure 5.9 with normal-stress profiles.

The results shown on figure 5.6 show that, with the inlet conditions stated above, none of the models results in values of the half-width or of the centre-line velocity which are in close agreement with the measurements. The differences resulting from the three models and from a doubling of the inlet value of dissipation is small compared to those resulting from an 80% decrease in the values of the inlet radial velocity or from an augmentation of the turbulence close to the baffle tip. The decreased velocity corresponds to that suggested by Carmody while augmenting

the turbulence close to the baffle tip by setting $u'/U_E = v'/U_E = w'/U_E = .14$ and $l/R = .4$ for $1.0 < y/R < 2.0$ (i.e. $0 < U/U_E < .95$) is intended to simulate a thick shear layer in that region. Such a shear layer is not indicated by the data nor is it likely to exist: it does, however, represent an upper bound of the uncertainty in the boundary conditions of turbulent quantities. As can be seen from figure 5.6, the decrease in V (from a maximum of $.74\ U_E$) and the increase in turbulence intensity have large influences on the predicted growth rates and centreline velocity distribution. The poor agreement between the measurements and the prediction with V decreased confirms that the present estimate is more reliable. The predictions with the higher turbulence intensity at inlet increase the spreading rate, $\frac{dy_{\frac{1}{2}}}{dx}$, from .025 to .05. However these values must be compared with the experimental value of .1 and the difference cannot reasonably be attributed to uncertainties in the boundary conditions. The two Reynolds stress models fare better than model I in the recirculation zone but, bearing in mind experimental difficulties in this region and the sizeable discrepancies downstream, no model may be distinguished as being better than the others.

The shear stress results of figure 5.8 demonstrate differences between the results of the three models but, once again, the influence of V and turbulence initial conditions are larger than those of the models. Clearly the augmented initial turbulence intensity and model III lead to results which are in remarkably good agreement with experiment and particularly in the downstream region where the measurements are more accurate. The normal stress results of figure 5.9 allow the same tentative conclusion as figure 5.8. In addition, however, the measurements reveal unexplicable behaviour in the upstream region and must be considered suspect. Also, models II and III will always be more successful for the calculation of normal stresses since they are not made equal in plane shear flow as with model I.

The flow of Durão and Whitelaw (1974). Figure 5.10 shows measurements and predictions of the centre-line velocity and the velocity profile at $x/R = 0.6$. The predictions of centre-line velocity are virtually the same for each turbulence model and show similar discrepancies to those encountered with Carmody's data. The length of the recirculation zone is again under-predicted. The almost constant predicted value of U_t/U_{in} further downstream is due to a balance between the decay of the wake (tending to increase the velocity) and the spreading of the flow (tending to decrease the velocity). Further measurements by Durão (1975) show that the wake decays more quickly than is predicted, thus accounting for the different shapes of the two curves.

The predicted velocity profiles are again virtually the same for each of the turbulence models and show a significant discrepancy as compared with the measurements.

5.1.3 Discussion

The previous section shows that significant discrepancies exist between measurements and predictions which may be attributed both to inaccurate measurements, leading to erroneous boundary conditions, and to deficiencies in the turbulence models.

An approach which would overcome the first problem is to increase the size of the solution domain so that known boundary conditions may be applied upstream of the body. This approach is, in principle, advantageous but may present difficulties in practice. The correct representation of the boundary-layer flows around the solid body requires a finite-difference grid with a comparatively larger number of nodes. This is expensive in terms of computer time and may still not allow calculated values of flow properties, at the downstream plane of the solid body, which are more precise than the presently available measurements. The present calculations quantify the precision with which the flow around the solid body must be

calculated and, at the same time, they indicate that the uncertainties in the boundary conditions are insufficient to explain the large discrepancies between calculated and measured quantities.

Two particular defects, which result from the turbulence models, are evident in the prediction of the recirculating flows. The length of the region of recirculation is underpredicted as is the rate at which the wake decays. The same defects have been observed by Vasilić (1975) who used model I to predict the two-dimensional flow over a thin obstruction mounted normal to a plane surface. Also, in connection with the present investigation, Assaf (1975) measured and predicted (using model I) the flow behind a disc mounted on the centre-line of a confining, round tube. The results, shown on figure 5.11, again demonstrate the same shortcomings of the turbulence model.

In order to understand the more serious defect, the underprediction of the spreading rate, it is necessary to consider the nature of round wake flows, a useful discussion of which is given by Rodi (1972). Far downstream, round wakes have the potential of displaying profile-similarity; that is, as $U_{\ell}/U_E \rightarrow 1$, appropriately normalised mean quantities and the spreading parameter, $S = U_E/(U_E-U_{\ell})dy_{\frac{1}{2}}/dx$, may become independent of x. Rodi (1972) considered nine sets of experimental data and concluded that round wakes do display profile-similarity. However, unlike all other commonly encountered free shear flows, the profiles of mean quantities and in particular the spreading parameter are strongly dependent upon the way in which the flow is initiated. Of particular interest here are the values of S for the flows measured by Chevray (1968) and Carmody (1964) which are $S = .105$ and $S = .8$ respectively. The reason for the non-uniqueness of profile-similar round wakes may be attributed to the fact that they are weak-shear flows; that is, the effect of local velocity gradients upon the Reynolds stresses is up to an order of magnitude less

than the effect of dissipation. The consequences of these observations for the turbulence models are twofold. First, as convection is a dominant factor, unless the flow around the recirculation zone is predicted accurately, the downstream predictions are unlikely to be correct: secondly, the dissipation equation will govern the spreading rate almost entirely.

Although the discrepancies in the predictions of the recirculation zones are not as great nor as well substantiated as that of the spreading rate, the above arguments indicate that great precision is required in the recirculation zone if the wake is to be correctly represented. In the recirculation region the Reynolds stress models offer the potential advantages over a two equation model that the differential transport of Reynolds stresses is permitted and that the use of the isotropic viscosity hypothesis is obviated. The effect of allowing for the differential transport of the Reynolds stresses is difficult to assess. Certainly, the gross features of the flows considered here are not dependent on this transport in contrast to asymmetric channel flow or annular pipe flow for example. However, the results demonstrate that the Reynolds stress closures are necessary to represent the different magnitudes of the stresses and that they result in slightly better predictions of mean velocity. This advantage might also be obtained with a mean flow closure incorporating the more realistic effective viscosity hypothesis described in sub-section 2.4.1.

While the Reynolds stress closures have a slight advantage over model I, the differences between the predictions obtained with the various models are negligible compared with the discrepancy between the predictions and the experimental data. This observation suggests that the discrepancy is caused by the common factor in the different models, namely, the dissipation equation. The findings of sub-section 2.4.2 support this supposition: it

was concluded that any dissipation equation, closed by quantities pertaining to low wave numbers, has no foundation in non-similar flows. The recirculation zone and the evolving flow immediately downstream of it are distinctly not similar and, consequently, the dissipation equation is particularly suspect in these regions. For these reasons, it is the author's firm belief that the dissipation equation is responsible for the large discrepancies and, further, that complex, rapidly evolving flows cannot be represented by closures of the level employed here. On the other hand, the finding of sub-section 2.4.2 also indicate that a closure based on the spectral energy equation can, in principle, represent such flows since the energy spectrum contains information about the evolution of the turbulence structure. Such an approach, although computationally more expensive, can be expected, therefore, to remedy the observed discrepancies in the calculation of flows behind bluff bodies.

5.2 Reacting Flows

In this section calculations of bluff body stabilised flames are reported. A literature survey, Pope (1973), revealed that there was a paucity of experimental data of local properties in these flows: while bluff body stabilised flames were widely studied in the 1950's, the main objective of these works was to determine the blow-off velocity and, consequently, local properties were not measured. The more recent works of Harrison (1973) and Harrison (1974) do, however, provide a complete set of measurements of mean velocity and combustion efficiency for a propane/air flame stabilised behind an annular V-gutter in a circular duct. The flows measured by Harrison are more fully described in the next sub-section where the boundary conditions for the calculations are given. The calculations were performed with the two combustion models

described in section 3.5 and it is noted that, with the applied boundary conditions, model A provides an ambiguous closure: the reasons for this and the remedy employed are also stated in the next sub-section. The results of the calculations, which are presented in sub-section 5.2.2, are discussed in sub-section 5.2.3 where it is seen that the calculations performed, albeit for only one class of flow, are sufficient to compare the two combustion models and to assess the validity of the assumptions on which they are based.

5.2.1 Description of the Flows Considered

The test rig used by Harrison, which was the same for both investigations (Harrison (1973) and Harrison (1974)), comprised a 30° included angle, annular, V-gutter mounted centrally in a circular duct: the inner and outer radii of the annulus were 52.0 mm and 75.0 mm respectively and the duct radius, R, was 101.6 mm. Propane was injected into the air stream 3.5 m upstream of the V-gutter which resulted in the fuel/air ratio being uniform to within 5% at the plane of the gutter. Downstream of the gutter, the duct continued for 1.05 m and was cooled by water jets in order to minimise the distortion due to thermal stresses.

The axial velocity was measured by means of a 3.2 mm diameter cylindrical pitot probe: calibration tests showed that the dynamic head was proportional to 0.53 times the pressure difference across the probe. The accuracy of this method of measuring the velocity depends upon the accuracy with which the density can be determined and also upon the probe Reynolds number and the turbulence intensity. The two last dependencies indicate that the measurements may be particularly suspect in the recirculation region where the presence of the probe may also affect the flow. These possible inaccuracies should be borne in mind although they are not cited below as reasons for discrepancies between calculations and measurements.

In order to determine the chemical composition of the flame, gas samples were taken through a 3.2 mm diameter probe. The gases were analysed for carbon dioxide and carbon monoxide using the I.R.G.A. technique and the concentration of hydrogen was assumed to be half that of carbon monoxide. The fraction of unburnt fuel was deduced from an analysis of the sample after complete combustion over hot copper oxide. The concentrations of oxygen and nitrogen could then be obtained with the assumption that they were the only remaining species. Hence the combustion efficiency, defined on the basis of oxygen consumption, was determined directly while the density and temperature were deduced from the equation of state and from the assumption of uniform enthalpy respectively. It may be noted that a basic assumption of both combustion models is that the reaction proceeds directly to carbon dioxide and water and consequently denies the existence of carbon monoxide and hydrogen. Consequently, in the models, the density and temperature are uniquely related to the combustion efficiency whereas this is not the case for the experimental procedure. In this connection it is unfortunate that the measured carbon monoxide concentration was not reported and consequently the error incurred by the models through its neglect cannot be estimated directly.

Calculations were performed for four of the experimental tests which were distinguished by different inlet values of velocity, fuel/air ratio, temperature and pressure; the conditions for each test are shown in Table II.

Table II. Test Conditions

Test	U_{in} (m/s)	fuel/air (kg/kg)	Equivalence Ratio	$T^{\circ}K$	P (bar)
1	111.0	0	0	720	0.572
2	107.0	.05	.783	720	0.591
3	85.8	.0333	.522	720	0.862
4	36.2	.047	.736	300	0.828

The calculations of test 1, in which there is no combustion, provide another check on the performance of the turbulence model while the three tests with combustion allow the models to be assessed under the different conditions indicated in the table.

In contrast to the calculations of isothermal flows reported in the previous section, the solution domain for these flows extended from 1.25 duct radii upstream to 3.1 radii downstream of the trailing edge of the gutter. Thus, the gutter was encompassed by the solution domain, a measure which overcomes the previously encountered problems associated with inlet boundary conditons. The boundary conditions for velocity, fuel and pressure at inlet were taken as uniform with values appropriate to Table II while the turbulence quantities were set by,

$$k = .003\ U^2$$

$$\ell = .03R\ ;\ \varepsilon = C_\mu k^{3/2}/\ell$$

$$g_{fu} = 0$$

The values of k and ε represent nominal free stream values while g_{fu} is identically zero owing to the absence of combustion products. The boundary conditions for the centre-line and outlet plane were the same as for the isothermal calculations and the wall functions, described in sub-section 2.3.3, were employed at the duct wall. For $<m_{fu}>$ and g_{fu} the zero normal gradient boundary condition appropriate to impervious walls was applied. The boundary conditions applied over the perimeter of the V-gutter were zero slip velocity and zero transport of scalars: this represents the treatment advocated by Runchal (1973).

The application of these boundary conditions to the equations appropriate to model A leads to an important, though novel, observation; namely, the boundary conditions are insufficient to produce a unique

solution. This mathematical point is best demonstrated by considering the hypothetical case in which the density is uniform and consequently the velocity and turbulence fields are independent of $\langle m_{fu} \rangle$ and g_{fu}. The homogeneity of the equations for $\langle m_{fu} \rangle$ and g_{fu} ensure that, if one solution is given by $\langle m_{fu} \rangle_1$ and $(g_{fu})_1$, an infinity of solutions are given by

$$\langle m_{fu} \rangle = \langle m_{fu} \rangle_{in} - a(\langle m_{fu} \rangle_{in} - \langle m_{fu} \rangle_1)$$

$$g_{fu} = a^2 (g_{fu})_1$$

where $\langle m_{fu} \rangle_{in}$ is the inlet boundary condition on $\langle m_{fu} \rangle$ and a is an arbitrary positive number. These solutions include negative values of $\langle m_{fu} \rangle$ which, by definition, is a non-negative quantity. The infinity of solutions for this situation is directly analogous to the more familiar ambiguity in Poisson's equation with zero gradient boundary conditions. In practical situations, in which the density is not unifrom, if a unique solution were to exist it would result from the direct influence of density on the turbulent transport terms and from the indirect influence of density upon the velocity and turbulence fields. While density variatons play an important rôle in turbulent combustion, it would be unrealistic to suppose that they alone dictate the level of the scalar fields.

The reason that this defect in model A has gone unnoticed is probably that most solution procedures, for reasons of stability, relax the reaction rate term in such a way that the combustion efficiency can never exceed 100%. This measure not only guarantees plausible solutions but also, by destroying the homogeneity of the equations, overcomes the non-uniqueness problem. That is, in addition to the applied boundary conditions, the value of $\langle m_{fu} \rangle$ is effectively specified at one or more points within the solution domain: thus, as with Poisson's equation, the additional restraint on the equations provides a unique solution. The same treatment was used

in the present calculations and the observation that, for every flow, 100% combustion efficiency was predicted at some point (namely the apex of the V-gutter) confirms that the solution depends upon this inhomogeneity for its uniqueness. The predictions of Mason and Spalding (1973) did not suffer from this problem since the homogeneity of the equations was destroyed by the non-uniform boundary conditions imposed on $\langle m_{fu} \rangle$ and g_{fu} at the inlet plane of their solution domain. The fact that the flows calculated here and those calculated by Khalil et al. (1975) had homogeneous boundary conditions, while Mason and Spalding used inhomogeneous boundary conditions, may account for the different value of C_{EBU} used by these authors.

5.2.2 Presentation of Results

The calculated mean velocity profiles for test 1 are shown on figure 5.12 together with the available experimental data: x denotes the axial distance downstream of the trailing edge of the gutter and y represents the radial distance from the centre-line. The results for this test, in which there was no combustion, allow an assessment of the accuracy of the turbulence model for the given flow geometry. The discrepancies observed for the isothermal flows reported in the last section are again apparent; the profiles at $x/R = 0.25$ indicate the position of the end of the predicted recirculation zone whereas at the same location the measurements show significant negative velocities. The profiles at $x/R = 1.25$ demonstrate that the predicted recovery of the minimum velocity is far less than that measured, the calculated velocity deficit being twice the measured value. Thus, these calculations confirm that the turbulence model results in the prediction of a too short recirculation zone and a too slow rise in minimum velocity.

The calculated combustion efficiency, temperature and velocity profiles for tests 2, 3 and 4 are shown on figures 5.13 to 5.21: the solid lines

represent the calculations using model A and the dashed lines represent those using model B; the available experimental data are indicated on the figures for comparison. In section 3.5 it was stated that the reaction rate constants, C_{EBU} and C_2, were chosen so as to produce agreement between calculated and measured combustion efficiencies; this was done by reference to the maximum combustion efficiency for test 2 at $x/R = 2.25$. It is seen that for all the tests the two combustion models predict similar values of combustion efficiency; the major differences occur for $x/R < 0.25$ where model A consistently predicts higher values. A comparison between the calculations and measurements indicates that for each test and at each location the predicted width of the flame exceeds the measured value. For test 2, the predicted and measured values of maximum combustion efficiency are in good agreement except at the first location, $x/R = 0.05$, where the former exceeds the latter. For tests 3 and 4, the disagreement at the first location is less pronounced but the subsequent profiles, $0.25 < x/R < 1.25$, show the maximum measured combustion efficiency to be greater than that calculated.

As expected, the calculated temperature profiles mirror the combustion efficiency profiles; a minor exception to this observation is test 4 where it is seen that model A predicts slightly higher temperatures than does model B. The reason for this is that the low inlet temperature of test 4 results in higher maximum to minimum temperature and density ratios than do the other tests, thus accentuating the different ways in which the two models evaluate temperature. A comparison between measured and calculated temperatures shows that there is a large discrepancy; for example, the maximum temperature predicted at $x/R = 0.05$ for test 4 is $1600^{\circ}K$ which may be compared with the measured value of $2099^{\circ}K$ and the calculated adiabatic flame temperature of $1750^{\circ}K$. While the presence of carbon monoxide can cause the temperature to exceed the adiabatic flame temperature, an excess

of 350°K cannot reasonably be expected. Rather, it appears that the gas analysis is subject to a considerable error since the fuel air ratio obtained from it is up to 30% higher than the known value, based on the air and propane mass flow rates. The error, which is sufficient to account for the discrepancy, denies the usefulness of considering further the comparison between the predicted and calculated temperature. It is to be hoped that the error is systematic and consequently the combustion efficiency, being a normalised quantity, is unaffected by it.

The profiles of mean axial velocity reflect not only the influence of Reynolds stresses but also the acceleration due to the expansion of the gasses caused by combustion. In particular, the measured profiles at $x/R = 2.25$ for test 4, in which there is a 1:6 expansion, show a velocity maximum downstream of the gutter rather than the minimum experienced in isothermal flows. The velocity profiles predicted by the two models are virtually the same, the slight differences being greatest for test 4. It was shown in sub-section 3.3.1 that models A and B determine the lower and upper bounds of density, respectively, and the difference between the predicted velocity profiles reflects this fact. A comparison between predictions and measurements shows that the disagreement is no greater than for isothermal flows; the predicted length of the recirculation zone is again shorter than that measured and far downstream, at $x/R = 2.25$, it is evident that rate of wake recovery is underestimated. However, at intermediate locations, $0.75 < x/R < 1.25$, the agreement is quite good and certainly better than for the isothermal flow, test 1.

5.2.3 Discussion

In discussing the results presented in the last sub-section, attention will be focussed on the prediction of combustion efficiency: the probable error in the temperature measurement does not allow firm conclusions to be made and, bearing in mind the limitations of the turbulence model, the

velocity predictions are adequate. The success of the models in predicting combustion efficiency may be judged from the figures; the error in the maximum combustion efficiency decreases with distance and, at most, is 30%. The width of the flame is consistently overpredicted by 10-40% although the precision of the measurements does not allow an accurate measure of this defect.

These achievements and defects of the models may be used to assess the assumption on which they are based: sub-sections 3.3.1 and 5.2.1 indicate that, in spite of its equal performance, model A is based on contradictory and implausible assumptions and consequently only model B will be considered. Two basic assumptions in the model, which are subject to doubt, are that the reaction rate is rapid, and that the reaction only involves fuel, oxygen, carbon dioxide and water. For a given high Reynolds number flow it follows, irrespective of the detailed modelling or the composition of the fuel, that the predicted combustion efficiency is solely a function of the minimum to maximum density ratio and that if this is unity, $< S_{fu} >$ is symmetric about $\eta = 1/2$. The first of these deductions is demonstrated by the calculations; tests 2-4 have minimum to maximum density ratios of .327, .408 and .166 respectively and the predicted combustion efficiency is seen to increase slowly with increasing density ratio. The experimental data is seen to follow the same trend except for test 2 in the vicinity of the gutter ($x/R < 0.75$). This exception can be explained by the invalidity, for this test, of the assumption that carbon dioxide and water are the only products: test 2 is distinguished by a combination of a high inlet temperature and high equivalence ratio, conditions conducive to the formation of carbon monoxide. While this is the probable explanation, it would, of course, be more satisfactory to have direct evidence. For tests 3 and 4, on the other hand, the near 100% combustion efficiency measured at $x/R = 0.25$ indicates

that the carbon monoxide concentration is negligible at this location and probably, therefore, downstream of it.

The experimental data suggests that the assumption of a high reaction rate is valid; hydrocarbon reactions rates increase approximately exponentially with temperature (see, Kretschmer and Odgers (1972)) and consequently, if the assumption were not valid, the low inlet temperature of test 4 would cause the combustion efficiency to be considerably lower than for the other tests. As indicated above, the slightly lower combustion efficiency may be explained in terms of the lower density ratio. Although conclusive evidence is not available, it appears, therefore, that for tests 3 and 4 the two basic assumptions are valid and so the deficiencies in the predictions stem from the details of the modelling.

The modelling of the molecular mixing term, G, and the reaction rate deduced from it are particularly suspect; the failure of G to predict Gaussian probability distributions in homogeneous inert flows and the difference between the value $C_2 = 4.5$ obtained in Chapter 3 and the value $C_2 = 1.0$ used in the calculations indicate that the modelling is a poor representation of the physical situation. Further, the modelled reaction rate is the predominant influence on the predicted combustion efficiency and is capable of producing the observed deficiencies. The overprediction of the width of the flame suggests that the reaction rate is too large at low combustion efficiencies while an increase at high efficiencies would improve the predicted maximum. These suggestions, together with the observation that $< S_{fu} >$ is symmetric about $\eta = \frac{1}{2}$ in constant density systems, indicate that density variations cause $< S_{fu} >$ to be asymmetric. While such asymmetry is provided by the reaction rate term employed by model B, it is evident that the basic term and the modelling of its dependence upon density variations are quantitatively incorrect. The strong dependence of $< S_{fu} >$ upon density variations is unfortunate for it means that the effects of turbulence on combustion cannot be studied independently of the effects of combustion on turbulence.

CHAPTER 6

CLOSURE

In the first section of this chapter, the main findings of the work are summarised; this allows the achievements to be compared with the objectives and the present capability of predicting turbulent reacting flows to be assessed. On this basis, in section 6.2, the remaining problems are identified and an approach to overcome them is suggested.

6.1 Summary and Conclusions

6.1.1 The Reynolds Stress Closure Procedure

It was found that the incorporation of the Reynolds stress equations into the basic solution procedure results in numerical instabilities which stem from the lack of linkage between adjacent grid nodes. A new procedure has been developed which overcomes this problem by solving the shear stress equation on a separate grid.

Test calculations show that, for simple flows (e.g. the wake behind a disc), grid independent solutions are obtained with a 20 x 20 grid: for such a calculation, the computer program requires 24,000 words storage and 1 sec/iteration on a CDC 6600. The number of iterations required to obtain a converged solution was found to depend on the complexity of the flow and on the number of grid nodes; for the flow of Carmody (1964), 600 iterations were required for a 30 x 30 grid resulting in a computer time requirement of 27 minutes. Although this time requirement appears excessive, as compared with parabolic procedures, it is not a result of solving the Reynolds stress equations. Indeed, the new procedure is more economical than the basic procedure in all respects. Thus, the objective of developing a numerical algorithm for Reynolds stress closures has been achieved without increasing the computation expense of the solution procedure.

6.1.2 The Calculation of Isothermal Wakes

Four wakes, two with significant regions of reversed flow, have been calculated with a mean flow closure, model I, and with two Reynolds stress closures, models II and III. By comparing the results with experimental data, the ability of the turbulence models to represent such flows has been assessed. It was found that the boundary conditions applied at the inlet plane, which in some cases were not known with certainty, had a significant influence on the calculations. However, test calculations show that the resultant uncertainties in the predictions are insufficient to affect the conclusions summarised below.

The mean velocity, calculated with all three models, is in excellent agreement with the data of Chevray and Kovasznay (1969) and the shear stress is also predicted well. Consequently, the relative merits of the models may be assessed by the values of normal stresses predicted by each: model III provides calculated values which are in good agreement with experiment, model II is slightly less satisfactory and model I, which predicts equal normal stresses, is inadequate. A comparison between calculated and measured velocity for the flow of Carmody (1964) reveals significant defects in all the models which are confirmed by the prediction of other wake flows with recirculation. The calculated length of the recirculation zone is 30% less than that measured and the spreading rate, $\frac{dy_{\frac{1}{2}}}{dx}$, is underpredicted by a factor of four. The first defect is equally apparent for the flows of Durão and Whitelaw (1974) and Assaf (1975) and, to a lesser extent, so also is the second. The Reynolds stress models fare slightly better than model I but the improvement is small compared with the discrepancy with the data. The inaccurate prediction of the velocity field in these flows does not allow a meaningful comparison of the predicted Reynolds stresses although, as is evidenced by the flow of Chevray and Kovasznay, models II and III clearly provide a better

representation of the normal stresses.

While the application of Reynolds stress closures to near-wake flows does not provide a significant improvement over model I, this series of calculations has served to fulfil the objective of assessing the performance of the turbulence models in these flows.

6.1.3 Turbulence Modelling

The three turbulence models have been examined term by term in the light of a consideration of the implications of the mean closure approach. As a result, the limits of validity of the modelling have been determined and neglected influences have been identified.

It was shown that the isotropic viscosity hypothesis is incapable of representing the Reynolds stress tensor even in simple situations although the effective viscosity approach is valid for nearly homogeneous flows. An improved effective viscosity hypothesis, based on model III, has been proposed: as well as providing a realistic representation of the Reynolds stress tensor, it has the advantage of accounting for the influence of streamline curvature.

The modelling of the second redistributive term, $\phi_{ij,2}$, in model III is well-founded: several authors, using different approaches, have arrived at the same result and, as has been shown above, the modelling remains valid as the flow departs from homogeneity. The first redistributive term, $\phi_{ij,1}$, was considered in conjunction with the anisotropy of dissipation. The two terms have the same properties and, although neither theoretical arguments nor experimental evidence have determined their respective rôles unequivocally, the modelling can be expected to be of the right form. The calculations of the data of Chevray and Kovasznay (1969) confirm this supposition and demonstrate the loss of accuracy resulting from the truncated form of $\phi_{ij,2}$ used by model II.

The turbulent transport terms were not examined in detail because, it was argued, their magnitude is insufficient to account for the large, observed discrepancies between calculations and experiment.

By a process of elimination, because of its controlling influence on the scale of turbulence and on theoretical grounds, the modelling of the source term in the dissipation equation, S_ε, has been identified as the principal deficiency of the turbulence models. It has been shown that the modelled form of S_ε is only appropriate to similar flows: even in these situations, the simplicity of the detailed modelling and the lack of dependence on streamline curvature suggest that its generality is suspect. For non-similar flows, such as those behind bluff bodies, the inapplicability of the dissipation equation stems from the inadequate representation of the turbulence structure by single-point closures. A two-point closure, based on the energy spectrum, has been suggested as an alternative approach which has the potential of representing non-similar flows.

6.1.4 Combustion Modelling

The probability approach of Lundgren (1967) has been applied to the equations of turbulent reacting flows. The joint probability distribution equations provide a clear picture of the mechanisms involved: the mean and fluctuating velocities transport the joint probability in position space and transport in probability space is caused by the source and by mixing on the microscale. The key to understanding turbulent reacting flows lies in the interrelation of the two latter effects. The term representing microscale mixing has been modelled for the single probability distribution equation and solutions of this equation have been obtained for a simplified premixed combustion system. While the modelling is not completely satisfactory, the solutions, which can be expected to be qualitatively

correct, demonstrate the interrelation of the reaction rate and microscale mixing as a function of the time scales of the system. Consequently, to an extent, the objective of developing a combustion model incorporating the effects of finite reaction rates has been achieved. While the joint probability equations can, potentially, account for finite reaction rates in any combustion system, the difficulty in modelling the microscale mixing term has prevented this potential from being realised.

Combustion models in current usage have been assessed by reference to the probability distribution equations. The theoretical foundations of the models for diffusion and arbitrarily fuelled flames, Lockwood and Naguib (1975a and 1975b), have been consolidated while the eddy-break-up model has been found to be poorly based. A variant of the eddy-break-up model, model B, has been proposed which is consistent with the assumption of a very high reaction rate. The influence of density variations, which is virtually ignored by the above models, has been considered and the practice of mass averaging has been shown to decrease the problems of modelling that it poses.

6.1.5 The Calculation of Bluff Body Stabilised Flames

Calculations have been made of premixed propane/air flames stabilised behind an annular V-gutter in a circular duct. The predictions, obtained with the k-ε turbulence model and both models A and B, have been compared with the measurements of Harrison (1973 and 1974). The similar values of combustion efficiency predicted by both combustion models are in reasonable agreement with the data although the width of the flame is over-predicted by approximately 30%. The agreement between the measured and calculated velocity fields is surprisingly good, bearing in mind the deficiencies of the turbulence model in isothermal flows. It can be concluded from these results that the basic assumption of a very fast single step

reaction is applicable to these flows and, consequently, the inaccuracy in the predictions stem from the detailed modelling rather than from the form of closure adopted.

6.2 Suggestions for further work

Future theoretical investigations of turbulent reacting flows should endeavour to increase the accuracy and generality of turbulence and combustion models. Present models appear to be capable of representing simple flows and reacting systems where the assumption of a very fast single step reaction is valid and so the refinement of the detailed modelling, by reference to experimental data, can be expected to increase the accuracy. In particular, the isotropic viscosity hypothesis, the source of dissipation, the reaction rate in eddy-break-up type models and the treatment of density fluctuations are probable sources of inaccuracy and are worthy of further investigation.

In order to represent many flows of engineering importance, the generality of the models must be increased: for example, the flow in gas turbine combustion chambers is complex and the reaction does not proceed rapidly to produce carbon dioxide and water. The inability of the turbulence models to represent such complex flows has been attributed to the inapplicability of the dissipation equation and, consequently, the development and use of a two-point closure, as described in sub-section 2.4.2, is an important area of further work. The probability approach has the potential of accounting for finite rate multi-stage reactions and the next step towards realising this potential is the modelling of the joint probability distribution equation. As this equation is

computationally expensive to solve, a model based on transport equations for the free parameters in an assumed joint probability distribution (see sub-section 3.3.1) may prove to be a good compromise between accuracy and economy.

REFERENCES

Assaf, H. (1975), "Measurement and calculation of flow properties downstream of blunt body flame stabilisers." M.Sc. Thesis, University of London.

Bilger, R.W. (1975), "A note on Favre averaging in variable density flows." University of California, La Jolla, Dept. of Applied Mechanics and Engineering Sciences Report.

Boussinesq, V.J. (1877), Mem. pres. Acad. Sci. Third Edition, Paris XXIII, p.46.

Bradshaw, P. (1973), "Effects of streamline curvature on turbulent flow." AGARDograph 169.

Bradshaw, P., Ferriss, D.H. and Atwell, N.P. (1967), "Calculation of boundary-layer development using the turbulent energy equation." J. Fluid Mech. 28, p.593.

Bray, K.N.C. (1973), "Equations of turbulent combustion I. Fundamental equations of reacting turbulent flows." University of Southampton, AASU Report 330.

Bray, K.N.C. (1974), "Kinetic energy of turbulence in flames." University of Southampton, AASU Report 332.

Bray, K.N.C. and Moss, J.B. (1974), "A unified statistical model of the premixed turbulent flame." University of Southampton AASU Report 335.

Carmody, T. (1964), "Establishment of the wake behind a disk". J. Basic Eng., 86, p.869.

Champagne, F.H., Harris, V.G. and Corrsin, S. (1970), "Experiments on nearly homogeneous shear flow." J. Fluid Mech. 41, p.81.

Chevray, R. (1968), "The turbulent wake of a body of revolution." J. Basic Eng., 90, p.275.

Chevray, R. and Kovasznay, L.S.G. (1969), "Turbulence measurements in the wake of a thin flat plate." AIAA Journal 7, p.1641.

Chigier, N.A. and Beér, J.M. (1964), "The flow region near the nozzle in double concentric jets." J. Basic Eng., 86, p.797.

Childs, J.H. (1960), "Flame stabilization." Design and Performance of Gas Turbine power plants. Vol. IX Ed W.R. Hawthorne, Oxford.

Chou, P.Y. (1945), "On velocity correlations and the solution of the equations of turbulent fluctuation." Quart. Appl. Math. 3, p.38.

Cushing, B.S., Baucher, J.E., Gandbhir, S. and Shipman, C.W. (1967), "Turbulent mass transfer and rates of combustion in confined, turbulent flames, II." Eleventh Symposium (Int'l) on Combustion, p.817.

Daly, B.J. and Harlow, F.H. (1970), "Transport equations of turbulence." Phys. Fluids, 13, p.2634.

Davies, T.W. and Beér, J.M. (1971), "Flow in the wake of bluff-body flame stabilizers." Thirteenth Symposium (Int'l) on Combustion, p.637.

Dopazo, C. and O'Brien, E.E. (1973). Paper presented at the 4th International Colloquium on Gas Dynamics of Explosions and Reaction Systems, La Jolla, Calif.

Durão, D.F.G. (1975). Private Communication.

Durão, D.F.G., Melling A., Pope, S.B. and Whitelaw, J.H. (1973), "Laser-anemometry measurements in the vicinity of a gutter-stabilised flame." Imperial College, Dept. of Mech. Eng. Report EHT/TN/41.

Durão, D.F.G. and Whitelaw, J.H. (1974), Proceeding of Laser Velocimeter Workshop, Purdue University, (See also, Imperial College, Dept. Mech. Eng. Report HTS/74/14.)

Durst, F., Melling, A. and Whitelaw, J.H. (1972a), "The application of optical anemometry to measurement in combustion systems." Combustion and Flame 18, p.197.

Durst, F., Melling, A. and Whitelaw, J.H. (1972b), "Laser anemometry measurements in a square duct with and without combustion oscillations." Imperial College, Dept. of Mech. Eng. Report HTS/72/25.

Elgobashi, S.E. and Pun, W.M. (1974), "A theoretical and experimental study of turbulent diffusion flames in cylindrical furnaces." Fifteenth Symposium on Combustion, Tokyo, Japan.

Favre, A. (1969), "Statistical equations of turbulent gases." Problems of Hydrodynamics and Continuum Mechanics, Society of Industrial and Applied Mathematics, Philadelphia, P.A. p.231.

Fetting, F., Choudhury, A.P.R. and Wilhelm, R.H. (1959), "Turbulent flame blow-off stability effect of auxiliary gas addition into separation zone." Seventh Symposium (Int'l) on Combustion, p.621.

Fillipi, F. and Fabrovich-Mazza,L. (1962), "Control of bluff-body flame-holder stability limits." Eighth Symposium (Int'l) on Combustion, p.956.

Gordon, S. and McBride, B.J. (1971), "Computer program for calculation of complex chemical equilibrium compositions, rocket performance, incident and reflected shocks, and Chapman-Jouguet detonations." NASA SP-273.

Gosman, A.D. and Lockwood, F.C. (1973), "Prediction of the influence of turbulent fluctuations on flow and heat transfer in furnaces." Imperial College, Dept. of Mech. Eng. Report, HTS/73/53.

Gosman, A.D., Pun, W.M, Runchal, A.K., Spalding, D.B. and Wolfshtein, M. (1969), "Heat and Mass Transfer in Recirculating Flows." Academic Press, London.

Hanjalic, K. and Launder, B.E. (1972), "Asymmetric flow in a plane channel." J. Fluid Mech. 51, p.301.

Harlow, F.H. and Nakayama, P.I. (1967), "Turbulent transport equations." Phys. Fluids, 10, p.323.

Harrison, A.J. (1973), "Combustion tests on an 8" diameter reheat unit with a V-gutter stabiliser burning propane (premix) or kerosine fuels - velocity traverses in the gutter wake." Lucas Aerospace, Burnley Report B.49, 113.

Harrison, A.J. (1974), "Combustion tests on an 8" diameter reheat unit with a V-gutter stabiliser burning propane fuel - velocity traverses in the gutter wake for premixed and line source fuel systems." Lucas Aerospace, Burnley Report B49, 149.

Howe, N.M., Shipman, C.W. and Vranos, A. (1963), "Turbulent mass transfer and rates of combustion in confined turbulent flames." Ninth Symposium (Int'l) on Combustion, p.36.

Jones, W.P. (1971), "Laminarisation in strongly accelerated boundary layers." Ph.D. Thesis, University of London.

Khalil, E.E., Spalding, D.B. and Whitelaw, J.H. (1975), "The calculation of local flow properties in two-dimensional furnaces." Int. J. Heat and Mass Transfer, 18, p.775.

Klebanoff, P.S. (1954), "Characteristics of turbulence in a boundary layer with zero pressure gradient." NACA TN 3178.

Kolmogorov, A.N. (1942), "Equations of turbulent motion of an incompressible fluid." Itr. Ak. Nauk SSSR. (Translation from Russian by D.B. Spalding, Imperial College, 1968).

Launder, B.E., Morse, A.P., Rodi, W. and Spalding, D.B., (1972), "The prediction of free shear flows - a comparison of six turbulence models." NASA Report SP-321, p.361.

Launder, B.E. and Spalding, D.B. (1972)., "Mathematical models of turbulence." Academic Press, London.

Launder, B.E., Reece, G.J. and Rodi, W. (1975), "Progress in the development of a Reynolds-stress turbulence closure." J. Fluid Mech. 68, p.537.

Libby, P.A. (1973). "A provisional analysis of two-dimensional turbulent mixing with variable density." NASA SP-311, p.427.

Lockwood, F.C. and Naguib, A.S. (1975a), "The prediction of the fluctuations in the properties of free, round-jet, turbulent diffusion flames." Combustion and Flame, 24, p.109.

Lockwood, F.C. and Naguib, A.S. (1975b), "A unified method for the prediction of turbulent diffusion and premixed flames." Second European Combustion Symposium, Orleans, France.

Longwell, J.P. (1953), "Flame stabilization by bluff bodies and turbulent flames in ducts." Fourth Symposium (Int'l) on Combustion, p.90.

Longwell, J.P., Chenevey, J.E., Clark, W.W. and Frost, E.E. (1949), "Flame stabilization by baffles in a high velocity gas stream." Third Symposium on Combustion and Flame and Explosion Phenomena, p.41.

Lumley, J.L. (1970), "Towards a turbulent constitutive relation." J. Fluid Mech., 41, p.413.

Lumley, J.L. and Khajeh Nouri, B. (1973), "Modelling homogeneous deformation of turbulence." Pennsylvania State University Report.

Lundgren, T.S. (1967), "Distribution functions in the statistical theory of turbulence". Phys. Fluids 10, p.969.

Mason, H.B. and Spalding, D.B. (1973), "Prediction of reaction rates in turbulent premixed boundary layer flows." Comb. Inst. European Symp. (Ed. F.J. Weinberg) p.601, Academic Press.

McGuirk, J.J. (1971), "Flame stabilisation by recirculation." M.Sc. thesis, University of London.

Murthy, S.N.B. (1974), "Turbulent mixing in non-reactive and reactive flows: a review." Project Squid Workshop on Turbulent Mixing in Nonreactive and Reactive Flows, Purdue University.

Naot, D. Shavit, A. and Wolfshtein, M. (1973), "Two-point correlation model and the redistribution of Reynolds stress." Phys. Fluids, 16, p.738.

Newhall, H.K. and Shahed, S.M. (1971), "Kinetics of nitric oxide formation in high-pressure flames." Thirteenth Symposium (Int'l) on Combustion, p.381.

Ng, K.H. (1971), "Predictions of turbulent boundary-layer developments using a two-equation model of turbulence." Ph.D. thesis, University of London.

Nicholson, H.M. and Field, J.P. (1949), "Some experimental techniques for the investigation of the mechanism of flame stabilization in the wake of bluff bodies." Third Symposium on Combustion and Flame and Explosion Phenomenon, p.45.

Patankar, S.V. and Spalding, D.B. (1970). "Heat and Mass Transfer in Boundary Layers." 2nd Edition, Intertext Books, London.

Patankar, S.V. and Spalding, D.B. (1973), "A calculation procedure for heat, mass and momentum transfer in three-dimensional parabolic flows." Int. J. Heat and Mass Transfer, 15, p.1787.

Pein, R., Peschel, H. and Fetting, F. (1970). "Recirculation zone concentrations and temperatures of bluff body stabilized flames." Combustion Science and Technology, 1, p.327.

Pope, S.B. (1973), "Review of information suitable for testing the prediction of flow in the vicinity of afterburner type flame stabilisers." Imperial College, Dept. of Mech. Eng. Report HTS/73/10.

Pope, S.B. (1975), "A more general effective viscosity hypothesis." J. Fluid Mech. 72, p.331.

Pope, S.B. and Whitelaw, J.H. (1976), "The calculation of near wake flows." J. Fluid Mech. To be published.

Prandtl, L. (1925), "Uber die ausgebildete Turbulenz." Zamm, 5, p.136.

Prandtl, L. and Wieghardt, K. (1945), "Uber ein neues Formelsystem fur die ausgebildete Turbulenz." Nach. Akad. Wiss. Gottingen, Math.-phys. Kh. p.6.

Priddin, C.H. (1975), "The behaviour of the turbulent boundary layer on curved, porous walls." Ph.D. Thesis, University of London.

Reynolds, W.C. (1974), "Computation of turbulent flows." AIAA paper no. 74-556.

Ribeiro, M.M. (1975), Private Communication. (See also, Ph.D. thesis, University of London, to be published).

Rodi, W. (1971), "On the equation governing the rate of turbulent energy dissipation. "Imperial College, Dept. of Mech. Eng. Report TM/TN/A/14.

Rodi, W. (1972), "The prediction of free turbulent boundary layers by use of a two-equation model of turbulence." Ph.D. Thesis, University of London.

Rotta, J.C. (1951), "Statistische Theorie nichthomogener Turbulenz. "Zeitsch f. Physik, 129, p.541.

Runchal, A.K. and Spalding, D.B. (1971), "Steady turbulent flow and heat transfer downstream of a sudden enlargement in a pipe of circular cross-section." Imperial College, Dept. of Mech. Eng. Report, HTS/71/15.

Runchal, A.K. (1973), "Combustion in ducts: the CID3 computer program." Combustion Heat and Mass Transfer Ltd., report. (Not for general circulation.)

Schlicting, H. (1960), "Boundary Layer Theory". McGraw-Hill, New York.

Spalding, D.B. (1970), "Concentration fluctuations in a round turbulent free jet." Imperial College, Dept. of Mech. Eng. Report BL/TN/A/30.

Spalding, D.B. (1971), "Mixing and chemical reaction in steady confined turbulent flames." Thirteenth Symposium (Int'l) on Combustion, p.649.

Spalding, D.B. (1975), "Mathematical models of turbulent flames; a review." Imperial College, Dept. of Mech. Eng. Report HTS/75/1.

Tennekes, H. and Lumley, J.H. (1972), "A first course in turbulence." M.I.T. Press, Cambridge, Mass.

Toor, H.L. (1962), "Mass transfer in dilute turbulent and non-turbulent systems with rapid irreversible reactions and equal diffusivities." A.I.Ch.E.J., 8 p.70.

Townsend, A.A. (1954), "The uniform distortion of homogeneous turbulence." Q.J. Mech. and Appl. Math., 7, p.104.

Tucker, H.J. and Reynolds, A.J. (1968), "The distortion of turbulence by irrotational plane strain." J. Fluid Mech., 32, p.657.

Uberoi, M.S. (1963), "Energy transfer in isotropic turbulence." Phys. Fluids, 6, p.1048.

Uberoi, M.S. (1957), "Equipartition of energy and local isotropy in turbulent flows." J. Appl. Phys. 28, p.1165.

Williams, G.C., Hottel, H.C. and Scurlock, A.C. (1949), "Flame stabilization and propagation in high velocity gas streams. "Third Symposium on Combustion and Flame and Explosion Phenomena, p.21.

Winterfeld, G. (1965), "On processes of turbulent exchange behind flame holders." Tenth Symposium (Int'l) on Combustion, p.1265.

NOMENCLATURE

A	mass fraction of activated species
A_P, A_N, A_S, A_E, A_W	finite-difference coefficients
a_{ij}	normalised Reynolds stress tensor
B_1, B_2, B_3	derived constants in modelled Reynolds
b_1, b_2, b_3	stress equations (model III)
C_{EBU}	eddy-break-up constant
C_{g1}, C_{g2}	constants in g-equation
C_p	specific heat
Cs, $C_\varepsilon, C_{\varepsilon 1}, C_{\varepsilon 2}$	constants in modelled Reynolds stress
$C_{\phi 1}, C_{\phi 2}$	equations
C_μ	effective viscosity constant
C_1, C_2	constants in modelled probability distribution equations
$E(\kappa)$	energy spectrum
$F_{x_i}(\kappa)$	flux of spectral energy in position space
$F_\kappa(\kappa)$	flux of spectral energy in wave number space
f	mixture fraction
G	coefficient in general effective viscosity hypothesis
$G(\tilde{\phi})$	molecular action term in probability distribution equation
g	function in effective viscosity hypothesis
g_{fu}	mean square fuel concentration fluctuations
$g(\tilde{\phi})$	functions in modelled probability
$H(\tilde{\phi})$	distribution equation

H_{fu}	heat of formation of fuel
h	enthalpy
I, I_2	unit matricies in 3 and 2 dimensions
k	kinetic energy of turbulence
m_α	mass fraction of species α
$N(\tilde{f})$	clipped-Gaussian probability distribution
P	pressure
P, P_{ij}	production of kinetic energy and Reynolds stress
$p(\tilde{\phi})$	probability distribution of ϕ
p'	pressure fluctuation
R_{ij}	two-point correlation tensor
r	radius
S_ε	source in dissipation equation
$S_\alpha(\underline{\phi})$	source of species α
s	stoichiometric coefficient
s_{ij}	normalised rate of strain tensor
T	temperature
T_{ij}	tensor function in effective viscosity hypothesis
t	time
U_i, u_i	velocity and fluctuating velocity vectors
U, u	velocity and fluctuating velocity in
V, v	orthogonal coordinates
W, w	
x, y, z	orthogonal coordinates
Γ	diffusive coefficient
$\delta(\tilde{\phi})$	Dirac delta function
δ_{ij}	Kronecker delta
ε	dissipation of kinetic energy of turbulence

η	combustion efficiency
κ	wave number
μ, μ_{eff}	laminar and effective viscosities
ρ	density
σ	rate of strain invariant
$\sigma_k, \sigma_\varepsilon, \sigma_g, \sigma_{fu}$	effective Prandtl-Schmidt numbers
τ, τ_t	turbulent time scale
τ_R	residence time
τ_k	chemical kinetic time scale
ϕ	scalar quantity
$\phi_{ij,1}, \phi_{ij,2}$	redistribution terms
Ω	rotation invariant
ω_{ij}	normalised rotation tensor

Subscripts

A	activated species
fu, ox, pr	fuel, oxygen and products
N,S,E,W,p	grid node locations

Conventions

$\langle\phi\rangle$, ϕ'	mean and fluctuating component of ϕ
$\overline{\phi}$, ϕ''	mass weighted mean and fluctuating component of ϕ
$\hat{\phi}$	$\langle \phi'^2 \rangle^{\frac{1}{2}}$
$\tilde{\phi}$	independent variable in probability space
{ }	(Chapter 2) trace of a matrix (Appendix) term to be omitted in Cartesian coordinates.

APPENDIX

Modelled Equations in Two-Dimensional Cartesian and Polar Cylindrical Coordinates

The modelled equations are stated here in the form in which they are solved by the numerical procedures. In addition to the coordinate system introduced in section 4.2, an additional convention is used to permit the expression of the equations in a common form; namely, terms in curled brackets, { } , are only appropriate to polar cylindrical coordinates. Further, for brevity, the convective and diffusive terms are denoted by $\frac{D\rho\phi}{Dt}$ and $D(\phi)$ where,

$$\frac{D\rho\phi}{Dt} = \frac{\partial \rho U \phi}{\partial x} + \frac{1}{r} \frac{\partial \rho V r \phi}{\partial y} \qquad (A.1)$$

$$D_1(\phi) = \frac{\partial}{\partial x} \left(\mu_{eff} \frac{\partial \phi}{\partial x}\right) + \frac{1}{r} \frac{\partial}{\partial y} \left(r \mu_{eff} \frac{\partial \phi}{\partial y}\right) \qquad (A.2)$$

and $$D_2(\phi) = \frac{\partial}{\partial x} \left(\rho \frac{k}{\varepsilon} \langle u^2 \rangle \frac{\partial \phi}{\partial x}\right) + \frac{1}{r} \frac{\partial}{\partial y} \left(r \rho \frac{k}{\varepsilon} \langle v^2 \rangle \frac{\partial \phi}{\partial y}\right)$$

$$+ \frac{\partial}{\partial x} \left(\rho \frac{k}{\varepsilon} \langle uv \rangle \frac{\partial \phi}{\partial y}\right) + \frac{1}{r} \frac{\partial}{\partial y} \left(r \rho \frac{k}{\varepsilon} \langle uv \rangle \frac{\partial \phi}{\partial x}\right) \qquad (A.3)$$

D_1 is the diffusion model used by model I and D_2 is that employed by both Reynolds stress closures. The right hand sides of equations A.1 and A.2 are incorporated implicitly in the finite-difference equations as are the first two terms in equation A.3: the final two terms in this equation are added to the source.

For all calculations performed, the continuity relation is,

$$\frac{D\rho}{Dt} = 0 \qquad (A.4)$$

A.1 Equations for Combustion Calculations.

The calculations of reacting flows were performed with the basic procedure, described in section 4.2, incorporating the k-ε turbulence model, model I. Model A solves transport equations for the unweighed mean values of U, V, k, ε, m_{fu} and g_{fu} while model B solves for their mass averaged values, excepting g_{fu}.

$$\frac{D}{Dt}\rho U = D_1(U) + \frac{\partial}{\partial x}(\mu_{eff}\frac{\partial U}{\partial x}) + \frac{1}{r}\frac{\partial}{\partial y}(r\,\mu_{eff}\frac{\partial V}{\partial x}) - \frac{\partial}{\partial x}(p + {}^2/_3\,\rho k) \quad * \qquad (A.5)$$

$$\frac{D}{Dt}\rho V = D_1(V) + \frac{\partial}{\partial x}(\mu_{eff}\frac{\partial U}{\partial y}) + \frac{1}{r}(\frac{\partial}{\partial y}\,r\,\mu_{eff}\frac{\partial V}{\partial y}) -$$

$$- \frac{\partial}{\partial y}(p + {}^2/_3\,\rho\,k) - \{\,2\,\mu_{eff}\,V/r\,\} \qquad (A.6)$$

$$\frac{D}{Dt}\rho k = D_1(k/\sigma_k) + P - \rho\varepsilon \qquad (A.7)$$

$$\frac{D}{Dt}\rho\varepsilon = D_1(\varepsilon/\sigma_\varepsilon) + \frac{\varepsilon}{k}(C_{\varepsilon 1}P - C_{\varepsilon 2}\rho\varepsilon) \qquad (A.8)$$

$$\frac{D}{Dt}\rho\, m_{fu} = D_1(m_{fu}/\sigma_{fu}) + S_{fu} \qquad (A.9)$$

$$\frac{D}{Dt}\rho\, g_{fu} = D_1(g_{fu}/\sigma_g) + C_{g1}\,\rho\,\frac{k^2}{\varepsilon}[(\frac{\partial m_{fu}}{\partial x})^2 + (\frac{\partial m_{fu}}{\partial y})^2] - C_{g2}\,\rho\,\frac{\varepsilon}{k}\,g_{fu} \qquad (A.10)$$

$$\mu_{eff} = C_\mu\,\rho\,k^2/\varepsilon \qquad (A.11)$$

$$P = \mu_{eff}[(\frac{\partial U}{\partial y} + \frac{\partial V}{\partial x})^2 + 2(\frac{\partial U}{\partial x})^2 + 2(\frac{\partial V}{\partial y})^2 + 2\,(V/r)^2] \qquad (A.12)$$

---

* The lower case p is used to denote pressure in order to avoid confusion with the production of kinetic energy, P.

The determination of the density, ρ, and the reaction rate of fuel, S_{fu}, is described in section 3.5.

A.2 Equations for Isothermal Calculations

The isothermal flows were predicted with all three turbulence models. The Reynolds stress closures necessitated the use of the new procedure described in section 4.3 which was used even in conjunction with model I. This procedure solves the momentum equations in their exact form,

$$\frac{D}{Dt}\rho U = -\frac{\partial}{\partial x}\rho\langle u^2\rangle - \frac{1}{r}\frac{\partial}{\partial y} r\,\rho\langle uv\rangle - \frac{\partial p}{\partial x} \qquad (A.13)$$

$$\frac{D}{Dt}\rho V = -\frac{\partial}{\partial x}\rho\langle uv\rangle - \frac{1}{r}\frac{\partial}{\partial y} r\,\rho\langle v^2\rangle - \frac{\partial p}{\partial y} + \{\rho\langle w^2\rangle/r\} \qquad (A.14)$$

Model I. The Reynolds stresses are given by,

$$\begin{aligned}
\rho\langle uv\rangle &= -\mu_{eff}\left(\frac{\partial U}{\partial y} + \frac{\partial V}{\partial x}\right)\\
\rho\langle u^2\rangle &= 2/3\,\rho k - 2\mu_{eff}\frac{\partial U}{\partial x} \qquad (A.15)\\
\rho\langle v^2\rangle &= 2/3\,\rho k - 2\mu_{eff}\frac{\partial V}{\partial y}\\
\rho\langle w^2\rangle &= 2/3\,\rho k - \{2\mu_{eff}\,V/r\}
\end{aligned}$$

The effective viscosity is given by equation A.11 and the equations solved for k and ε are identical to equations A.7 and A.8.

The production of kinetic energy is given by,

$$P = -\rho\left(\langle uv\rangle\left(\frac{\partial U}{\partial y} + \frac{\partial V}{\partial x}\right) + \langle u^2\rangle\frac{\partial U}{\partial x} + \langle v^2\rangle\frac{\partial V}{\partial y} + \{\langle w^2\rangle\ V/r\}\right) \qquad (A.16)$$

Reynolds Stress Models. The two Reynolds stress closures differ only in the redistribution term: their common form is,

$$\frac{D}{Dt}\rho\langle u^2\rangle = D_2\left(C_s\langle u^2\rangle\right) + P_{11} + R_{11} - {}^2/_3\,\rho\varepsilon$$

$$\frac{D}{Dt}\rho\langle v^2\rangle = D_2\left(C_s\langle v^2\rangle\right) + P_{22} + R_{22} - {}^2/_3\,\rho\varepsilon$$

$$- \left\{2\rho C_s \frac{k}{\varepsilon}\langle w^2\rangle\left(\langle v^2\rangle - \langle w^2\rangle\right)/r^2\right\}$$

$$\frac{D}{Dt}\rho\langle w^2\rangle = D_2\left(C_s\langle w^2\rangle\right) + P_{33} + R_{33} - {}^2/_3\,\rho\varepsilon \qquad \text{(A.17)}$$

$$+ \left\{2\rho C_s \frac{k}{\varepsilon}\langle w^2\rangle\left(\langle v^2\rangle - \langle w^2\rangle\right)/r^2\right\}$$

$$\frac{D}{Dt}\rho\langle uv\rangle = D_2\left(C_s\langle uv\rangle\right) + P_{12} + R_{12} - \left\{\rho C_s \frac{k}{\varepsilon}\langle w^2\rangle\langle uv\rangle/r^2\right\}$$

$$\frac{D}{Dt}\rho\varepsilon = D_2\left(C_\varepsilon\varepsilon\right) + \frac{\varepsilon}{k}\left(C_{\varepsilon 1}P - C_{\varepsilon 2}\rho\varepsilon\right) \qquad \text{(A.18)}$$

where

$$P_{11} = -2\rho\left(\langle u^2\rangle\frac{\partial U}{\partial x} + \langle uv\rangle\frac{\partial U}{\partial y}\right)$$

$$P_{22} = -2\rho\left(\langle v^2\rangle\frac{\partial V}{\partial y} + \langle uv\rangle\frac{\partial V}{\partial x}\right) \qquad \text{(A.19)}$$

$$P_{33} = -\left\{2\rho\langle w^2\rangle V/r\right\}$$

$$P_{12} = -\rho\left(\langle v^2\rangle\frac{\partial U}{\partial y} + \langle u^2\rangle\frac{\partial V}{\partial x} - \left\{\langle uv\rangle\ V/r\right\}\right)$$

The redistribution terms for each model are,

Model 2

$$R_{11} = - C_{\phi 1} \frac{\rho\varepsilon}{k} (\langle u^2 \rangle - 2/3\ k) - C_{\phi 2} (P_{11} - 2/3\ P)$$

$$R_{22} = - C_{\phi 1} \frac{\rho\varepsilon}{k} (\langle v^2 \rangle - 2/3\ k) - C_{\phi 2} (P_{22} - 2/3\ P)$$

$$R_{33} = - C_{\phi 1} \frac{\rho\varepsilon}{k} (\langle w^2 \rangle - 2/3\ k) - C_{\phi 2} (P_{33} - 2/3\ P) \qquad \text{(A.20)}$$

$$R_{12} = - C_{\phi 1} \frac{\rho\varepsilon}{k} \langle uv \rangle - C_{\phi 2} P_{12}$$

Model 3

$$R_{11} = - C_{\phi 1} \frac{\rho\varepsilon}{k} (\langle u^2 \rangle - 2/3\ k) - B_1 (P_{11} - 2/3\ P)$$

$$- 2B_2\ \rho k \frac{\partial U}{\partial x} + 2B_3 \left(\rho \langle u^2 \rangle \frac{\partial U}{\partial x} + \rho \langle uv \rangle \frac{\partial V}{\partial x} + 1/3\ P\right)$$

$$R_{22} = - C_{\phi 1} \frac{\rho\varepsilon}{k} (\langle v^2 \rangle - 2/3\ k) - B_1 (P_{22} - 2/3\ P)$$

$$- 2B_2\ \rho\ k \frac{\partial V}{\partial y} + 2B_3 \left(\rho \langle v^2 \rangle \frac{\partial V}{\partial y} + \rho \langle uv \rangle \frac{\partial U}{\partial y} + 1/3\ P\right) \qquad \text{(A.21)}$$

$$R_{33} = - C_{\phi 1} \frac{\rho\varepsilon}{k} (\langle w^2 \rangle - 2/3\ k) - B_1 (P_{33} - 2/3\ P)$$

$$- \{2B_2\ \rho k\ V/r\} + 2B_3 \left(\{\rho \frac{\langle w^2 \rangle V}{r}\} + 1/3\ P\right)$$

$$R_{12} = - C_{\phi 1} \frac{\rho\varepsilon}{k} \langle uv \rangle - B_1 P_{12}$$

$$- B_2\ \rho k \left(\frac{\partial U}{\partial y} + \frac{\partial V}{\partial x}\right) + B_3\ \rho \left(\langle u^2 \rangle \frac{\partial U}{\partial y} + \langle v^2 \rangle \frac{\partial V}{\partial x} + \langle uv \rangle \left[\frac{\partial U}{\partial x} + \frac{\partial V}{\partial y}\right]\right)$$

where,

$$B_1 = (C_{\phi 2} + 8)/11$$

$$B_2 = (30\ C_{\phi 2} - 2)/55 \qquad \text{(A.22)}$$

$$B_3 = (8\ C_{\phi 2} - 2)/11$$

Table I Values of Constants

Model	I	II	III	A	B	Origin
C_μ	0.09			0.09	0.09	a
σ_k	0.9			0.9	0.9	a
σ_ε	1.3			1.3	1.3	a
$C_{\varepsilon 1}$	1.45	1.45	1.45	1.45	1.45	b
$C_{\varepsilon 2}$	1.90	1.90	1.90	1.90	1.90	b
$C_{\phi 1}$		2.5	1.5			b
$C_{\phi 2}$		0.4	0.4			b
C_s		0.25	0.25			b
C_ε		0.15	0.15			b
C_{g1}				2.8		c
C_{g2}				2.0		c
σ_g				0.7		c
$\sigma_{m_{fu}}$				0.7	0.7	c
C_{EBU}				1.1		d
C_2					1.0	d

a - Launder, Morse, Rodi and Spalding (1972)

b - Launder, Reece and Rodi (1975)

c - Elgobashi and Pun (1974)

d - Optimisation, see sub-section 5.2.2

LIST OF FIGURES

Page

Model III ————————

Model III with doubled inlet V velocity — — — —

Model III with inlet ε decreased by 20% —·—·—·—

Figs. 5.3 to 5.5 Flow of Chevray and Kovasznay (1969);

Measurements ⊙ ◇

Model I ----------

Model II — — — — —

Model III ————————

Model III with inlet ε increased by 20% – – – – – –

Figs. 5.6 to 5.9 Flow of Carmody (1964);

Measurements ⊙

Model I ----------

Model II — — — — —

Model III ————————

Model III Inlet V-velocity decreased by 80% —·—·—·—·—

Model III Inlet ε doubled – – – – – –

Model III Augmented turbulence at inlet —·—·—·—·—

Page

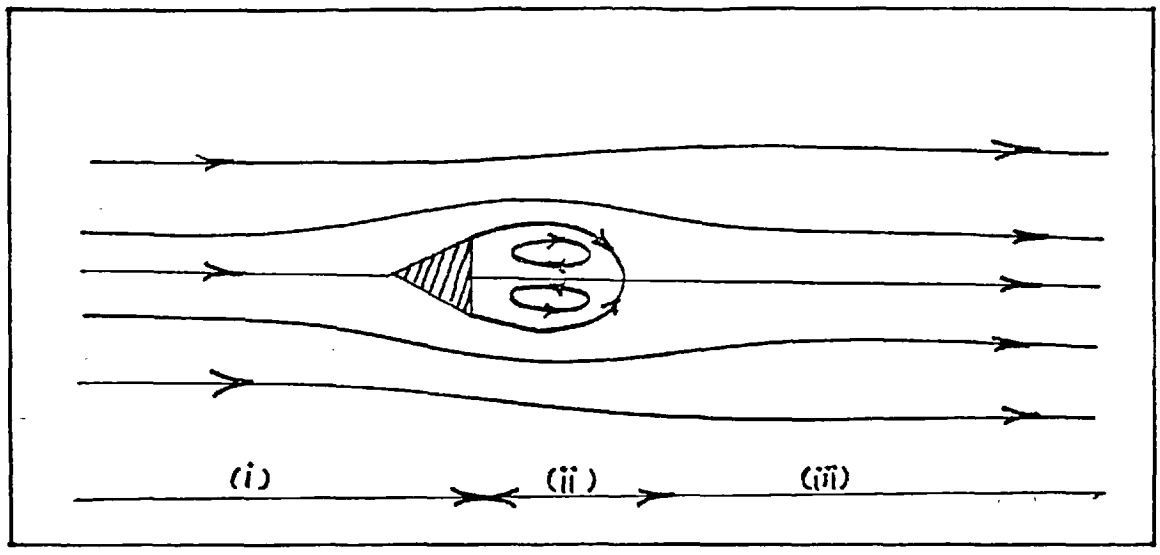

Figure 1.1 Isothermal flow behind a cone.

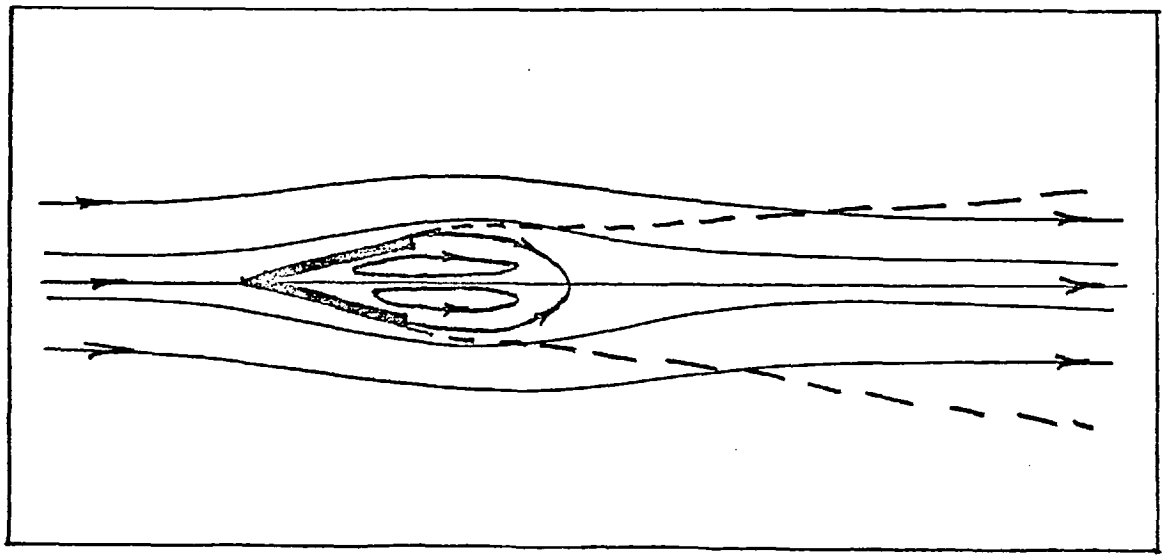

Figure 1.2 Flame stabilised behind a V-gutter.

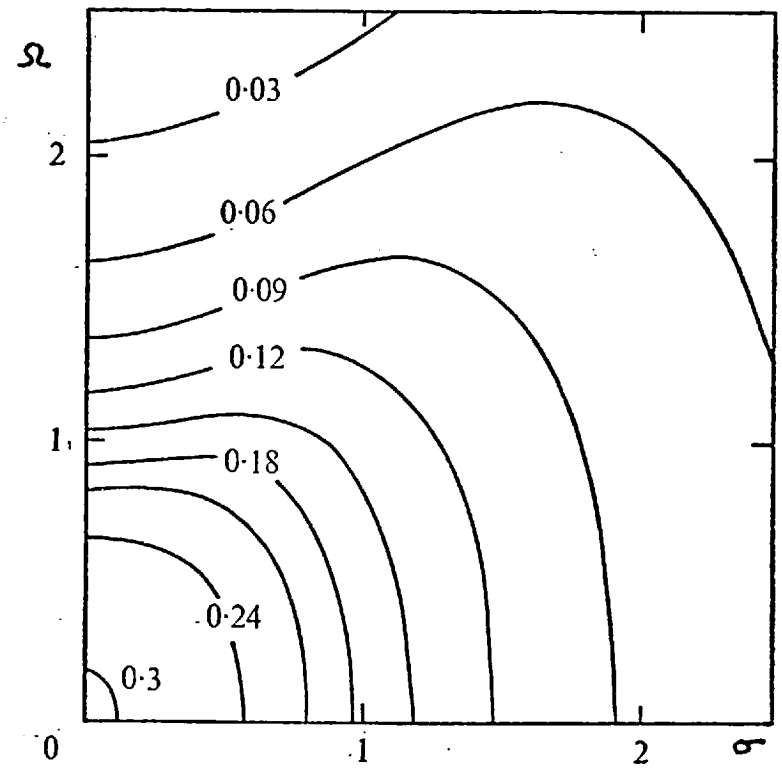

Figure 2.1 Variation of C_μ with σ and Ω .

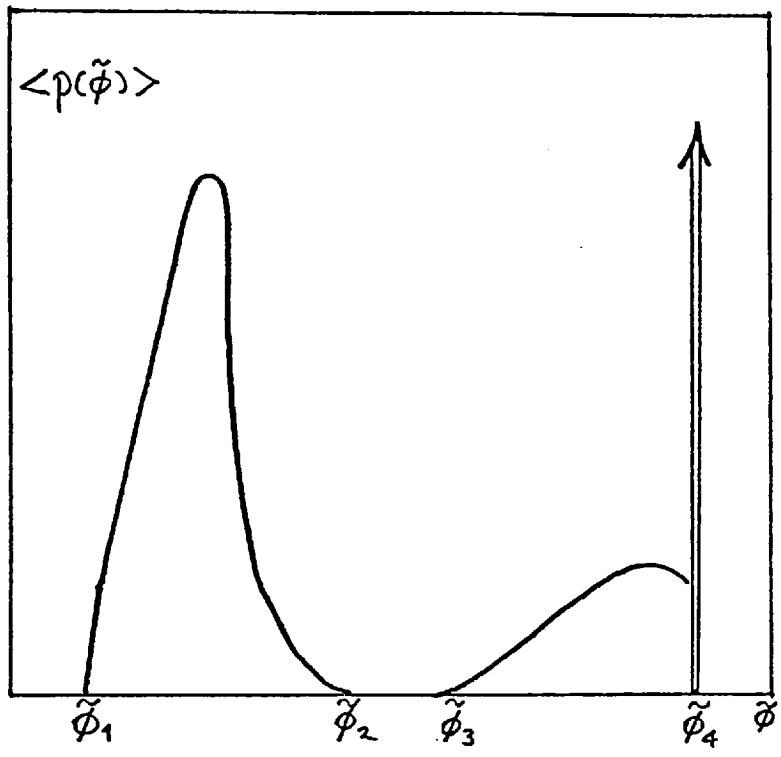

Figure 3.1 General single probability distribution :
$\langle p(\tilde{\phi}) \rangle$ against $\tilde{\phi}$.

Figure 3.2 Inert, homogeneous, flow: $\langle p(\tilde{\sigma}) \rangle$ against $\tilde{\sigma}$ and τ_R/τ_t.

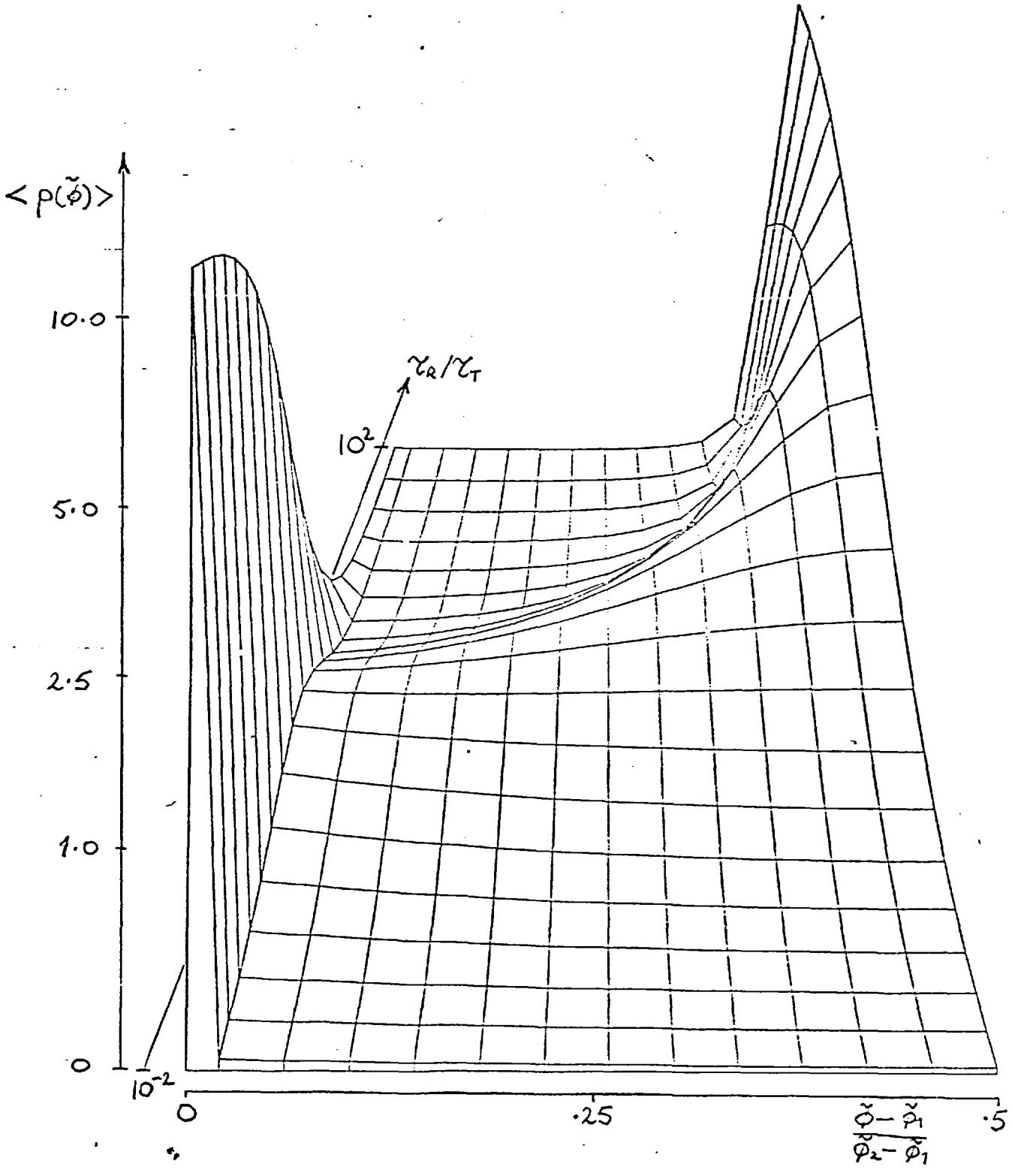

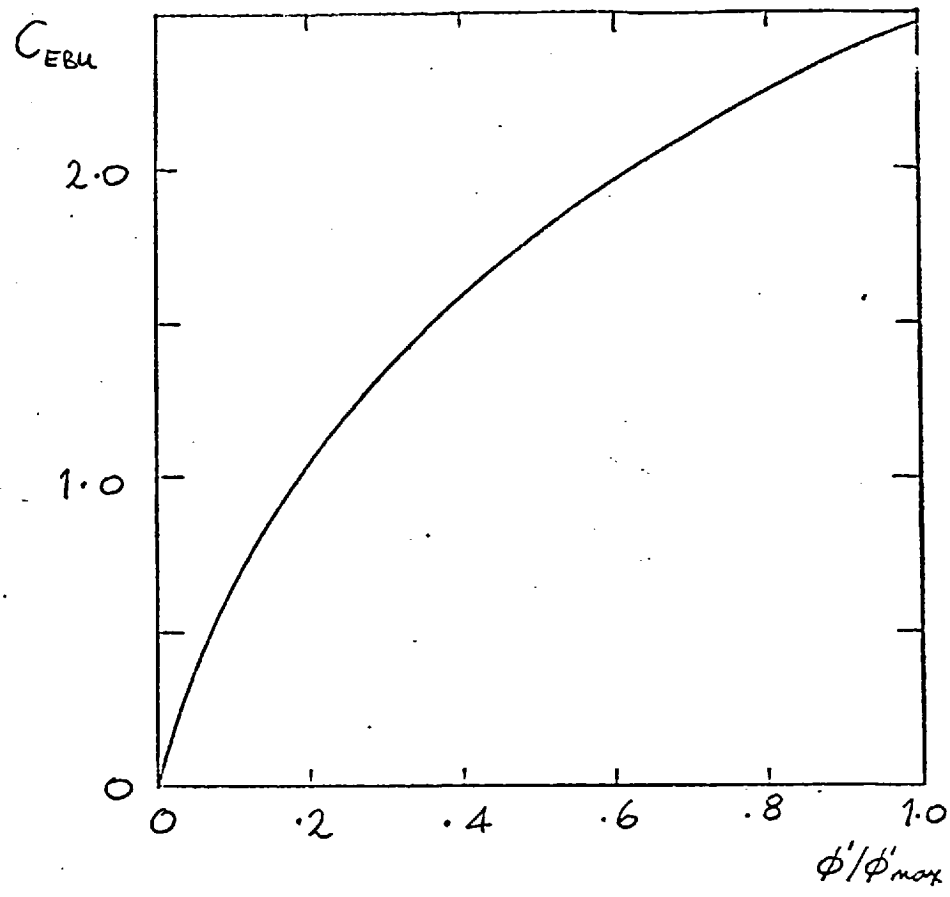

Figure 3.3 Reacting homogeneous flow:
C_{EBU} against $\hat{\phi}/\hat{\phi}_{max}$

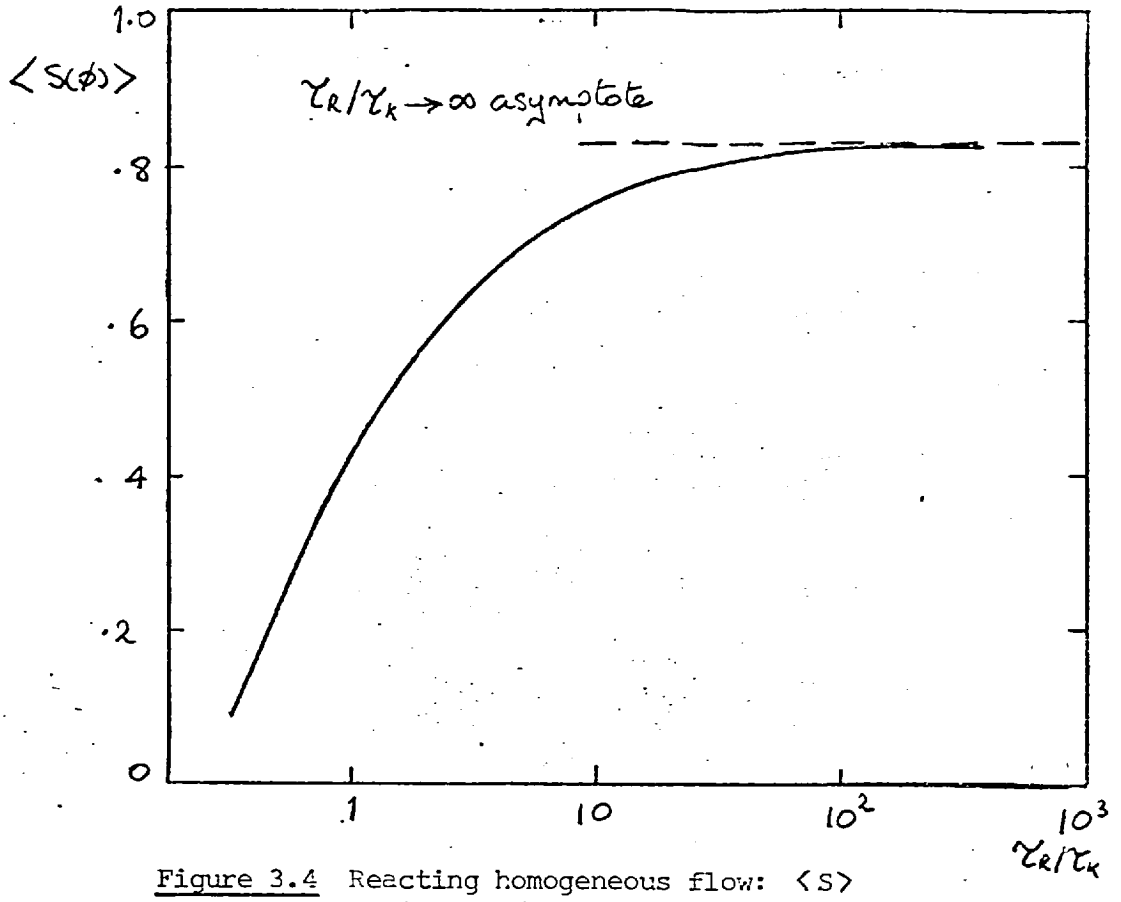

Figure 3.4 Reacting homogeneous flow: $\langle S \rangle$ against τ_R/τ_k, $\tau_R/\tau_t = 1$.

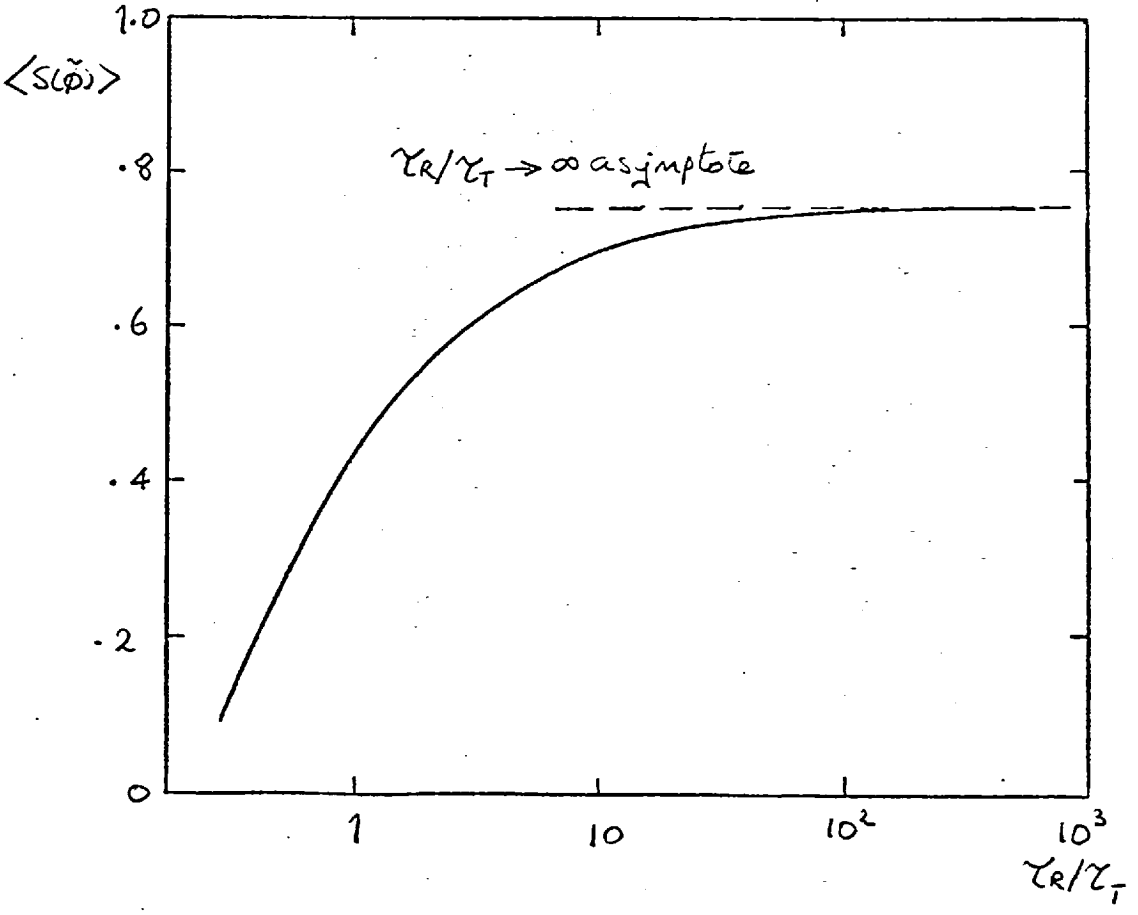

Figure 3.5 Reacting homogeneous flow: $\langle S \rangle$ against τ_R/τ_t, $\tau_R/\tau_k = 1$.

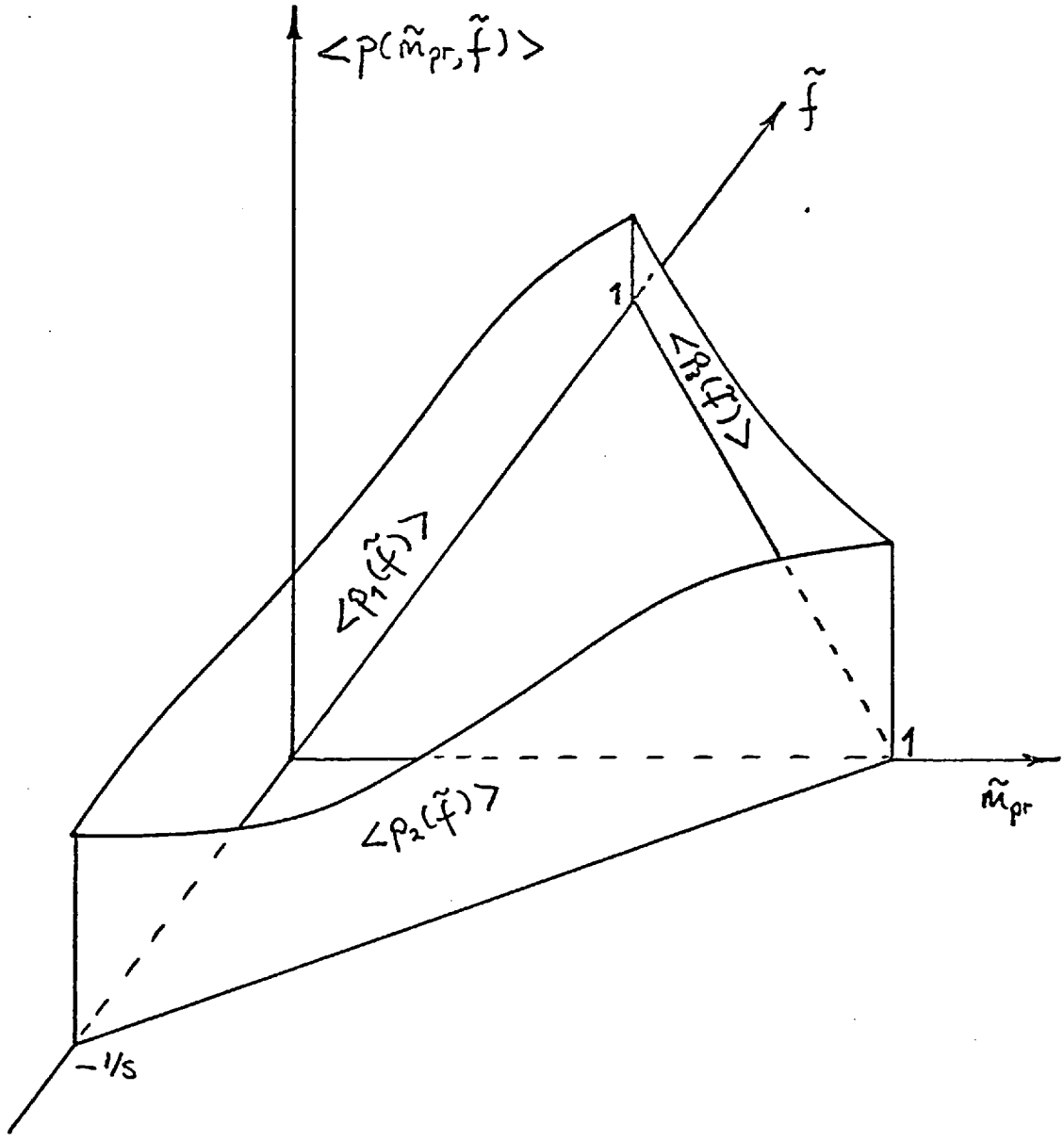

Figure 3.6 Joint probability distribution, equation 3.85: $\langle p(\tilde{m}_{pr},\tilde{f})\rangle$ against $\tilde{m}_{pr}$ and $\tilde{f}$.

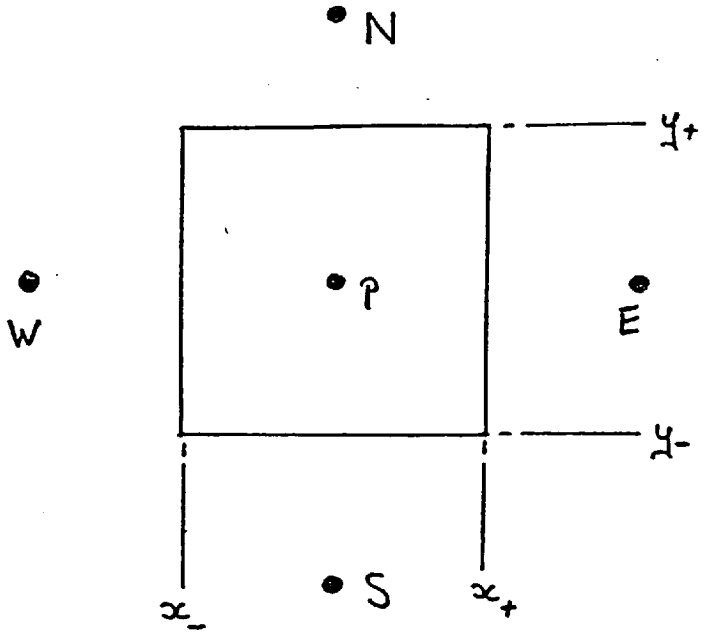

Figure 4.1 Finite-difference grid.

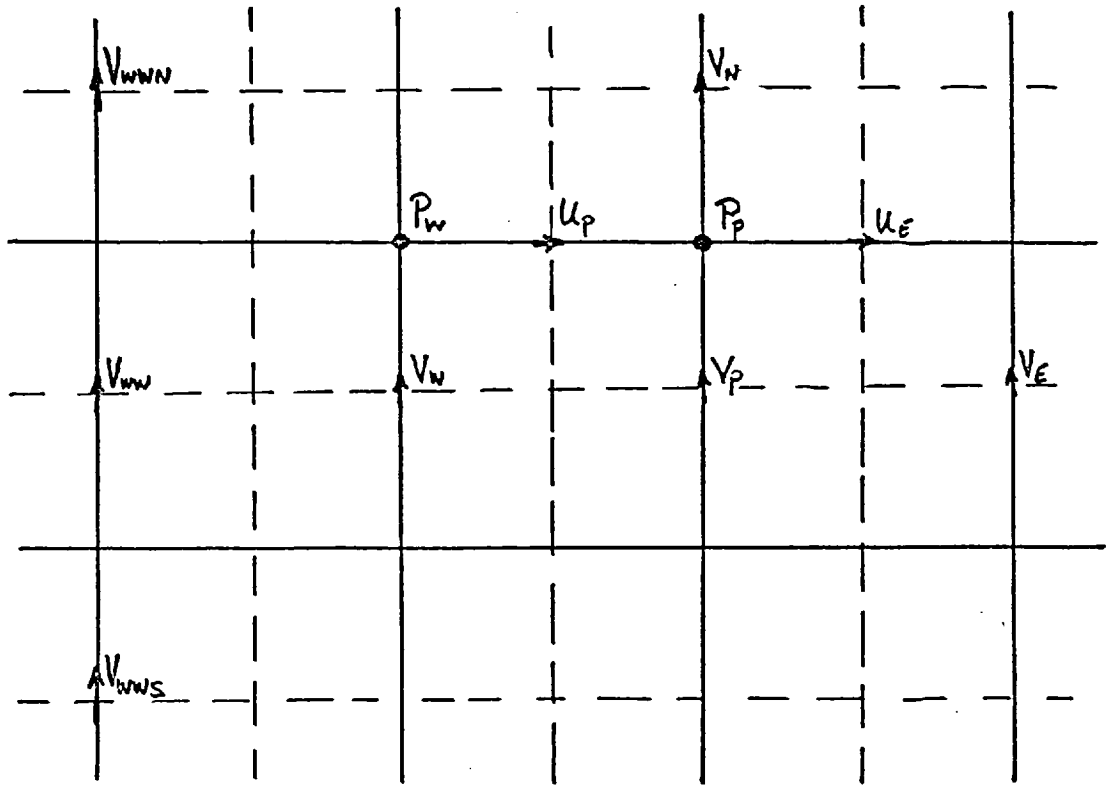

Figure 4.2 Finite-difference grids for the basic procedure.

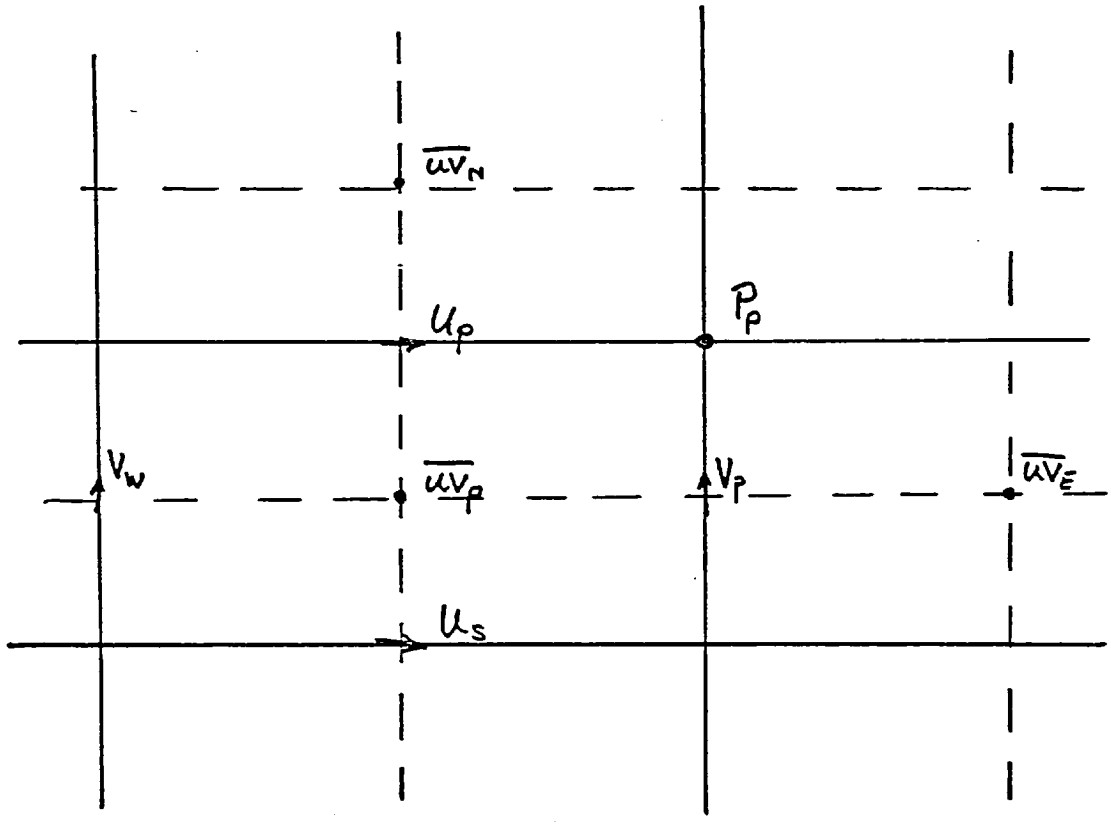

Figure 4.3 Finite-difference grids for the Reynolds stress procedure.

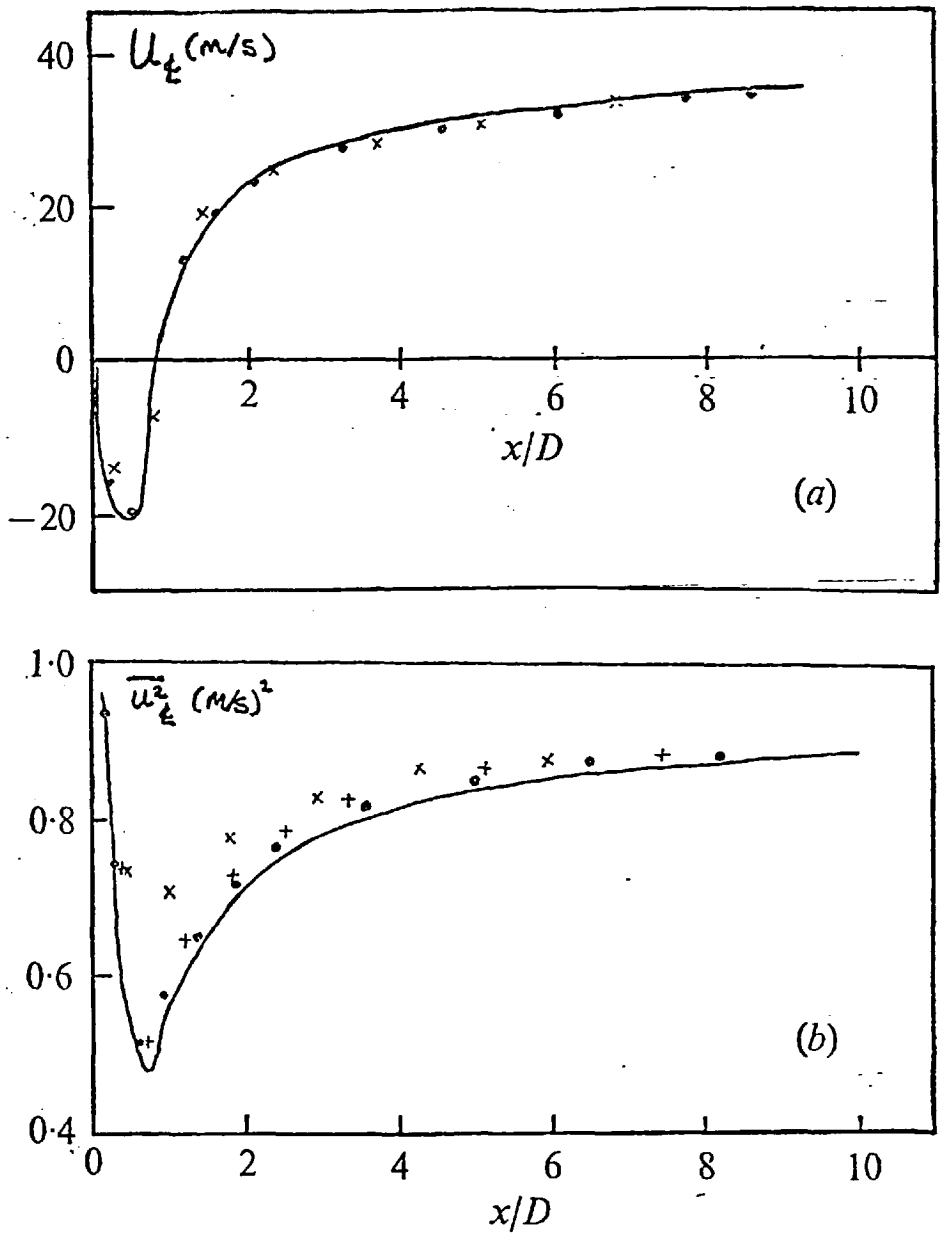

Figure 4.4 Solution algorithm test calculations: flow behind a disc.

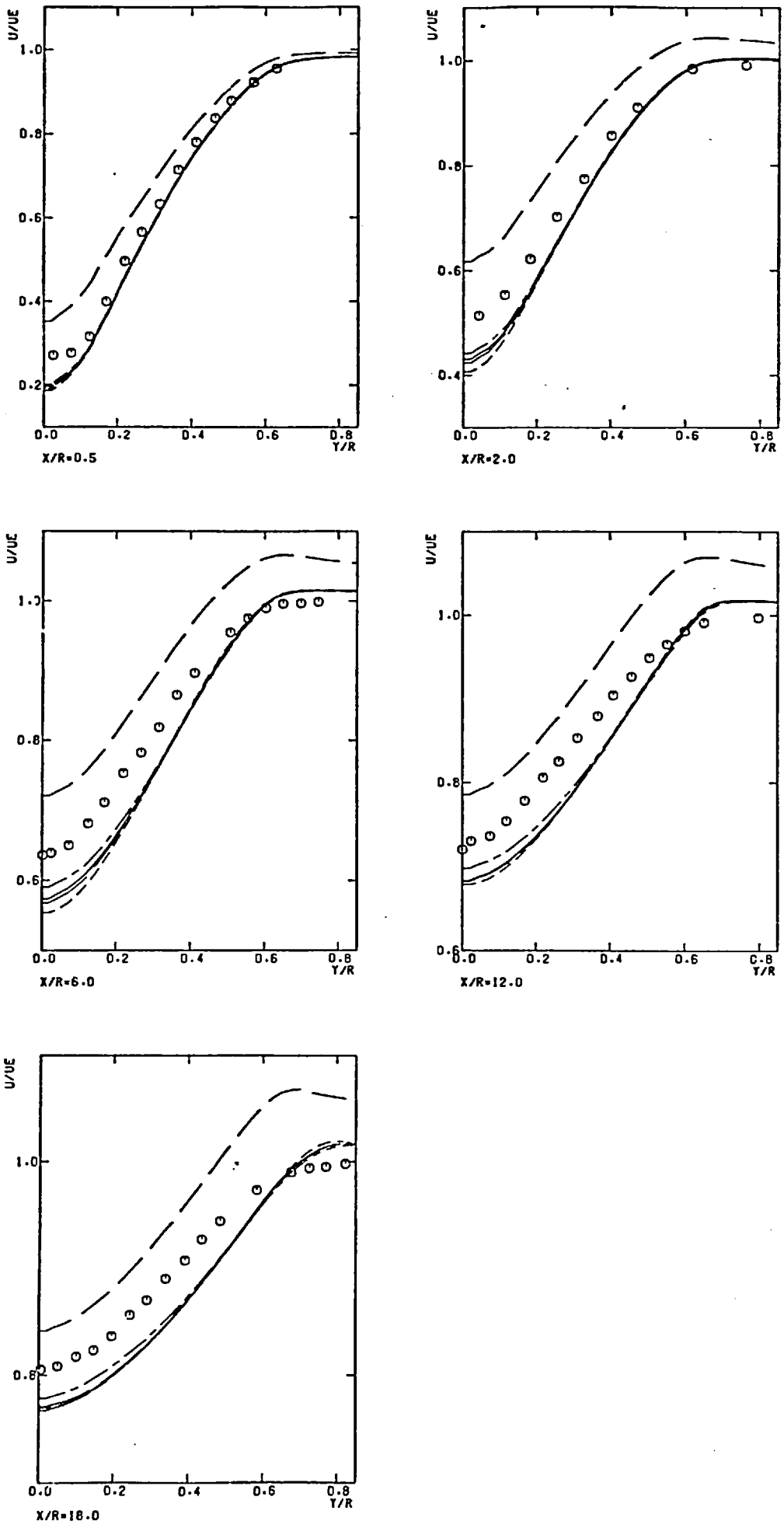

Figure 5.1 Flow of Chevray (1968): U/U_E against y/R.

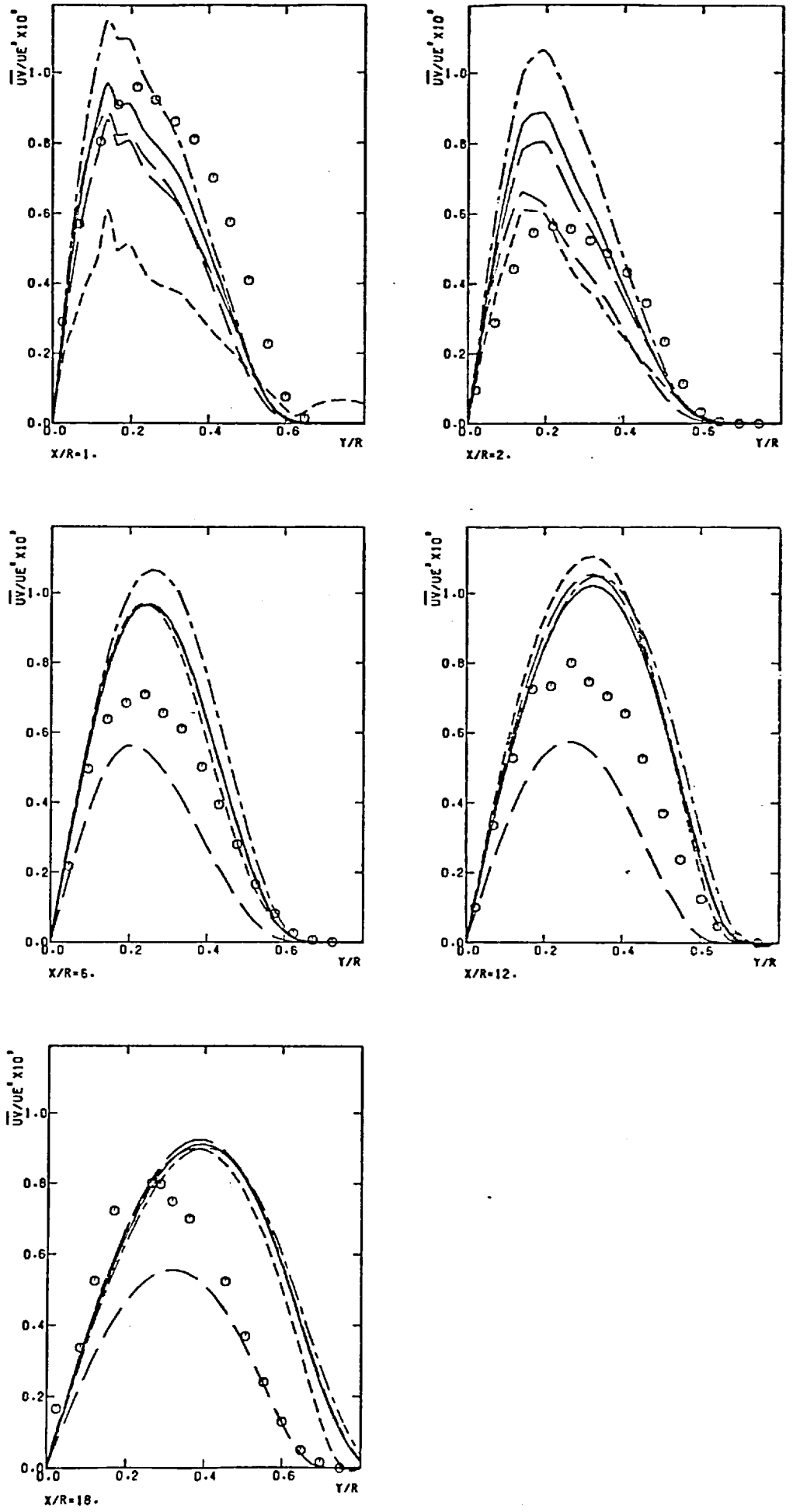

Figure 5.2 Flow of Chevray (1968): $\overline{uv}/U_E^2$ against y/R.

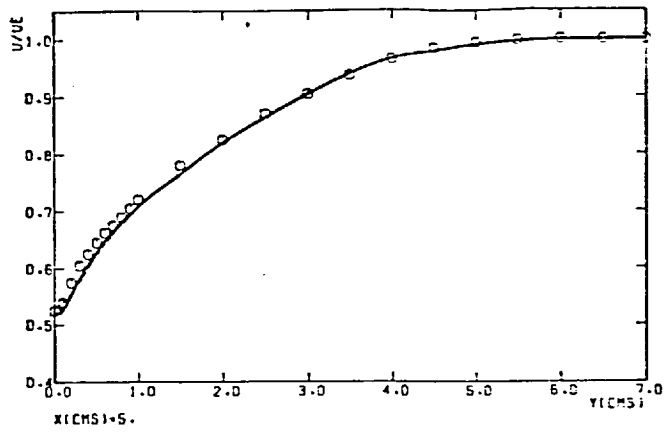

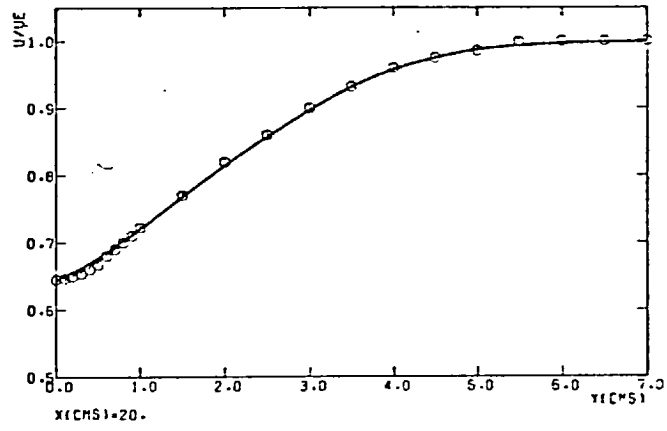

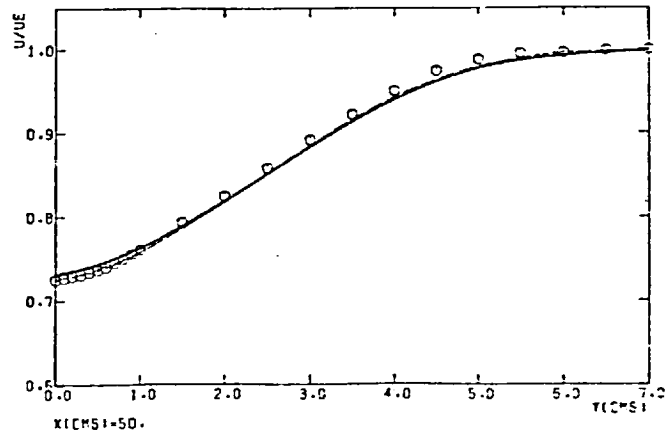

Figure 5.3 Flow of Chevray and Kovasznay (1969): U/U_E against y.

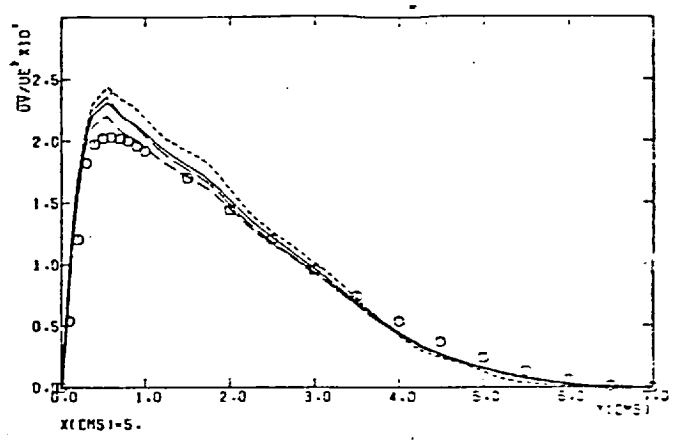

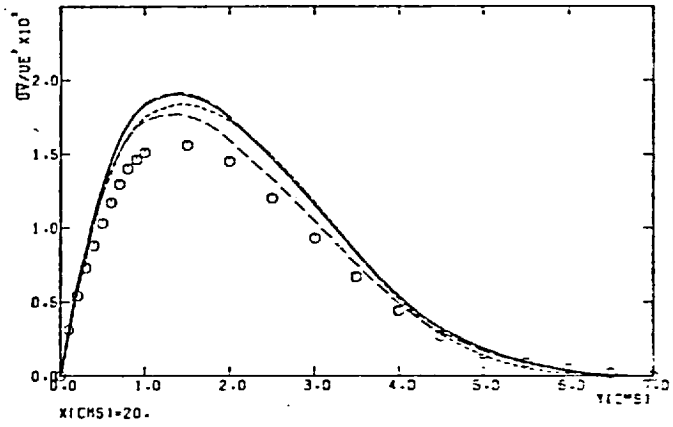

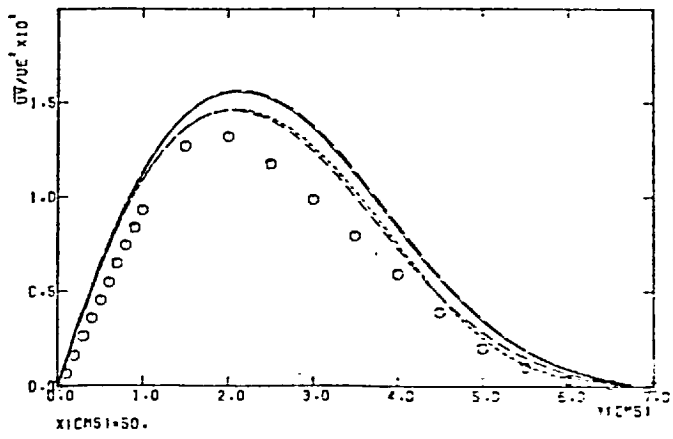

Figure 5.4 Flow of Chevray and Kovasznay (1969): $\overline{uv}/U_E$ against y.

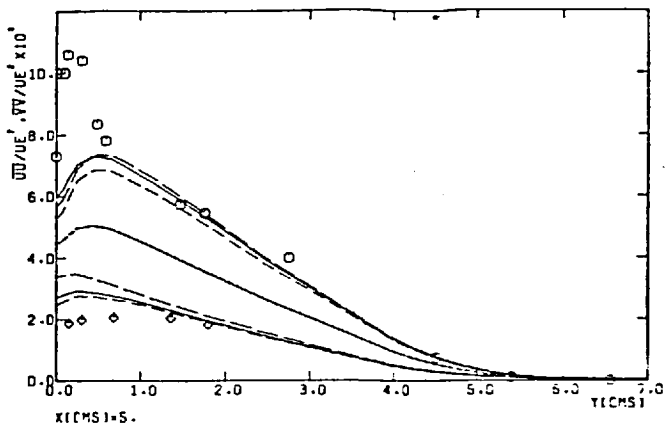

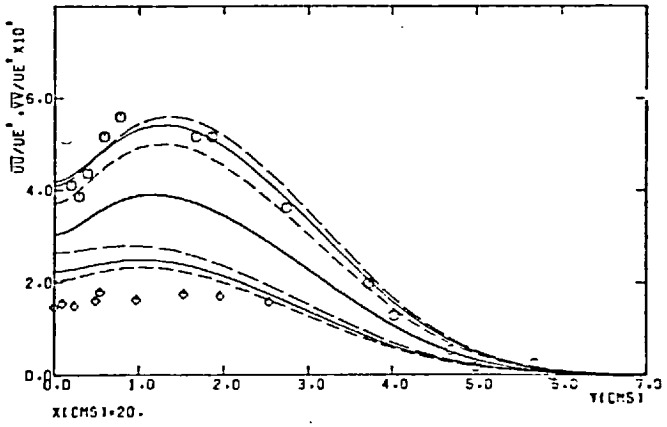

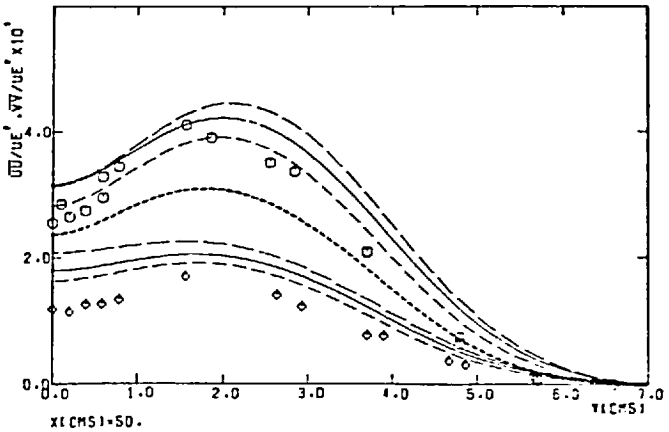

Figure 5.5 Flow of Chevray and Kovasznay (1969): $\overline{u^2}/U_E^2$ and $\overline{v^2}/U_E^2$ against y.

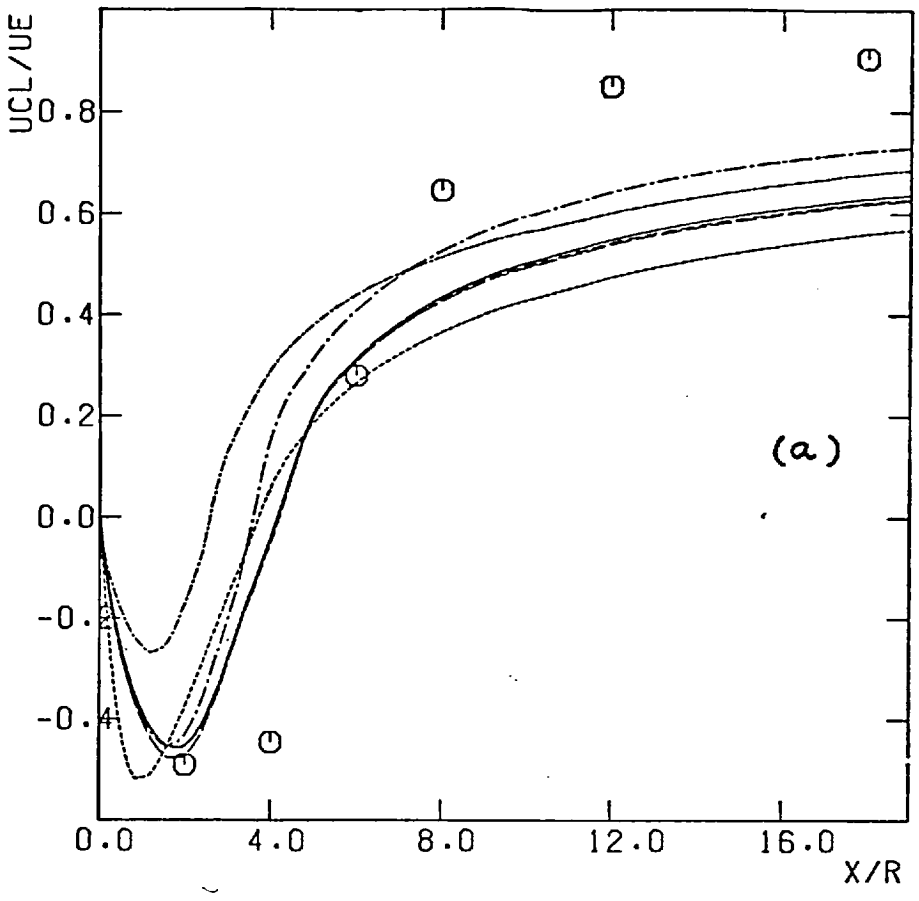

Figure 5.6 Flow of Carmody (1964):
(a) U/U_E against x/R and

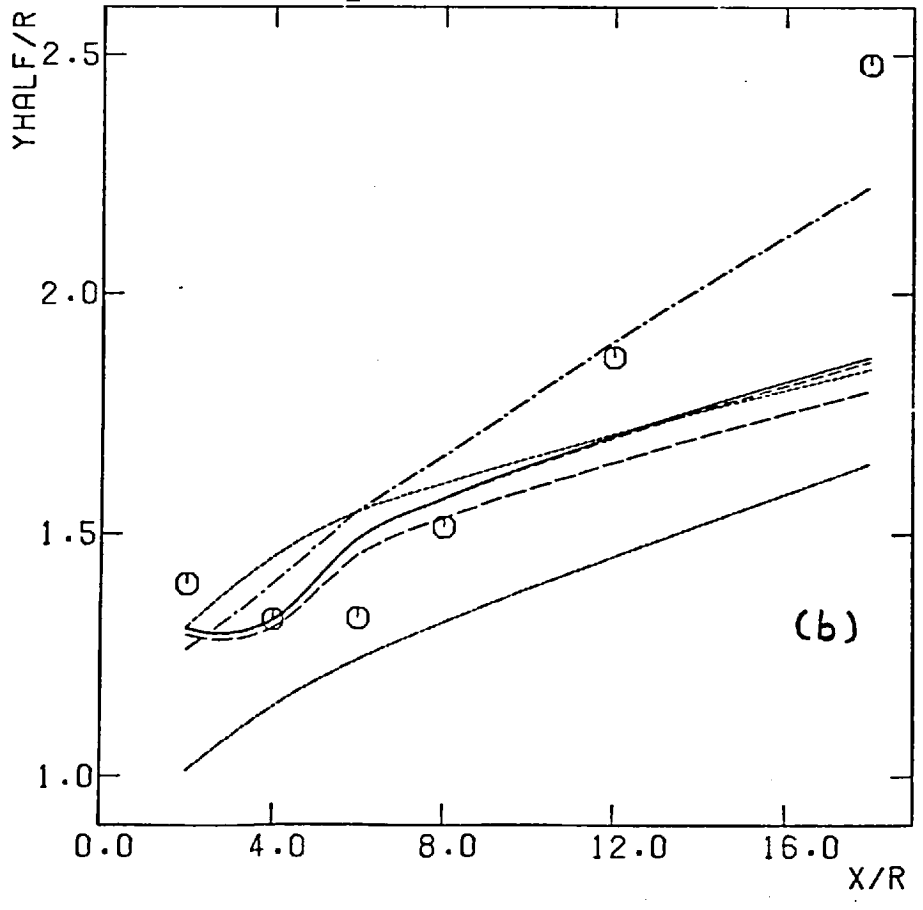

(b) $y_{\frac{1}{2}}/R$ against x/R.

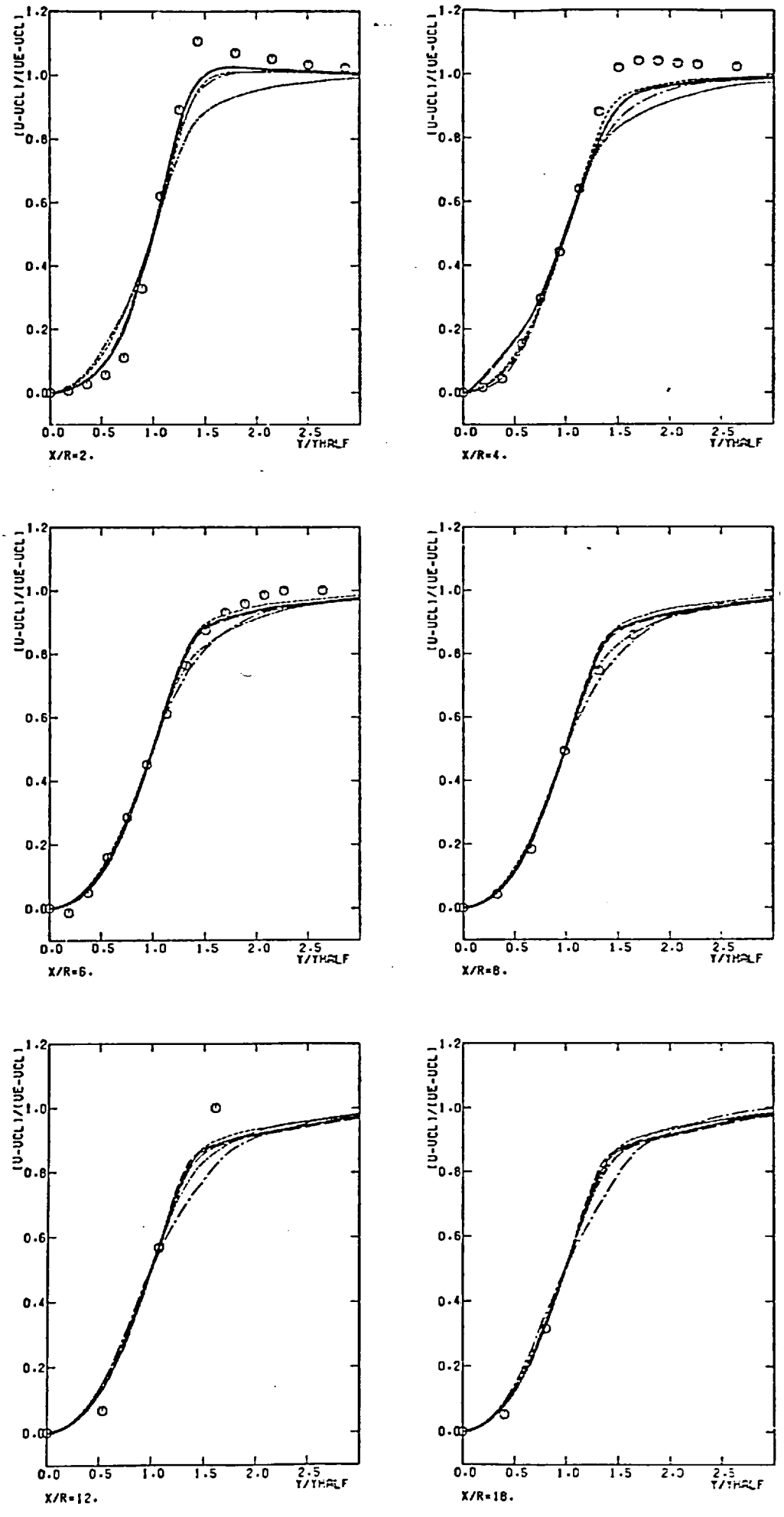

Figure 5.7 Flow of Carmody (1964): $(U - U_\ell)/U_E - U_\ell)$ against y/R.

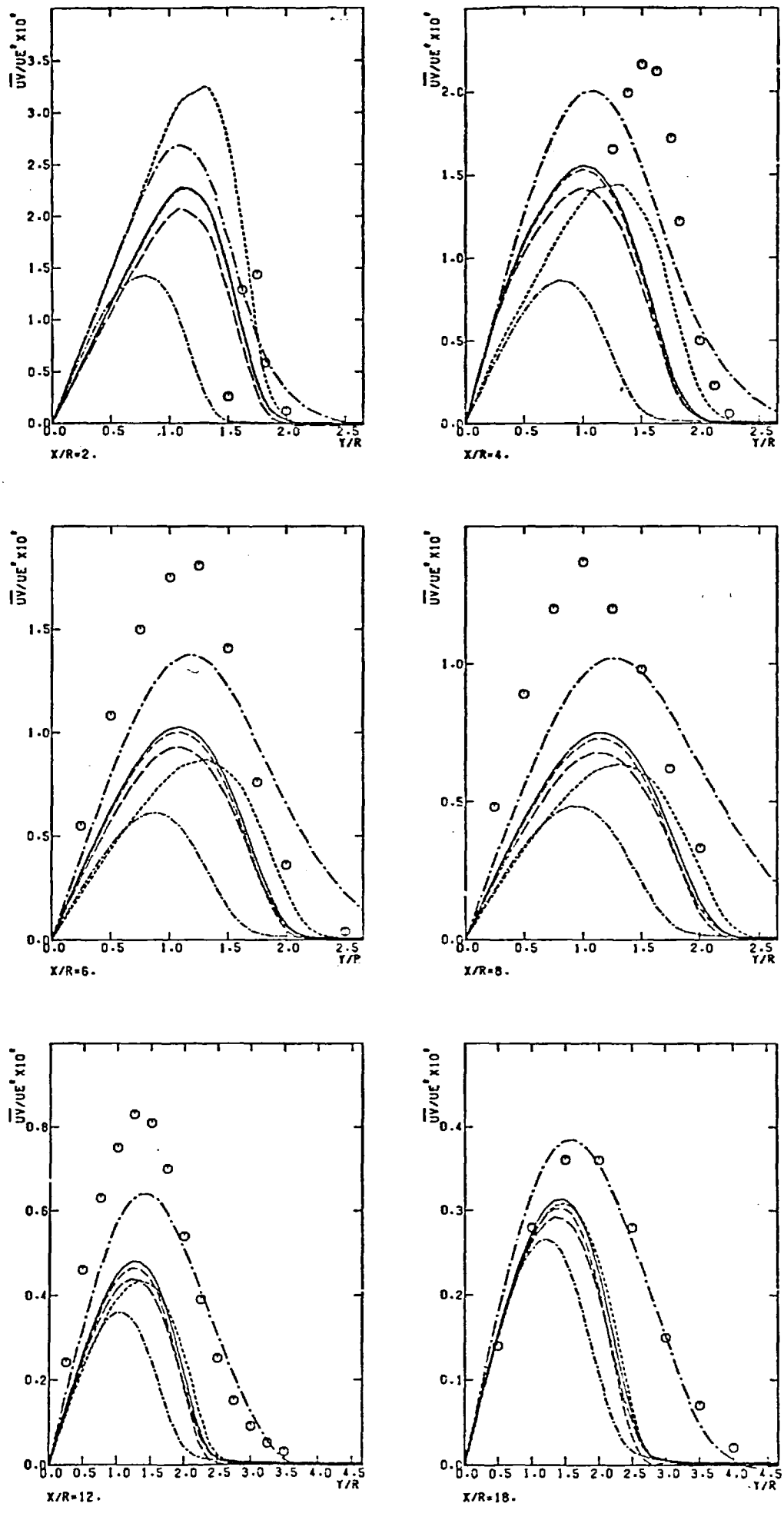

Figure 5.8 Flow of Carmody (1964)
$\overline{uv}/U_E^2$ against y/R.

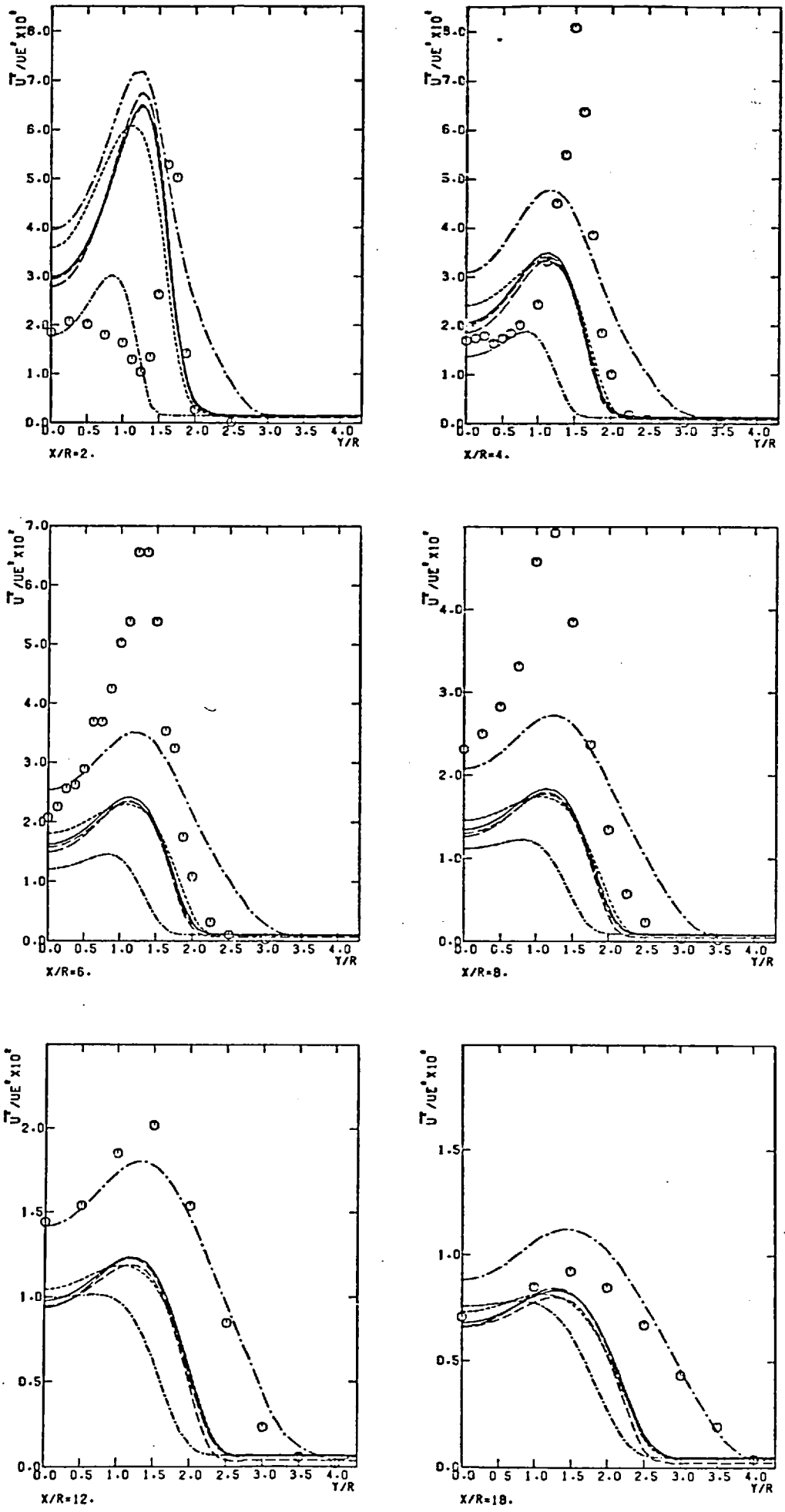

Figure 5.9 Flow of Carmody (1964):
$\overline{u^2}/U_E^2$ against y/R.

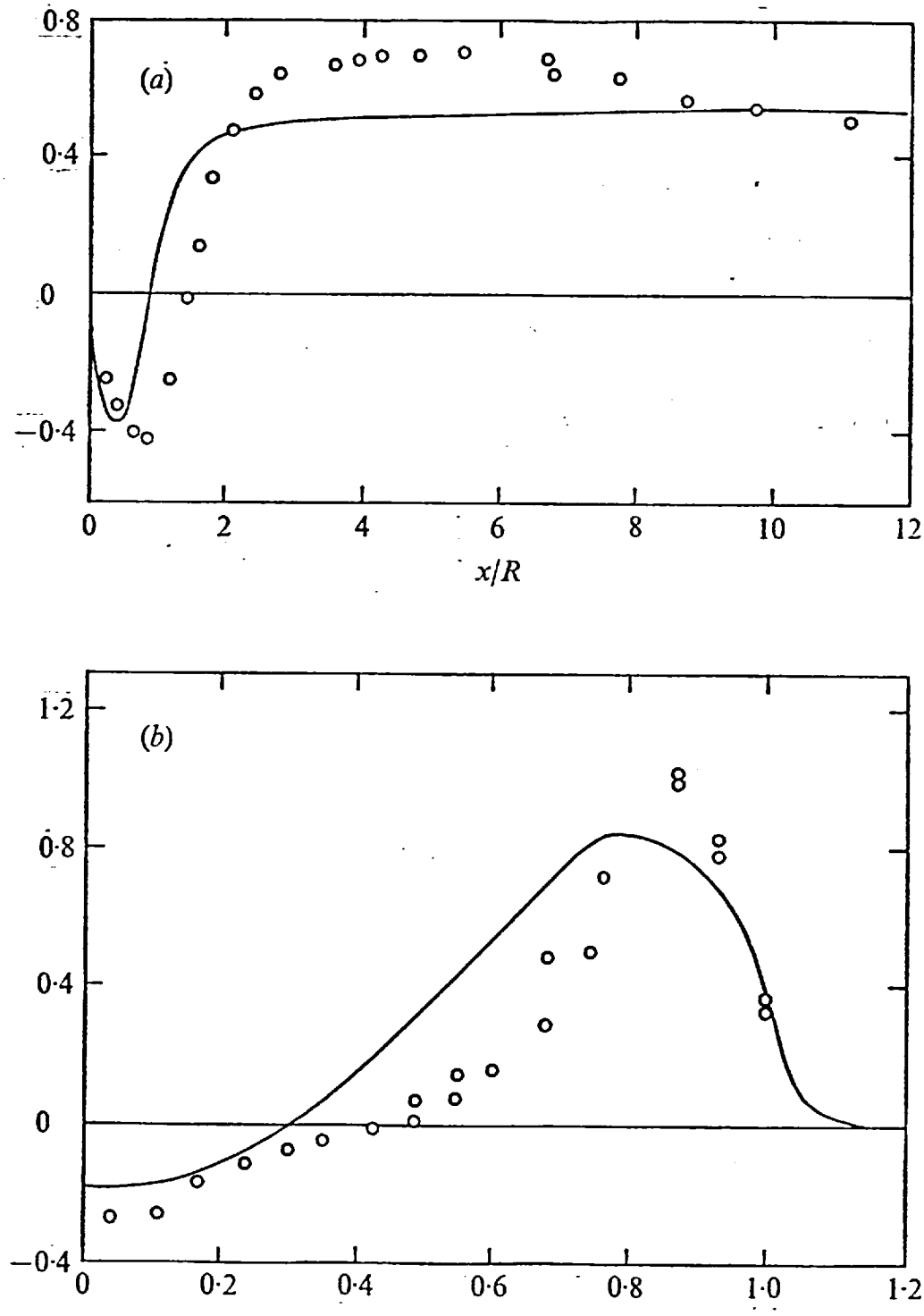

Figure 5.10 Flow of Durão and Whitelaw (1974):
(a) U/U_{in} against x/R,
(b) U/U_{in} against y/R, x/R = 0.6

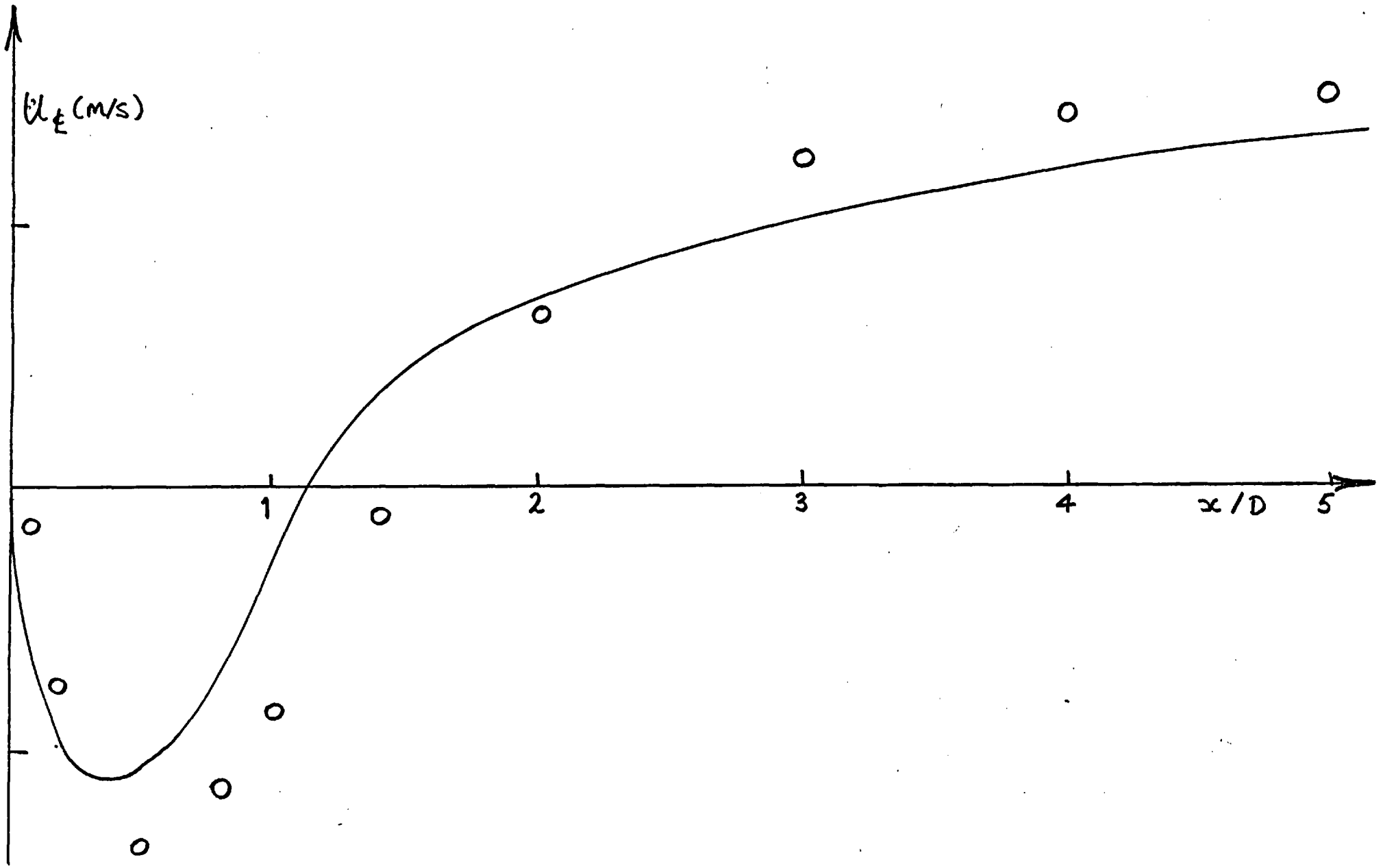

Figure 5.11 Flow of Assaf (1975); U_t against x/R

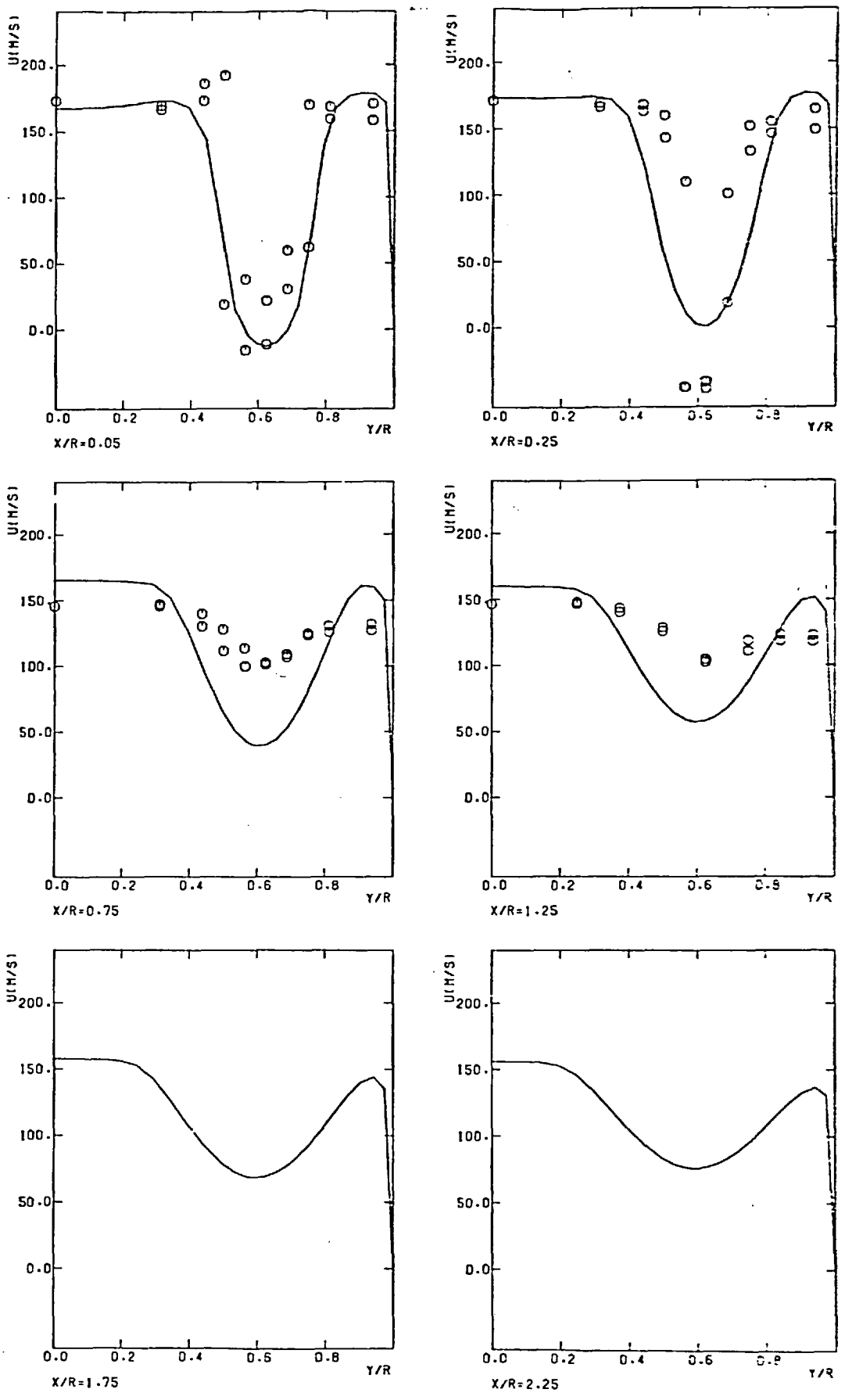

Figure 5.12 Test 1, U against y/R.

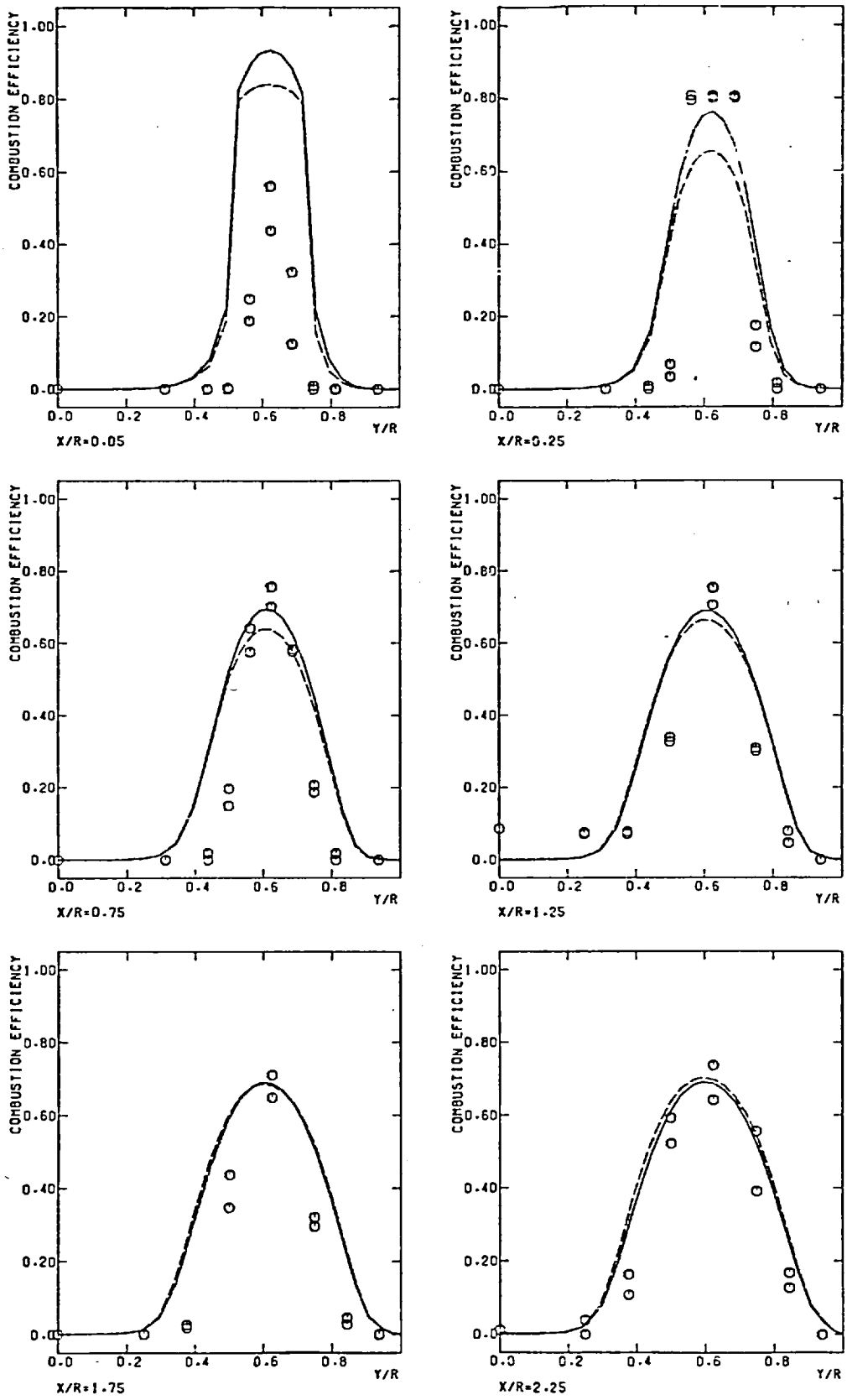

Figure 5.13 Test 2, η against y/R.

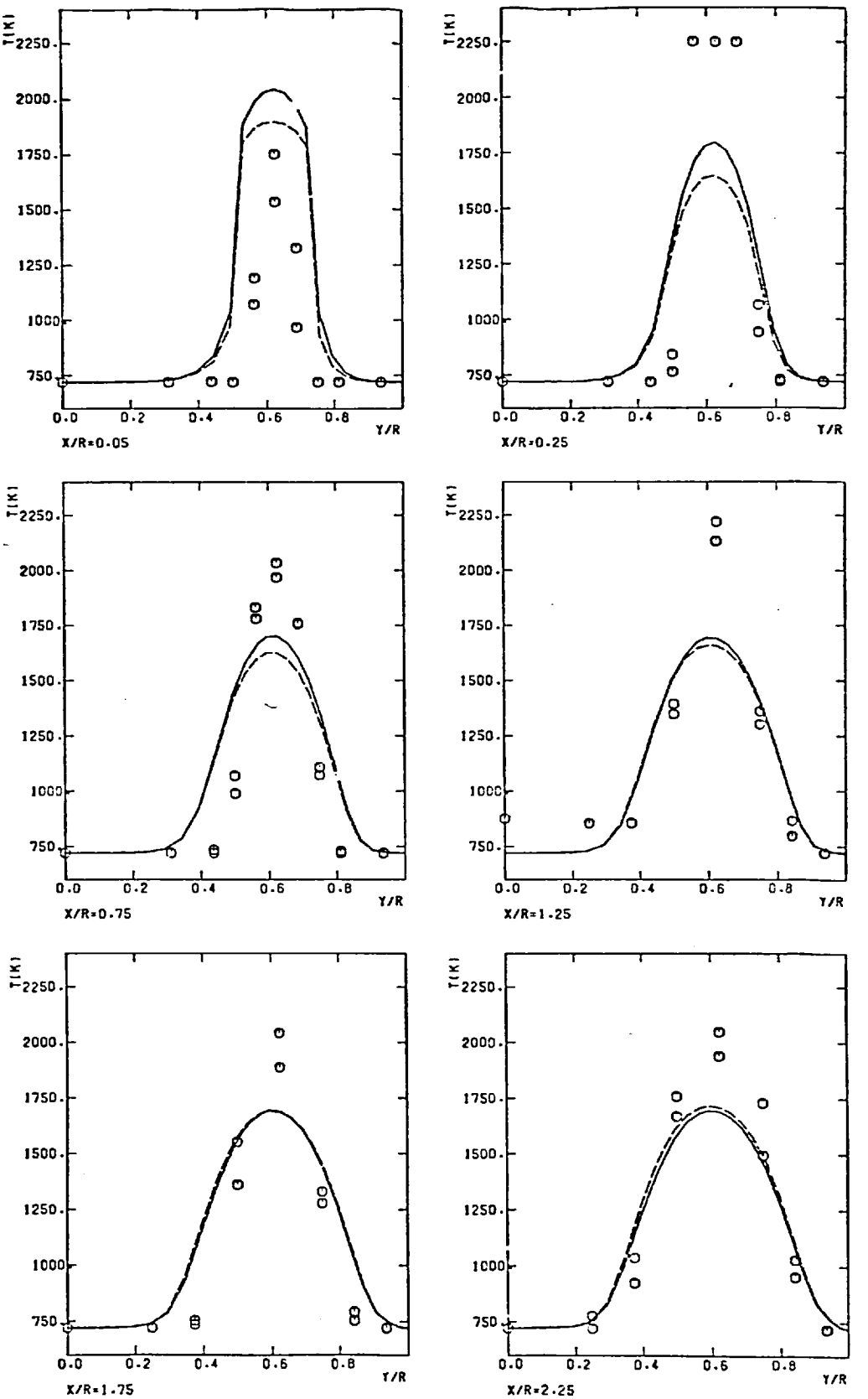

Figure 5.14 Test 2, T against y/R.

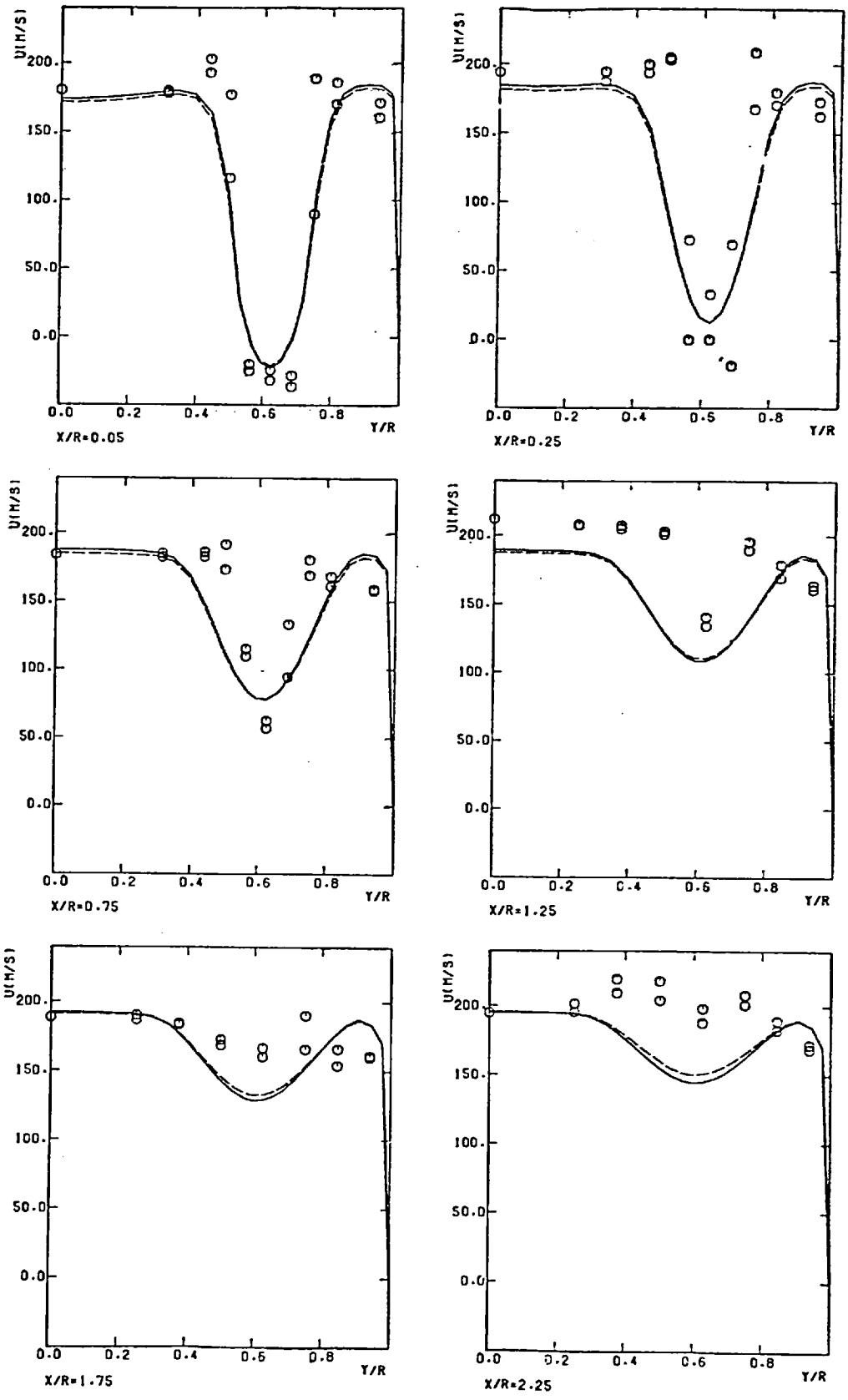

Figure 5.15 Test 2, U against y/R.

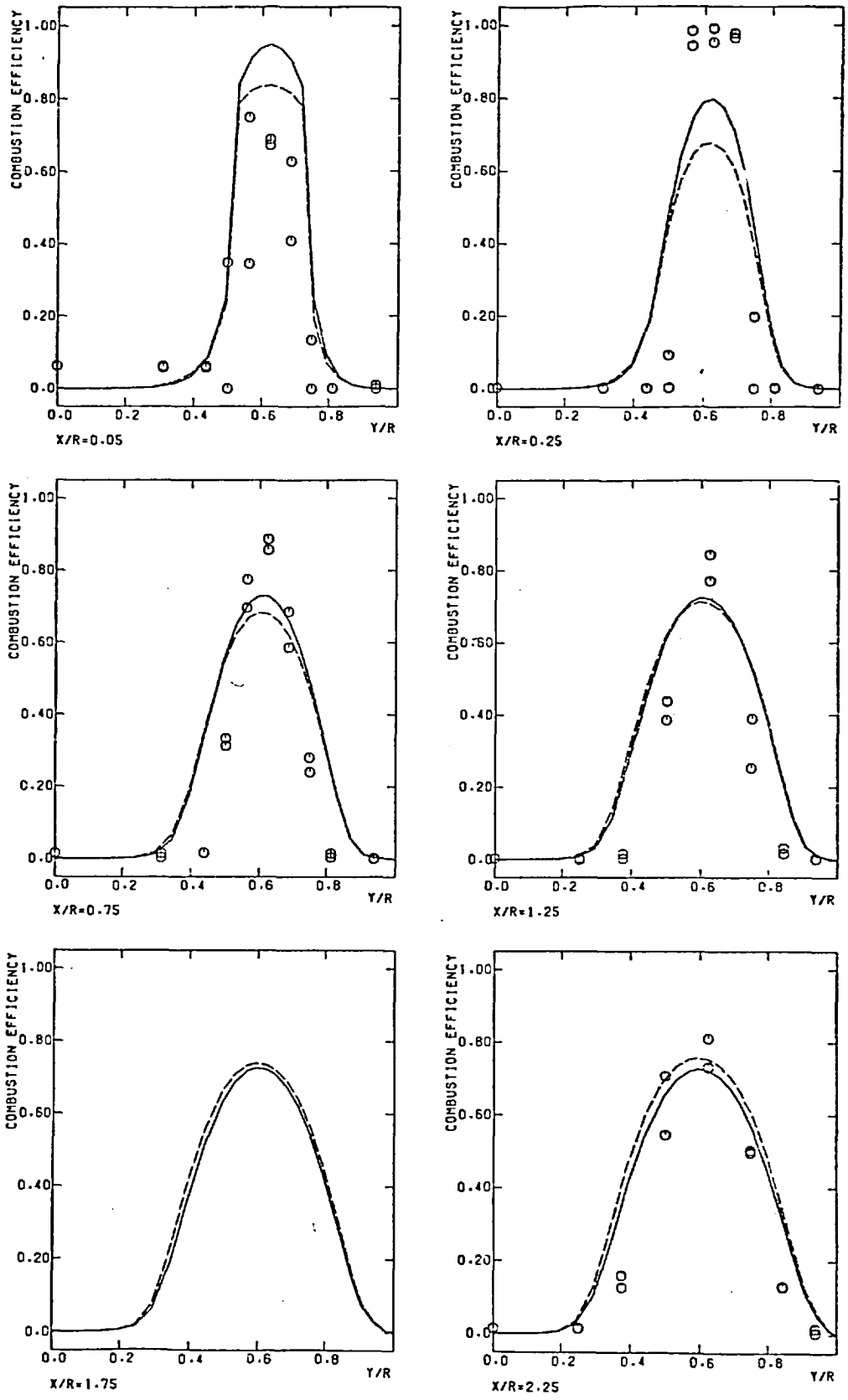

Figure 5.16 Test 3, η against y/R.

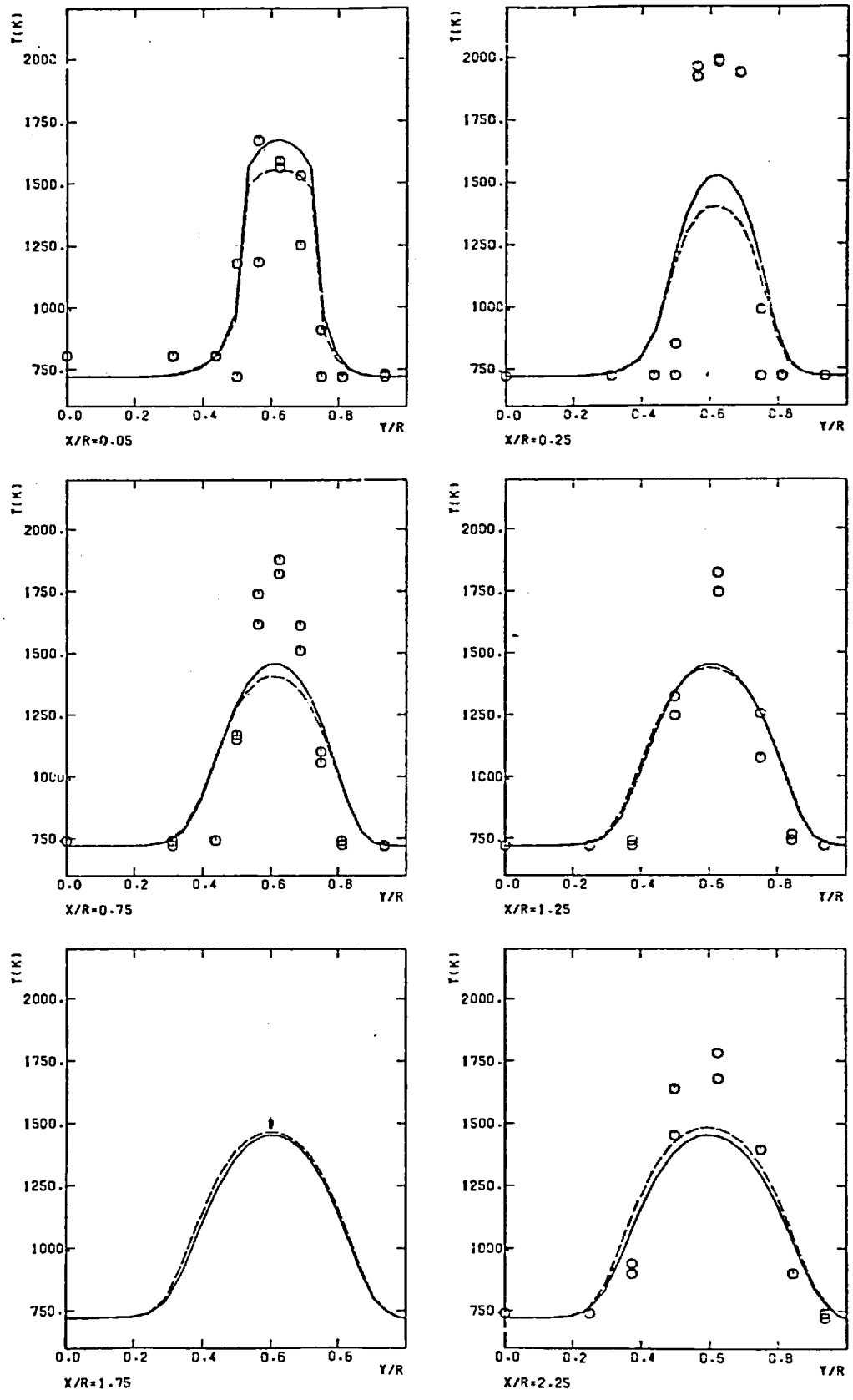

Figure 5.17 Test 3, T against y/R.

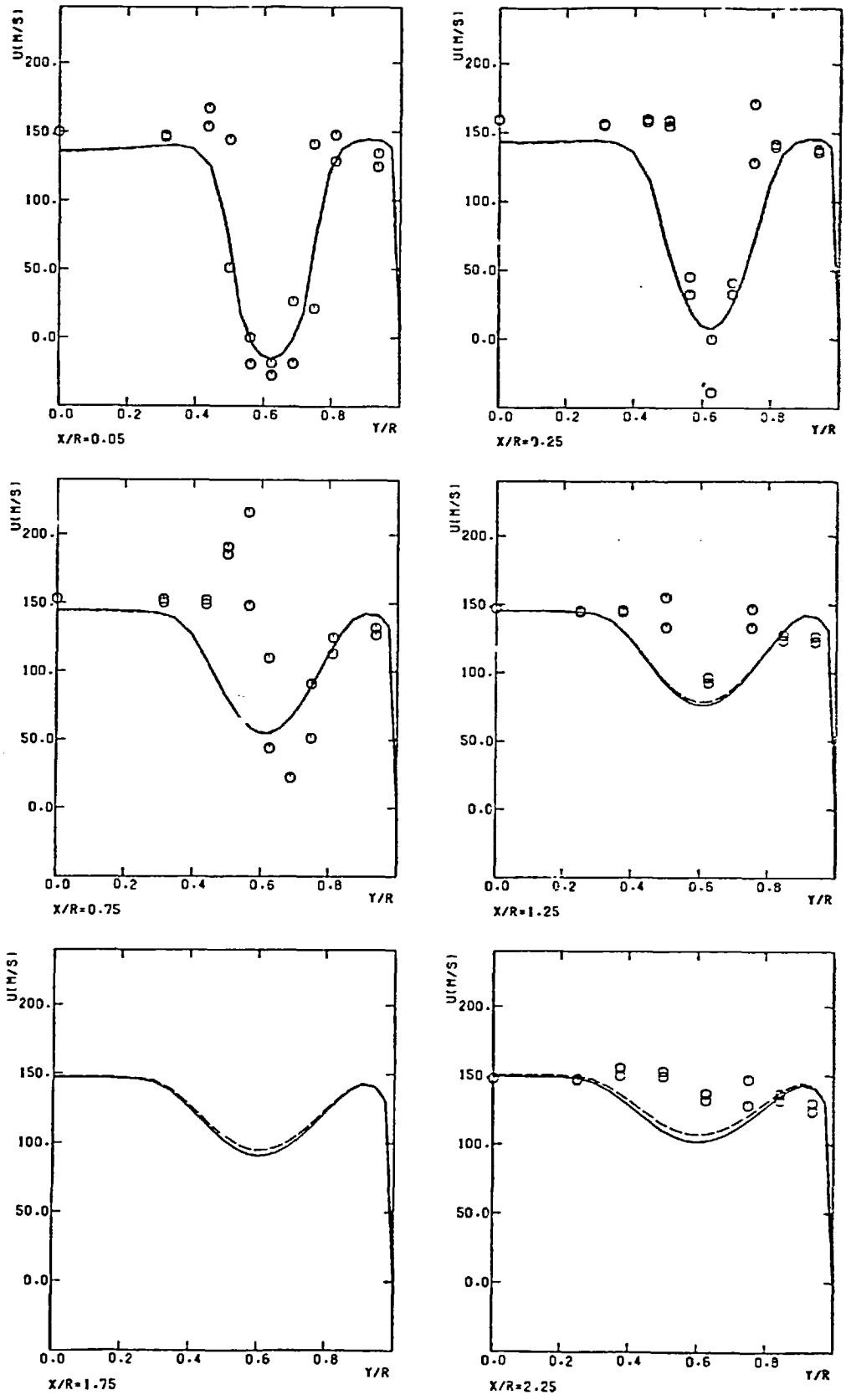

Figure 5.18 Test 3, U against y/R.

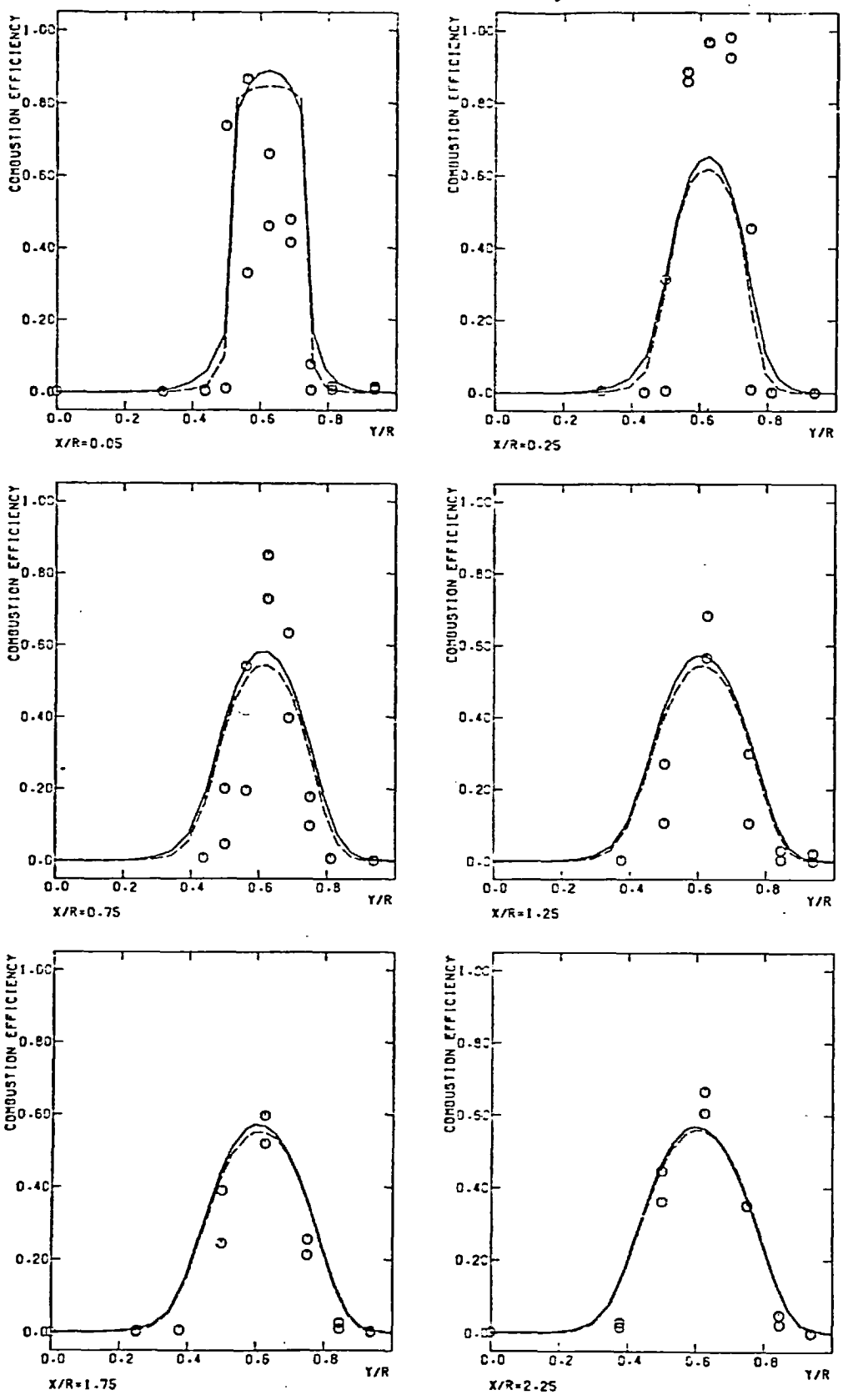

Figure 5.19 Test 4, η against y/R.

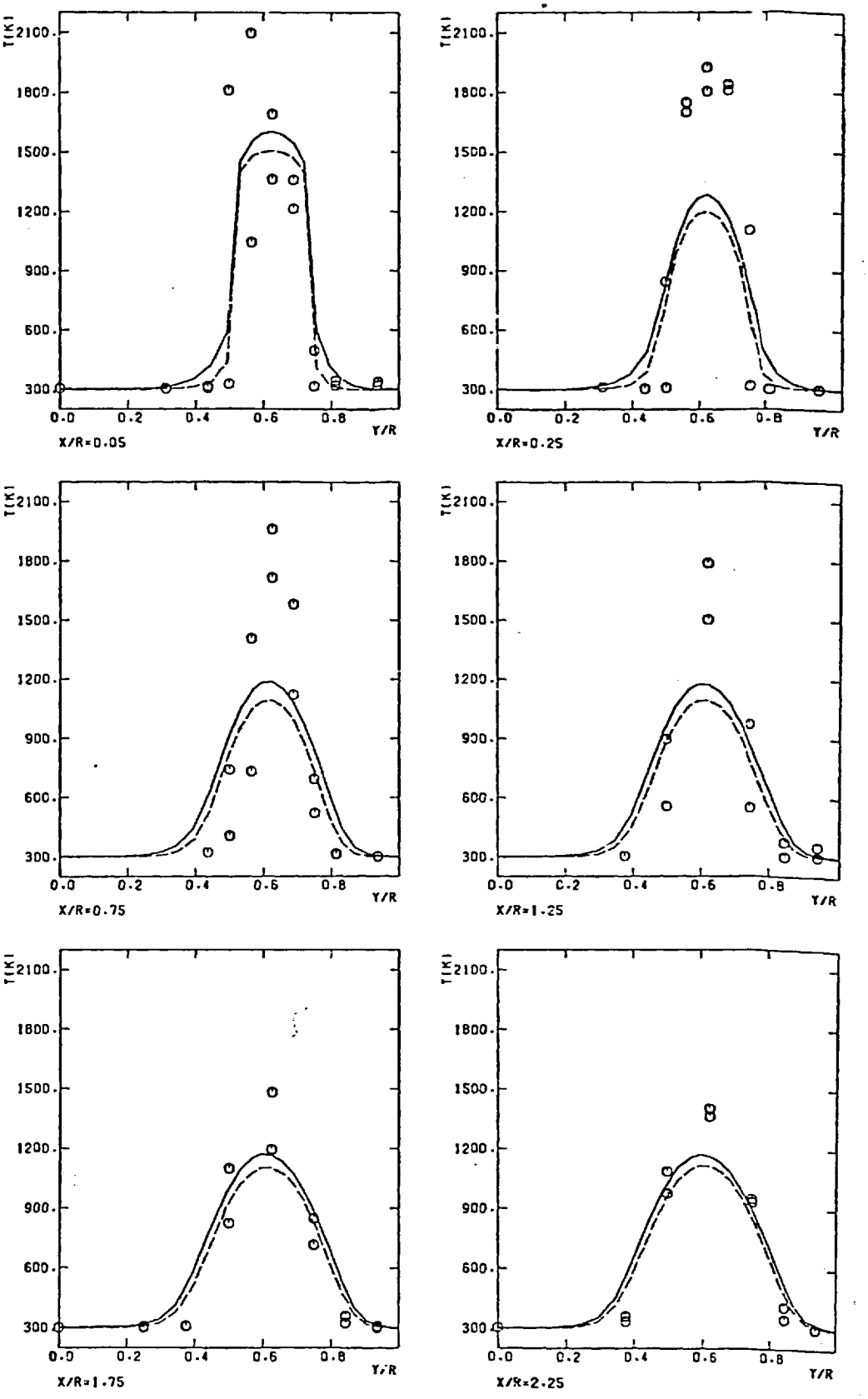

Figure 5.20 Test 4, T against y/R.

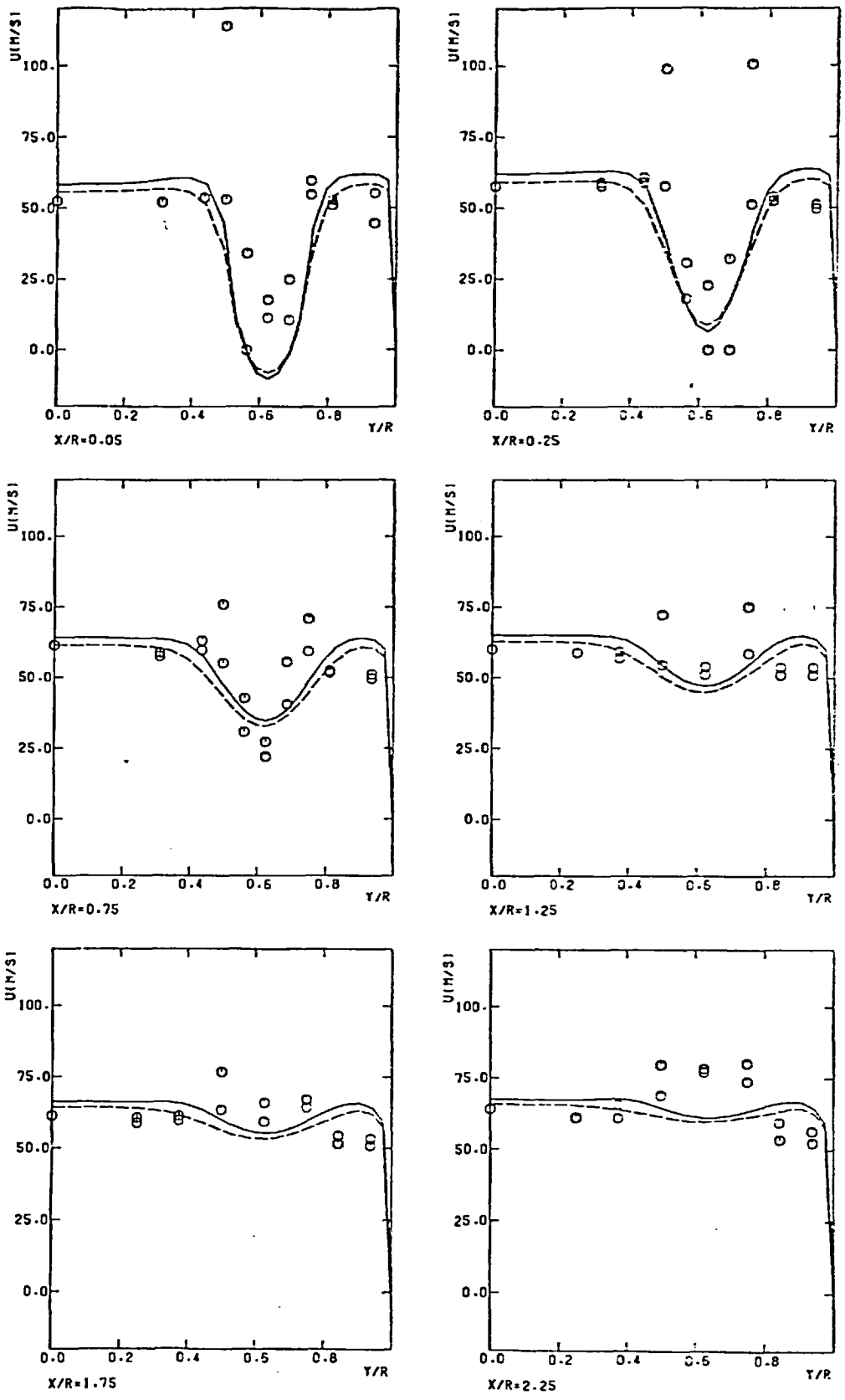

Figure 5.21 Test 4, U against y/R.